TU/e EINDHOVEN UNIVERSITY OF TECHNOLOGY

Dynamic covalent chemistry for UV curable networks

Citation for published version (APA):
Maassen, E. E. L. (2019). *Dynamic covalent chemistry for UV curable networks*. [Phd Thesis 1 (Research TU/e / Graduation TU/e), Chemical Engineering and Chemistry]. Technische Universiteit Eindhoven.

Document status and date:
Published: 02/10/2019

Document Version:
Publisher's PDF, also known as Version of Record (includes final page, issue and volume numbers)

Please check the document version of this publication:

• A submitted manuscript is the version of the article upon submission and before peer-review. There can be important differences between the submitted version and the official published version of record. People interested in the research are advised to contact the author for the final version of the publication, or visit the DOI to the publisher's website.
• The final author version and the galley proof are versions of the publication after peer review.
• The final published version features the final layout of the paper including the volume, issue and page numbers.

Link to publication

General rights
Copyright and moral rights for the publications made accessible in the public portal are retained by the authors and/or other copyright owners and it is a condition of accessing publications that users recognise and abide by the legal requirements associated with these rights.

• Users may download and print one copy of any publication from the public portal for the purpose of private study or research.
• You may not further distribute the material or use it for any profit-making activity or commercial gain
• You may freely distribute the URL identifying the publication in the public portal.

If the publication is distributed under the terms of Article 25fa of the Dutch Copyright Act, indicated by the "Taverne" license above, please follow below link for the End User Agreement:

www.tue.nl/taverne

Take down policy
If you believe that this document breaches copyright please contact us at:

openaccess@tue.nl

providing details and we will investigate your claim.

Download date: 04. Oct. 2023

Dynamic Covalent Chemistry for UV Curable Networks

PROEFSCHRIFT

ter verkrijging van de graad van doctor aan de Technische Universiteit Eindhoven, op gezag van de rector magnificus prof.dr.ir. F.P.T. Baaijens, voor een commissie aangewezen door het College voor Promoties, in het openbaar te verdedigen op woensdag 2 oktober 2019 om 16:00 uur

door

Eveline Elisabeth Leonardus Maassen

Geboren te Beek

Dit proefschrift is goedgekeurd door de promotoren en de samenstelling van de promotiecomissie is als volgt:

Voorzitter:	prof. dr. ir. E.J.M. Hensen
1e promotor:	prof. dr. R.P. Sijbesma
copromotor:	dr. ir. J.P.A. Heuts
Onafhankelijke leden:	prof. dr. D.J. Broer
	prof. dr. F. Picchioni (RUG)
	prof. dr. R.A.T.M van Benthem
Overig lid	prof. dr. G.W.M. Peters
Adviseur	dr. T. ten Cate (TNO)

Het onderzoek of ontwerp dat in dit proefschrift wordt beschreven is uitgevoerd in overeenstemming met de TU/e Gedragscode Wetenschapsbeoefening.

“Not everything that can be counted counts.

Not everything that counts can be counted.”

- William Bruce Cameron -

A catalogue record is available from the Eindhoven University of Technology Library.
ISBN: 978-90-386-4846-0

Copyright © 2019 by Eveline Maassen

Cover design: Jolien Paulussen
The cover illustrates a zoom-in on a polymeric network where dynamic covalent crosslinks are present. The network is based on the lines of Eveline's hand palms to represent the amount of work she put in this research.

Printed by: Gildeprint – the Netherlands

This work was financially supported by the TU/e Impuls program and carried out within the Additive Manufacturing program of Brightlands Materials Center.

Summary

Dynamic covalent chemistry for UV curable networks

Additive manufacturing (colloquially known as 3D printing) of polymers has gained much attention in the past few years, as customized products can be made on demand. In this thesis the focus is on stereolithography, a printing technique that uses photopolymerization to create three-dimensional objects from a liquid resin in a layer by layer process. Unfortunately, the application of printed products on a larger scale is hindered by often inferior mechanical properties of these products. The main components in resins used for stereolithography are monomers or oligomers. Due to their fast curing behavior (meth)acrylates dominate the market, but polymerization is often accompanied by stress development due to volumetric shrinkage. The shrinkage-induced stress can cause creep distortions or crack formation, leading to premature material failure. The work described in this thesis aims to reduce the shrinkage stress by using covalent adaptable networks. The focus is on thermally induced bond exchange to be applied in UV cured polymeric materials. Three different chemical approaches are reported.

In **Chapter 2**, a Diels-Alder containing di-acrylic monomer was synthesized successfully. Photopolymerization with bisphenol A ethoxylate diacrylate as a comonomer yielded a highly crosslinked network which contained Diels-Alder adduct moieties. Quantitative opening of the Diels-Alder bonds was achieved by thermally treating the material above 150 °C. This led to a material with a significantly lower crosslink density. The reformation reaction proved to be less efficient and only minimal reformation was achieved by thermal annealing. Nevertheless, the mechanical properties of the material after shrinkage compensation were investigated with tensile testing. The opening of the Diels-Alder bonds makes stress dissipation possible and it was shown that the opening of the bonds helps to improve the lifetime of the material.

The samples containing Diels-Alder bonds were subjected to consecutive heating cycles during a DMTA experiment, to study their thermal reversibility. In those experiments, an unexpectedly large shift in T_g from the first to the second heating cycle was observed. In **Chapter 3**, the origin of the increase in T_g is studied in detail. Highly crosslinked bisphenol A ethoxylate diacrylate networks without any dynamic covalent bonds also undergo additional curing during DMTA measurements. A detailed study of the conditions under which the change in properties takes place unequivocally shows that a small (0.1%) oscillatory strain applied above T_g is responsible for the observed additional curing. By shear induced curing above T_g, a similar increase in T_g was observed confirming the contribution of an oscillatory strain. It was also found that any optical anisotropy introduced by straining the material did not contribute to the shift in mechanical properties.

Chapter 4 describes the development of a reversible crosslinker based on transalkylation chemistry using benzyl bromide with 1,4-diazabicyclo[2.2.2]octane (DABCO). Kinetic experiments showed efficient exchange at relatively low temperatures (70 °C), with both excess of amine and excess of bromine without the addition of a catalyst. To study the

reversibility of this system in a polymer, a linear polymer with benzyl bromide side groups was crosslinked with DABCO as a divalent crosslinker. The resulting polymer network was insoluble but could be compression molded into various shapes. Again systems with excess of amine and excess of bromine were investigated. Both polymeric networks showed efficient stress relaxation around 120 °C. In accordance with the small molecule kinetic studies, the system with excess amine showed faster relaxation than the system with excess benzyl bromide groups.

The last experimental chapter, **Chapter 5**, reports a rapid one-step method for the formation of dynamic crosslinks in polymers containing hydroxyl groups. Bond exchange by transesterification is used in many interesting material applications. Most of these systems use a dispersed catalyst to tune the exchange kinetics and obtain efficient bond exchange. Here intrinsic carboxylic acid catalysts are formed simultaneously upon the formation of ester crosslinks. Stress relaxation experiments showed the effectiveness of the internal carboxylic acid catalyst in a system with free hydroxyl groups. However, thermally induced 'permanent' crosslinks prevent full stress relaxation. Surprisingly, a system without excess free hydroxyl groups also showed efficient stress relaxation, suggesting a contribution of an anhydride intermediate in the transesterification reaction mechanism.

Finally, in **Chapter 6** the impact of the research is discussed in more detail. Furthermore, additional directions for future work and incorporation of the transalkylation and transesterification chemistry in a photopolymerizable system are presented.

Samenvatting

Dynamisch covalente chemie voor UV polymeriseerbare netwerken

Het 3D printen van polymere materialen is de laatste jaren steeds meer in de aandacht gekomen omdat deze techniek mogelijkheden biedt voor de eenvoudige productie van gepersonaliseerde producten. In dit proefschrift ligt de nadruk op stereolithografie, een printmethode die fotopolymerisatie gebruikt om door middel van een laag voor laag proces driedimensionale producten te maken uit een vloeibaar startmateriaal. De toepassing van geprinte producten op een grote schaal wordt helaas beperkt door de slechte materiaaleigenschappen van deze producten. De belangrijkste componenten van het vloeibare startmateriaal zijn de monomeren of oligomeren. Door hun snelle uitharding worden (meth)acrylaten hiervoor het meest gebruikt. Maar de polymerisatie gaat gepaard met de ontwikkeling van krimpstress door een afname in het volume. Deze krimpstress kan leiden tot vervormingen van het materiaal of kleine scheurtjes in het materiaal. Het doel van het onderzoek beschreven in dit proefschrift is het verminderen van de krimpstress door het gebruik van covalent aanpasbare netwerken. De nadruk ligt hierbij op de thermische initiatie van het uitwisselen van bindingen in polymeren die gemaakt zijn door middel van UV-uitharding. Drie verschillende aanpakken worden beschreven.

In **Hoofdstuk 2** wordt de synthese van een diacrylaat monomeer dat Diels-Alder groepen bevat beschreven. Fotopolymerisatie van dit monomeer met bisfenol A ethoxylaat diacrylaat als comonomeer resulteerde in een sterk vernet netwerk dat Diels-Alder groepen bevat. De Diels-Alder groepen konden kwantitatief geopend worden door het materiaal thermisch te behandelen boven 150 °C. Het openen van de Diels-Alder groepen resulteerde in een verlaagde vernettingsgraad. De hervormingsreactie was minder efficiënt en het gebruik van verschillende thermische behandelingen leidde maar tot minimale hervorming van Diels-Alder groepen. Desondanks werden de mechanische eigenschappen van de materialen na thermische krimpcompensatie onderzocht met behulp van een trekproef. Het openen van de Diels-Alder groepen zorgt voor delokalisering van de stress waardoor het materiaal een langere levensduur heeft.

Om de thermische reversibiliteit van de materialen met Diels-Alder bindingen te bestuderen werden ze blootgesteld aan opeenvolgende verwarmingsstappen in een DMTA. Tijdens deze experimenten werd er een onverwachte toename van de glasovergangstemperatuur (T_g) waargenomen tussen de 1^e en de 2^e verwarmingscyclus. In **Hoofdstuk 3** wordt de oorsprong van deze toename in detail bestudeerd. Sterk vernette bisfenol A ethoxylaat diacrylaat netwerken zonder reversibele Diels-Alder bindingen laten eenzelfde toename zien tijdens DMTA-metingen. Een gedetailleerde studie van de condities waaronder deze T_g toename plaatsvindt toont aan dat het trekken aan het materiaal boven de T_g met een kleine kracht ervoor zorgt dat er extra uitharding plaatsvindt. Deze kracht zorgt er ook voor dat er een optische anisotropie geïntroduceerd wordt in het materiaal. Deze anisotropie draagt echter niet bij aan de verandering in materiaaleigenschappen.

In **Hoofdstuk 4** wordt de ontwikkeling van een reversibel netwerk gebaseerd op transalkylatie chemie met 1,4-diazabicyclo[2.2.2]octaan (DABCO) beschreven. Kinetische experimenten tonen aan dat er bij relatief lage temperaturen (70 °C) efficiënte uitwisseling van bindingen plaatsvindt. Deze reactie treedt op met zowel een overmaat aan amine als een overmaat aan bromide zonder dat er een katalysator aanwezig is. Om dit systeem verder te onderzoeken is er een lineair polymeer gemaakt met bromide zijgroepen. Door de toevoeging van DABCO konden deze zijgroepen worden vernet. Het gemaakte netwerk was onoplosbaar maar kon door middel van een warme drukpers wel gevormd worden. Ook in het vaste systeem werden zowel een overmaat aan amine als een overmaat aan broom onderzocht. Beide lieten efficiënte stress relaxatie zien rond 120 °C. Net als bij de kinetische experimenten reageerde ook hier het systeem met een overmaat aan amine sneller dan het systeem met een overmaat aan bromide.

Het laatste experimentele hoofdstuk, **Hoofdstuk 5**, beschrijft een snelle eenstapsmethode voor de vorming van een dynamische vernetting voor polymeren die hydroxylgroepen bevatten. Het uitwisselen van bindingen door middel van transesterificatiereacties heeft al tot veel interessante toepassingen geleid. De meeste van deze systemen bevatten een apart toegevoegde katalysator om de kinetiek te sturen en efficiënte uitwisseling te verkrijgen. In het ontwikkelde systeem wordt er een intrinsieke katalysator gevormd tijdens de vernetting van de polymere ketens. Stressrelaxatie experimenten tonen aan dat dit systeem efficiënt werkt als er hydroxylgroepen aanwezig zijn. Er worden echter wel vaste verbindingen gevormd tussen polymeerketens die ervoor zorgen dat volledige relaxatie niet mogelijk is. Tegen de verwachtingen in is er ook stressrelaxatie te zien bij een systeem zonder veel hydroxylgroepen. Dit suggereert dat de anhydriden die gevormd worden tijdens de omestering ook een rol spelen in de reactie.

Als laatste wordt in **Hoofdstuk 6** in meer detail de impact van dit onderzoek besproken. Ook worden aanvullende ideeën voor toekomstig werk en de implementatie van transalkylatie en transesterificatie chemie in een polymeriseerbaar systeem gepresenteerd.

Table of Contents

Chapter 1
General introduction **1**
1.1 Introduction 2
1.2 Stereolithography 3
1.3 Photopolymerization of acrylates 4
1.4 Shrinkage stress 7
1.5 Dynamic covalent chemistry 8
1.6 Aim and outline of this thesis 12
1.7 References 13

Chapter 2
Stress relaxation via Diels-Alder reactions **21**
2.1 Introduction 22
2.2 Monomers 24
2.3 Polymerization 25
2.4 Opening of the Diels-Alder groups 27
2.5 Mechanical properties 29
2.6 Conclusions 31
2.7 Experimental details 32
2.8 References 35

Chapter 3
Post curing of an acrylate network induced by oscillatory strain **39**
3.1 Introduction 40
3.2 Initial experiments 40
3.3 Effect of thermal treatment 42
3.4 Effect of oscillatory strain 45
3.5 Optical anisotropy 47
3.6 Conclusions 49
3.7 Experimental details 49
3.8 References 51

Chapter 4
Stress relaxation via transalkylation chemistry **53**
4.1 Introduction 54
4.2 Small molecule kinetics 57
4.3 Reversible crosslinking of linear chains 62
4.4 Stress relaxation 64
4.5 Conclusions 66
4.6 Experimental details 66
4.7 References 70

Chapter 5
Stress relaxation via internally catalyzed transesterification reactions **73**
5.1 Introduction 74
5.2 Network synthesis 76
5.3 System A: with free hydroxyl groups 79
5.4 System B: without free hydroxyl groups 82
5.5 Conclusions 84
5.6 Experimental details 85
5.7 References 87

Chapter 6
Epilogue **91**
6.1 Introduction 92
6.2 Overview of results 93
6.3 Future perspectives 94
6.4 Conclusions 97
6.5 References 97

Curriculum Vitae **99**
List of Publications **101**
Acknowledgements **103**

Chapter 1

General introduction

Abstract: 3D printing of polymers has gained much attention in the past few years, as customized products can be made on demand. Unfortunately, the application of printed products on a larger scale is hindered by often inferior mechanical properties of these products. In this chapter the fundamental aspects of 3D printing, more specifically stereolithography are outlined, followed by an explanation of polymerization induced volumetric shrinkage and resulting stress. Shrinkage stress is an important contributor to premature material failure, several examples of reducing this shrinkage stress are discussed. Furthermore, as the work in this thesis aims to reduce the shrinkage stress by using covalent adaptable networks, the basic concepts and some recent advances in this field are described.

1.1 Introduction

Polymeric materials are widely used and are an important part of our everyday life.[1] In 2017 the world plastic production almost reached 350 million tons per year, almost 50 kg for each inhabitant of our planet.[2] The most common classification of polymers is based on the molecular interactions between polymer chains.[3] A thermoplastic material consists of entangled macromolecules which can flow upon heating. The flow makes it possible to mold and remold thermoplastics into virtually any shape.[4] The second class of polymers, thermosets, are network polymers in which the mobility of chains is highly restricted due to covalent crosslinks between polymer chains, making flow upon heating impossible.[5] Although there are many different processing methods,[6] getting the right shape is still one of the biggest challenges for thermosets.[7–9]

It is in this field that additive manufacturing (colloquially known as 3D printing), offers new possibilities.[10] The layer by layer production makes the use of molds redundant, which leads to more freedom in design,[11] and more importantly, easy production of customized products.[12] A large number of 3D printing techniques have been developed, such as fused deposition modeling, selective laser sintering, material or binder jetting and stereolithography.[13] In this thesis the focus is on stereolithography, but the general principles of the 3D printing process are the same for all printing techniques. The first step is the creation of a computer-aided design (CAD) file of the desired product, in which the desired shape is virtually sliced into layers of a certain thickness (generally between 15-500 µm).[14] Using the CAD model to direct the motor of the printer, the first slice can be printed on a building platform. After a layer is printed, the platform or printing head moves in the vertical direction and the next layer can be added. Often, post processing steps are performed to remove support structures, remove surface defects or increase the mechanical properties.[15]

Although interest in 3D printing has rapidly grown during the past years, the mechanical properties of 3D printed products are often inferior to products produced via classical technologies such as injection molding.[14,16] A major issue is the presence of weak spots, caused by the layer-by-layer production, as the interaction between two layers is often weaker than the interaction within a single layer.[17,18] Another issue is the limited choice in starting materials, because the method has specific demands for the raw materials such as melt strength,[19] or viscosity.[20,21]
In the research described here, the focus is on stereolithography, a printing technique that uses photopolymerization to create three-dimensional objects from a liquid resin in a layer by layer process.[22] This research aims to improve the mechanical properties of the final product by a bottom-up approach that starts with designing better acrylic monomers.

In the remainder of this chapter, a more detailed explanation of stereolithography and acrylate polymerization is reported. The origin of shrinkage stress and known solutions to this issue are discussed. The next part explains the concept of dynamic covalent chemistry and how this can potentially solve the issue of shrinkage stress in photo polymerizations. Finally, the aim and outline of this thesis are presented.

1.2 Stereolithography

Stereolithography is classified as a vat polymerization,[23] in which an excess of resin is selectively photopolymerized into a solid product.[16] The resin consists of multivalent monomers or oligomers, a photo initiator, and further additives.[24] By using multifunctional monomers, crosslinking and thus hardening into a permanent polymeric network takes place.[25] When polymerization of a layer is finished, the building platform moves, so a subsequent layer can be printed. This process is schematically represented in Figure 1.1. There is a large variety of printers on the market, although the basic principles are the same.[22] In Figure 1.1, a top-down approach is depicted, in which the cured product is lowered into the liquid resin. More recently, bottom-up machines with an inverted geometry have been developed. With this configuration, light comes from the bottom through a transparent vat. This approach requires less resin and smaller vat sizes, as the printed object is pulled out of the resin.[26]

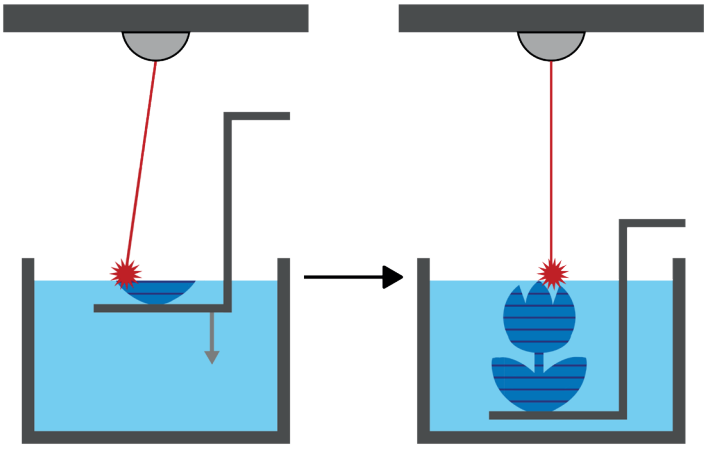

Figure 1.1. Schematic representation of stereolithography, a 3D object is formed slice by slice. A layer of monomer is polymerized by UV light. After formation of a layer, the platform is lowered into the resin allowing polymerization of the next layer.

The first stereolithographic printer was introduced in the late 1980s, making it the first commercialized 3D printing technique.[27,28] Although many different 3D-printing techniques have been developed over the years, stereolithography remains one of the most powerful and versatile techniques.[12,16] Compared to other 3D printing techniques, it offers high fabrication accuracy and resolution.[29] Another advantage is that if the monomer conversion is sufficiently high,[17] products produced via stereolithography have similar properties in the building direction and perpendicular to the building direction, due to good layer to layer adhesion.[29,30]

Since the first patent application in 1984, stereolithography has found its way in various fields.[27] For instance, different biomedical engineering applications have been developed. The freedom in design makes the production of patient specific models and implants readily

accesible.[30] By using computed tomography (CT) images or echocardiograms, body parts such as a heart or skeleton of a specific patient can be built to be used as a surgical guide.[31,32] These models can aid in diagnostics and even reduce surgical operation times. Dehurtevent *et al.*[33] were able to print dental restorations with a density and flexural strength similar to dental restorations manufactured using classical subtractive techniques. The main advantage of 3D printing (in biomedical applications) is the reduction of waste, and less instrument wear. In classical production methods using milling, unused portions of the raw material are not recyclable. The advantages of stereolithography in dental applications are such that dental printers and resins are nowadays commercially available through companies such as NextDent.[34]

The main components in resins used for stereolithography are monomers or oligomers. Characteristics such as viscosity, chemical structure and photo efficiency must be optimized by selection of the monomers.[35] The photoinitiator absorbs the light, and converts the energy into reactive species.[36] The rate of polymerization is determined by the reaction rate constant for the addition of a radical to a monomer.[37] For stereolithography, high photosensitivity is required to obtain a high printing resolution.[38] The viscosity must be low enough to allow formation of a new layer of resin after the polymerized part is lowered into the vat.[39] The final mechanical properties of the polymer are determined by tuning the molecular structure of the monomer or oligomers.[40] The two most common types of monomers for stereolithography are epoxides and (meth)acrylates.[35,41] (Meth)acrylate monomers or oligomers polymerize very fast,[42] and in general have a low viscosity and high photosensitivity.[43] An additional advantage is the presence of ester functionality which makes it possible to modify monomers and build in different funtionalities.[22] Drawbacks of the use of (meth)acrylates are the low strength and high brittleness of the polymerization products due to polymerization induced volume shrinkage.[35,44]
Epoxy based systems show exceptionally low volume shrinkage, giving excellent dimensional stability and better mechanical and thermal properties.[28,45] However, where acrylate polymerization takes only a few seconds, curing of an epoxy resin takes multiple minutes.[46] With advanced printing techniques, it is now possible to print acrylic products in minutes rather than hours.[21,47] This makes acrylates an attractive option, especially if the polymerization induced shrinkage can be minimized.
In commercially available resins, acrylic and epoxy-based monomers are combined leading to a dual-cure system. These systems have intermediate processing conditions and properties.[48,49]

1.3 Photopolymerization of acrylates

Photopolymerization is the chemical process that lies at the basis of stereolithography. During a photopolymerization, light initiates the transformation of a liquid monomer mixture into the corresponding solid polymer.[50] Photopolymerization has a long history of applications other than in stereolithography,[51] e.g. in dentistry,[52] coatings,[51,53] liquid-crystal displays,[54] inks and adhesives.[55,56] The use of photoreactions is attractive as they occur very fast and at room temperature.[57] Furthermore, they are generally performed in bulk which reduces the use of polluting solvents.[58] Another advantage is that the light-induced reaction

gives spatiotemporal control of the polymerization reaction,[59] a feature that is used extensively in photopolymerization for display applications.[60]
The liquid resin used in a photopolymerization consists of two main components, the monomer and a photoinitiator. A photoinitiator is an organic molecule which transforms the energy supplied by the light into chemical energy to initiate the polymerization reaction.[35] After absorption of a photon, the photoinitiator is consumed to form a reactive species, which is either a free radical or a cation.[61] Commonly used monomers for photopolymerization are styrenics, epoxides and (meth)acrylates. Due to their fast curing behavior, (meth)acrylates dominate the market.[28,42]

In general, photopolymerization of (meth)acrylates proceeds via a free radical polymerization mechanism.[62] This mechanism consists of four distinct steps: initiation, propagation, chain transfer and termination.[3,63] All four steps are shown in Scheme 1.1.

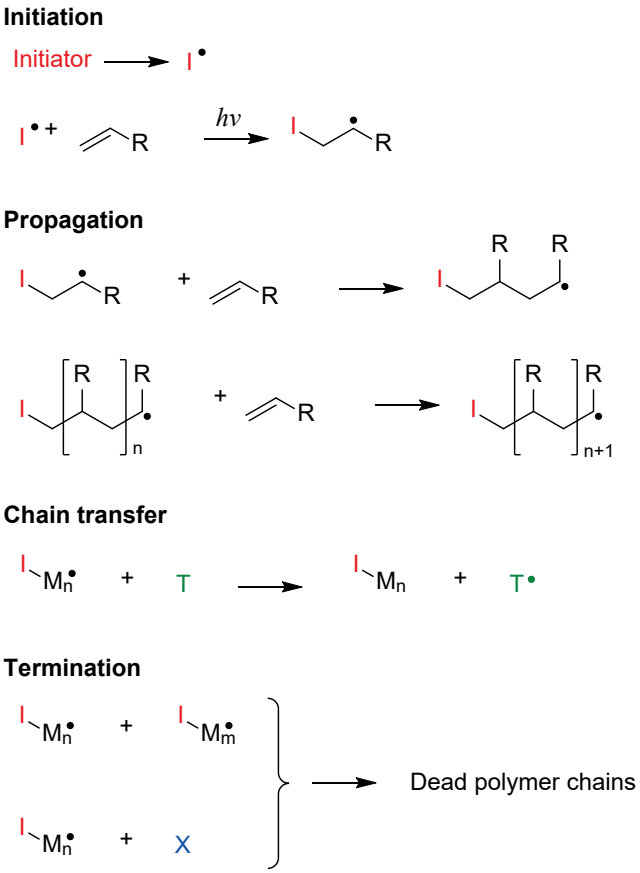

• = active radical, M = monomer, X = chain stopper, T = chain transfer agent

Scheme 1.1. Initiation, propagation, chain transfer and termination steps of a free radical polymerization mechanism.

During the initiation step, a radical initiator decomposes and produces one or more radicals, $I^{\bullet}$.[3] The lifetime of such a radical is generally very short, only 10^{-6} seconds, during which the radical can react with a monomer, initiating the growth of a chain.[61] There are two categories of free radical photoinitiators, Norrish Type I and Norrish Type II.[64] Type I initiators undergo a unimolecular reaction where two radical species are generated through cleavage of a bond in one molecule.[65] Type II initiators react in a bimolecular fashion to produce initiating species. The first step is the abstraction of a hydrogen atom from a co-initiator. Then, electron transfer leads to fragmentation of the initiator where one fragment is a radical.[66] With type II initiators both the initiator and the co-initiator have to be incorporated efficiently in the resin mixture. Due to their unimolecular mechanism, Type I initiators react faster and at lower concentrations.[61] A disadvantage of both Type I and Type II initiators is deactivation by oxygen. Oxygen can inhibit initiation by reacting with the photoinitiator, or it can form a peroxyl radical on a growing polymer chain. Peroxy radicals are very stable, and the chain growth will be virtually stopped as addition of monomers is very slow.[67] By performing the photopolymerization in the absence of oxygen, inhibition can be eliminated.[68] Another possibility is the use of additives to avoid or reinitiate peroxyl radicals.

In the propagation step, polymer chains are formed by successive monomer addition to a growing chain.[63] The chain length increases until chain transfer or termination occurs.[3] In the case of chain transfer, the polymerization continues on another chain. Termination occurs when two radicals combine, either by recombination of two active chains, or by reaction of an active chain with a chain stopper such as initiator radical or oxygen. Termination effectively removes radicals from the system, therefore stopping the polymerization.

If multifunctional monomers (shown in Figure 1.2) are used in a radical polymerization, they act as crosslinkers, forming a large network rather than long linear chains. The chains are now covalently crosslinked, creating a thermosetting polymer. The underlying mechanism of forming a crosslinked network is the same as that of forming linear chains,[69] but there are some important differences with linear polymerization.[70] Unless the system is very dilute, polymerization of multifunctional monomers increases the viscosity of the mixture, until at one point a gel is formed which limits further polymerization.[3,70] The restricted mobility of the radicals present in the gel will slow down the initiation and propagation reaction as the degree of polymerization increases. At some point vitrification will occur.[71] Upon vitrification, the partially cured resin is in the glassy state where the radicals are unable to react with monomer as they are trapped in the glass or bound to the network.[72] When the temperature is increased above the glass transition temperature (T_g), the chains regain their molecular mobility and polymerization can proceed, leading to an increase in conversion and therefore crosslink density,[73] and a higher T_g.[74] For this reason, thermally treating photopolymerization products can strongly influence the final mechanical properties and are often applied to produce products with uniform properties.[28,75] Even above T_g, conversion of networks is limited. Generally, conversion does not reach values above 90% for difunctional monomers, and 52% when using trifunctional monomers.[76]

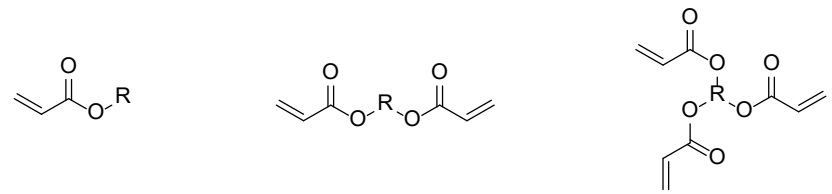

Figure 1.2. Schematic structure of a mono-, di-, and tri-acrylate.

1.4 Shrinkage stress

Polymerization of multifunctional (meth)acrylates into a highly crosslinked network is often accompanied by stress development due to volumetric shrinkage.[44,77] Shrinkage is the largest shortcoming in stereolithography,[78] and is an unavoidable result of the acrylate polymerization.[35] In the liquid monomer, the molecules interact weakly through van der Waals forces, which define the intermolecular distance.[79] During the polymerization, covalent bonds are formed, which are shorter than the van der Waals distances between monomers in the initial mixture. The density will increase and volumetric shrinkage will occur.[42,78] Furthermore, energy dissipation through material flow is inhibited by crosslinks, causing the stress to build in the material.[80,81] The shrinkage-induced stress can cause creep distortions or crack formation, leading to premature material failure.[82] Several methods towards reducing the volumetric shrinkage in (meth)acrylic systems have been investigated.

One approach is the use of composite materials, where inorganic fillers are added to the acrylic polymer matrix.[83] The filler particles do not contract upon matrix polymerization and will not contribute to shrinkage. The volume fraction occupied by fillers will be constant, and prevent the decrease of intermolecular distances during network formation. Munksgaard *et al*. found that large (65% v/v) amounts of filler particles are required to effectively reduce the shrinkage.[84] An additional effect of the use of fillers, is the change in properties of the final materials. In general, composite materials are harder and have an increased tensile strength.[85] Unfortunately, the use of fillers may not be suitable for stereolithography, because of possible inhomogeneities in the system as a result of sedimentation of the particles.[86]

Adjusting the resin composition also has a significant effect on the shrinkage stress, for instance the bulkiness of the monomers. Gonzales *et al.* found that by changing the ratios of Bis-GMA:TEGDMA (Figure 1.3) in a network from 3:7 to 7:3, the stress was reduced by up to 44 ± 0.5%.[87] Chains containing TEGDMA tend to pack closely, due to their flexible backbones and lack of bulky groups, increasing shrinkage. Consequently, a decrease in the TEGDMA content in these materials reduced the stress. However, an increase in Bis-GMA content in the material led to a decrease in conversion as Bis-GMA has a high viscosity and reduced flexibility.

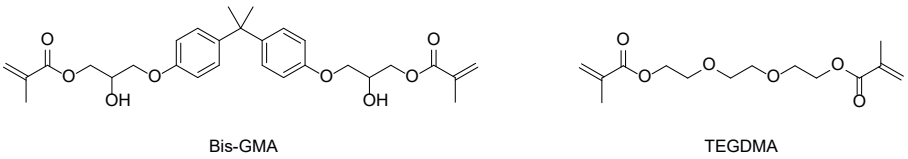

Figure 1.3. Structure of Bis-GMA and TEGDMA monomers.

This work is in accordance with the work of Kim *et al.* where Bis-GMA derivates with additional bulky side groups were synthesized.[88] The side groups increased the steric hindrance and created more free volume in the monomer solution which was retained in the polymer, leading to a reduction in volumetric shrinkage by 50%.

Molecular weight of diacrylate monomers is another parameter that may be optimized to limit stress formation. Increasing monomer molecular weight reduces the initial double bond concentration in the system, hereby reducing the shrinkage, as each C=C to C-C bond conversion results in a volumetric shrinkage of 23 cm^3/mol.[89] Trujillo-Lemon *et al.* used various dimethacrylate derivatives of a fatty acid to produce photopolymerized networks. All of these materials had extremely high conversions, with lower shrinkages than other tested acrylates. In particular, one of the fatty acid-dimethacrylate derivatives (DA-II) produced a network with acrylate conversion of 94 ± 2% with volume shrinkage of 2.4%. compared to a conversion of 65 ± 2% with volume shrinkage of 10.2% for Bis-GMA, under the same curing conditions.[90] However, other mechanical properties of this material, such as modulus and flexural strength, were poor compared to the material prepared with Bis-GMA. This would make the commercial use of this material unviable.

1.5 Dynamic covalent chemistry

It is clear that the ability to reduce volumetric shrinkage stress in photocurable (meth)acrylates would be highly advantageous. However, current methods to reduce shrinkage are not suitable for stereolithography, because changing the monomer composition lowers conversion and increases viscosity, while the use of fillers often results in an inhomogeneous resin.
An alternative, less explored approach is the use of covalent adaptable networks (CANs).[91] In recent years, CANs have been gaining attention as a third class of polymeric materials that bridge the gap between thermosets and thermoplastics.[92–94] By introducing reversible crosslinks in a thermoset material, enhanced properties such as reshapability,[95] recyclability,[95,96] self-healing,[97] or stress relaxation can be obtained.[96,98] These polymer networks contain specially designed reversible covalent bonds. Depending on the nature of the bond, a stimulus such as light,[99] temperature,[100] or pH,[101] triggers the reversibility of the bond. Based on their mechanism, CANs can be categorized in two groups being either reversible addition networks or reversible exchange networks.[92]

Reversible addition rearrangement is a dissociative process, in which first an existing bond is broken and then a new one is formed. This process is schematically illustrated in Figure 1.4. It is clear from this schematic picture that during the transition there is a temporary decrease in network connectivity and crosslink density.

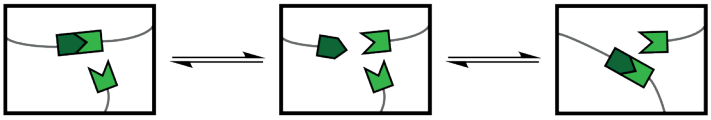

Figure 1.4. Dissociative exchange reaction where first the old bond is broken and in the second step a bond is reformed.

With reversible exchange rearrangements, there is no decrease in crosslink density as for these systems the sequence of events is exactly the opposite. First a new bond is formed leading to an intermediate state without decreased connectivity, then the old bond is broken. This is schematically illustrated in Figure 1.5.

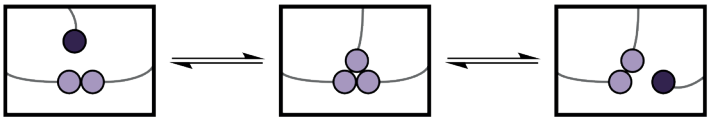

Figure 1.5. Associative exchange reaction, a new bond is formed prior to bond breakage.

When studying the frequency dependent flow of networks with rheology, it should in principle be easy to distinguish between both mechanisms by studying the rubber plateau. For a classical thermoset, the rubber plateau has a constant value which depends on the crosslink density of the material.[102] This plateau is independent of the frequency, and the temperature at which the measurement is performed. For a reversible addition rearrangement (dissociative), the plateau modulus is strongly dependent on the temperature, Figure 1.6. When the temperature is increased, some crosslinks dissociate, yielding a lower rubber plateau. Similar to permanent networks, reversible exchange networks (associative) have a rubber plateau modulus which is relatively independent of the absolute temperature during the measurement, as the crosslink density of the system is constant Figure 1.6. However, in contrast to permanent networks, both these systems will flow at low frequencies due to exchange reactions on the timescale of the experiment.[92]

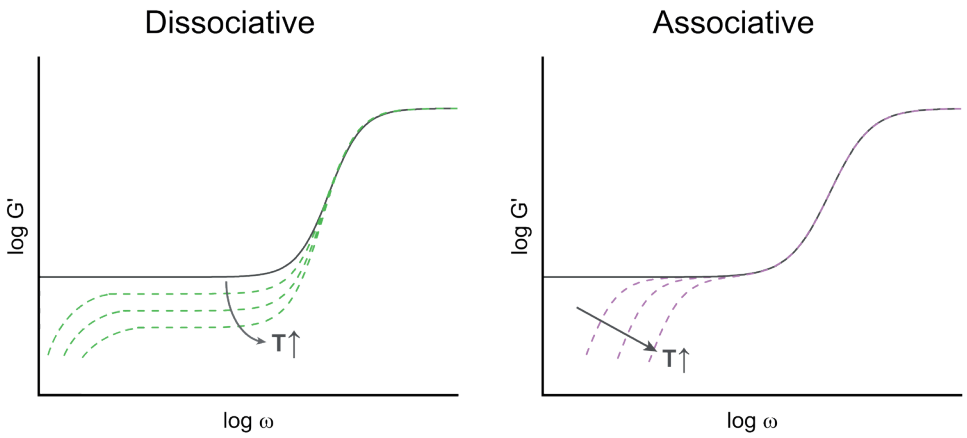

Figure 1.6. The modulus versus frequency for an ideal thermoset (grey line), compared to reversible crosslinked networks. Left a dissociative network (green dashes) and on the right an associative network (purple dashes).

As CANs undergo bond rearrangement, stressed chains can adopt more favorable configurations, leading to the relief of stresses. As the reversible bonds are part of the network, the rearrangements would occur through the material and with full reformation there would be no degradation of the network. Several stress relaxing systems for photopolymers have been reported in the literature.

Bowman *et al.* developed several controllable reversible addition-fragmentation (CRAFT) compounds which show efficient stress relaxation of acrylate networks.[98,99,103] The synthesized acrylic CRAFT monomers can either be used in an completely acrylic resin or copolymerized with thiols. Most efficient stress relaxation was observed in the thiol-acrylate system. Stress relaxation by CRAFT is radical mediated and is switched on upon exposure to UV light at ambient temperature. Radicals that are generated during or after polymerization first bind to the reactive center of the trithiocarbonate based CRAFT monomer, after which a rearrangement causes another substituent from the CRAFT monomer to be expelled as an active radical again (Scheme 1.2). This process leads to chain rearrangements and stress relaxation.

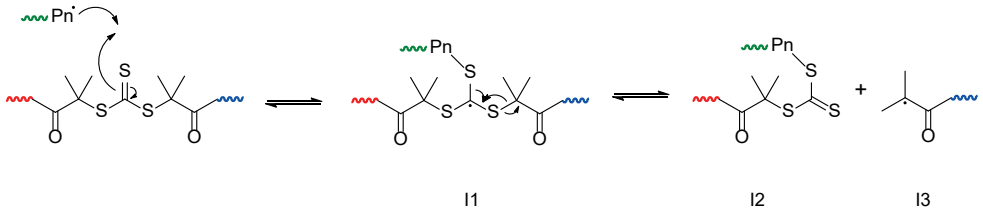

Scheme 1.2. Radical-mediated AFT bond-exchange mechanism.[99]

Another well investigated approach towards stress relaxation involves transesterification between ester bonds and free hydroxyl groups. This was first introduced by Leibler *et al.* in 2011 using an epoxy network (Figure 1.7).[95] By addition of zinc acetate to the covalently crosslinked polyester, so called 'vitrimers' were produced. This material is insoluble but above a certain temperature it behaves like a thermoplast and the materials can be recycled, reshaped and repaired. The system also shows stress relaxation with a characteristic relaxation time of ~58 hours at 100 °C.

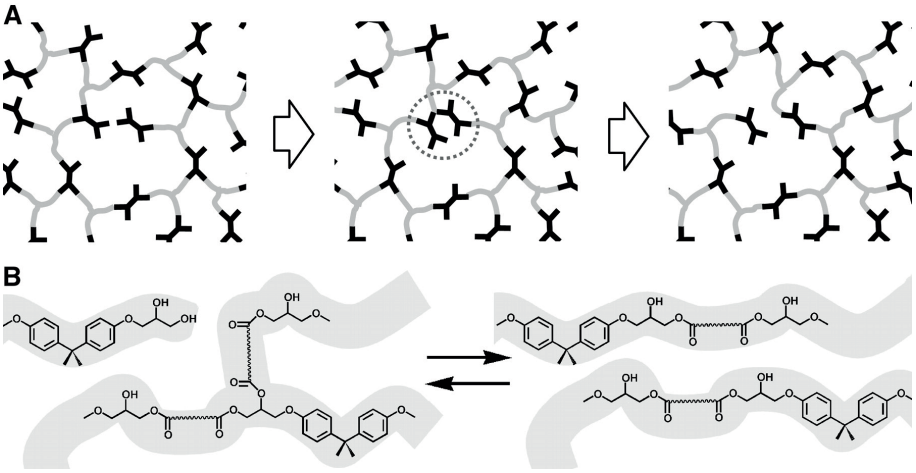

Figure 1.7. Transesterification in polyester epoxy resins as described by Leibler. (A) schematic representation and (B) a close up of the molecular rearrangements. From: Science, Vol 334, Issue 6058. Reprinted with permission from AAAS.[95]

The same strategy was used by Zhang *et al.* to develop reprocessable thermosets for stereolithography.[104] Acrylic monomers containing hydroxyl groups (Figure 1.8) were photo cured in the presence of zinc acetylacetonate hydrate as transesterification catalyst. The material could be reprocessed, repaired and reshaped at elevated temperatures, and 3D structures could be printed.

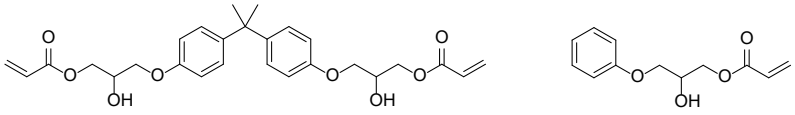

Figure 1.8. Bisphenol A glycerolate diacrylate and 2-hydroxy-3-phenoxypropyl acrylate monomers used for the reprocessable thermoset.[104]

1.6 Aim and outline of this thesis

The objective of the research presented in this thesis is to explore the potential of dynamic covalent chemistry to reduce stress in photopolymerizable acrylates. To achieve this aim, a variety of monomers are selected and synthesized. Subsequently, polymer samples are produced, and their mechanical properties and ability to relax stresses are investigated. The focus is on acrylic monomers, since these show great potential in fast stereolithographic printing applications. Three chemical strategies towards exchangeable bonds are reported. In all these systems, the reversibility is triggered by an increase in temperature, since thermal postcuring treatments are often part of the standard production process for photopolymerizations.

In Chapter 2, a monomer containing a thermally reversible Diels-Alder group is synthesized and copolymerized into polymer films via UV curing. Thin films are used to simulate a single layer in a stereolithographic printer. The reversibility of the Diels-Alder groups is studied in detail. Moreover, the mechanical properties of the Diels-Alder polymers after thermal stress relaxation are compared with a chemically similar non-reversible system.

During the optimization of the photopolymerization process, interesting additional curing is observed when samples are subjected to DMTA experiments. The origin of this curing is studied in more detail and the results are presented in Chapter 3.

Chapter 4 describes the use of transalkylation chemistry as reversible crosslinks. This system is much less known than the previously discussed Diels-Alder chemistry, and it is still not completely clear if the reaction follows a dissociative or an associative pathway. Kinetic studies are performed using ^{1}H NMR to investigate the potential of DABCO and gain more insight in the mechanism. Following the kinetic study, the designed system is incorporated in a polymeric material and the stress relaxation behavior is studied.

The fifth and last experimental chapter describes the use of self-catalyzed transesterification reactions towards reversible networks. A linear polymer with hydroxyl side groups is reacted with pyromellitic dianhydride, yielding a crosslinked network. Networks with and without abundant free hydroxyl groups are prepared and the reversibility is evaluated by stress relaxation experiments.

Finally, in Chapter 6, the different approaches toward reversible networks are compared and the relevance to industry is described.

1.7 References

(1) Namazi, H. Polymers in Our Daily Life. *BioImpacts* **2017**, *7* (2), 73–74.

(2) Plastics-Europe. Plastics – the Facts 2018 https://www.plasticseurope.org/application/files/6315/4510/9658/Plastics_the_facts_2018_AF_web.pdf.

(3) Young, R. J.; Lovell, P. A. *Introduction to Polymers*; CRC press, 2011.

(4) Vlachopoulos, J.; Strutt, D. Polymer Processing. *Mater. Sci. Technol.* **2003**, *19* (9), 1161–1169.

(5) Andrews, M.; Tamboukou, M. Handbook of Thermoset Plastics 2nd Ed - S. Goodman (Noyes, 1998) WW.Pdf. **2013**, 0–26.

(6) Herrera, F. A. Thermoplastic and Thermoset Processing Methods. *Cienc. los polímeros* **2014**, 1–5.

(7) W. Peng and B. Riedl. Thermosetting Resins. *J. Chem. Educ.* **1995**, *72* (7), 587–592.

(8) Kamal, M. R. Thermoset Characterization for Moldability Analysis. *Polym. Eng. Sci.* **1974**, *14* (3), 231–239.

(9) Kamal, M. R.; Ryan, M. E. The Behavior of Thermosetting Compounds in Injection Molding Cavities. *Polym. Eng. Sci.* **1980**, *20* (13), 859–867.

(10) Pîrjan, A.; Petroşanu, D.-M. The Impact of 3D Printing Technology on the Society and Economy. *J. Inf. Syst. Oper. Manag.* **2013**, *7* (2), 360–370.

(11) Sossou, G.; Demoly, F.; Montavon, G.; Gomes, S. An Additive Manufacturing Oriented Design Approach to Mechanical Assemblies. *J. Comput. Des. Eng.* **2018**, *5* (1), 3–18.

(12) Wong, K. V.; Hernandez, A. A Review of Additive Manufacturing. *ISRN Mech. Eng.* **2012**, *2012*, 1–10.

(13) ALL3DP. 3D Printing Technology Guide https://all3dp.com/1/types-of-3d-printers-3d-printing-technology/.

(14) Ligon, S. C.; Liska, R.; Stampfl, J.; Gurr, M.; Mülhaupt, R. Polymers for 3D Printing and Customized Additive Manufacturing. *Chem. Rev.* **2017**, *117* (15), 10212–10290.

(15) Kumbhar, N. N.; Mulay, A. V. Post Processing Methods Used to Improve Surface Finish of Products Which Are Manufactured by Additive Manufacturing Technologies: A Review. *J. Inst. Eng. Ser. C* **2018**, *99* (4), 481–487.

(16) Hofmann, M. 3D Printing Gets a Boost and Opportunities with Polymer Materials. *ACS Macro Lett.* **2014**, *3* (4), 382–386.

(17) Monzón, M.; Ortega, Z.; Hernández, A.; Paz, R.; Ortega, F. Anisotropy of Photopolymer Parts Made by Digital Light Processing. *Materials (Basel).* **2017**, *10* (1), 1–15.

(18) Kotlinski, J. Mechanical Properties of Commercial Rapid Prototyping Materials. *Rapid Prototyp. J.* **2014**, *20* (6), 499–510.

(19) Masood, S. H.; Song, W. Q. Development of New Metal/Polymer Materials for Rapid Tooling Using Fused Deposition Modelling. *Mater. Des.* **2004**, *25* (7), 587–594.

(20) Stampfl, J.; Baudis, S.; Heller, C.; Liska, R.; Neumeister, A.; Kling, R.; Ostendorf, A.; Spitzbart, M. Photopolymers with Tunable Mechanical Properties Processed by Laser-Based High-Resolution Stereolithography. *J. Micromechanics Microengineering* **2008**, *18* (12).

(21) Tumbleston, J. R.; Shirvanyants, D.; Ermoshkin, N.; Janusziewicz, R.; Johnson, A. R.; Kelly, D.; Chen, K.; Pinschmidt, R.; Rolland, J. P.; Ermoshkin, A.; et al. Continuous Liquid Interface Production of 3D Objects. *Science.* **2015**, *347* (6228), 1349–1352.

(22) Jorge Bártolo, P. Stereolithographic Processes. In *Stereolithography: Materials, Processes and Applications*; Jorge Bártolo, P., Ed.; Springer New York, 2011; pp 1–36.

(23) International Organization for Standardization. Additive Manufacturing—General Principles—Terminology. ISO/ASTM 52900, 2015.

(24) E. Selli, E.; Bellobono, I. R. Photopolymerization of Multifunctional Monomers: Kinetic Aspects. In *Radiation curing in polymer science and technology, Vol. III: Polymerisation mechanisms*; Fouassier, J.P.; Rabek, J. F., Ed.; Elsevier Science Publishers, London, 1993.

(25) Davis, F. J.; Mitchell, G. R. Polymeric Materials for Rapid Manufacturing. In *Stereolithography: Materials, Processes and Applications*; Bártolo, P. J., Ed.; Springer US: Boston, MA, 2011; pp 113–139.

(26) Peele, B. N.; Wallin, T. J.; Zhao, H.; Shepherd, R. F. 3D Printing Antagonistic Systems of Arti Fi Cial Muscle Using Projection Stereolithography. *Bioinspir. Biomim.* **2015**, *10*.

(27) Hull, C. W.; Arcadia, C. Apparatus for Production of Three-Dmensional Objects By Stereolthography . *Appar. Prod. Three-Dimensional Objects by Stereolithography* **1984**, No. 19.

(28) Kruth, J. P.; Leu, M. C.; Nakagawa, T. Progress in Additive Manufacturing and Rapid Prototyping. *CIRP Ann. - Manuf. Technol.* **1998**, *47* (2), 525–540.

(29) Kim, G. D.; Oh, Y. T. A Benchmark Study on Rapid Prototyping Processes and Machines: Quantitative Comparisons of Mechanical Properties, Accuracy, Roughness, Speed, and Material Cost. *Proc. Inst. Mech. Eng. Part B J. Eng. Manuf.* **2008**, *222* (2), 201–215.

(30) Melchels, F. P. W.; Feijen, J.; Grijpma, D. W. A Review on Stereolithography and Its Applications in Biomedical Engineering. *Biomaterials* **2010**, *31* (24), 6121–6130.

(31) Mankovich, N. J.; Cheeseman, A. M.; Stoker, N. G. The Display of Three-Dimensional Anatomy with Stereolithographic Models. *J. Digit. Imaging* **1990**, *3* (3), 200–203.

(32) Binder, T. M.; Moertl, D.; Mundigler, G.; Rehak, G.; Franke, M.; Delle-Karth, G.; Mohl, W.; Baumgartner, H.; Maurer, G. Stereolithographic Biomodeling to Create Tangible Hard Copies of Cardiac Structures from Echocardiographic Data. *J. Am. Coll. Cardiol.* **2002**, *35* (1), 230–237.

(33) Dehurtevent, M.; Robberecht, L.; Hornez, J. C.; Thuault, A.; Deveaux, E.; Béhin, P. Stereolithography: A New Method for Processing Dental Ceramics by Additive Computer-Aided Manufacturing. *Dent. Mater.* **2017**, *33* (5), 477–485.

(34) NextDent. Leading Dental Materials for 3D Printing https://nextdent.com/.

(35) Corbel S., Dufaud O., R.-C. T. Materials for Stereolithography. In *Stereolithography*; Bártolo P., Ed.; Springer US, 2011.

(36) Dartnall, H. J. A. Photosensitivity. In *Photochemistry of Vision. Handbook of Sensory Physiology*; Abrahamson, E. W., Baumann, C., Bridges, C. D. B., Crescitelli, F., Dartnall, H. J. A., Eakin, R. M., Falk, G., Fatt, P., Goldsmith, T. H., Hara, R., et al., Eds.; Springer Berlin Heidelberg: Berlin, Heidelberg, 1972; pp 122–145.

(37) Fouassier, J. P.; Lalevée, J. Efficiency of a Photopolymerization Reaction. In *Photoinitiators for Polymer Synthesis: Scope, Reactivity and Efficiency*; 2012; pp 103–122.

(38) Moussa, K.; Decker, C. Light-Induced Polymerization of New Highly Reactive Monomers. **1946**, *055* (1944), 2197–2203.

(39) Bird, D.; Caravaca, E.; Laquidara, J.; Luhmann, K.; Ravindra, N. M. Formulation of Curable Resins Utilized in Stereolithography. In *BT - TMS 2019 148th Annual Meeting & Exhibition*; Springer International Publishing: Cham, 2019; pp 1575–1587.

(40) Andrews, E. H. Structure-Property Relationships in a Polymer. *Int. J. Polym. Mater. Polym. Biomater.* **1973**, *2* (4), 337–359.

(41) Rossi, S.; Puglisi, A.; Benaglia, M. Additive Manufacturing Technologies: 3D Printing in Organic Synthesis. *ChemCatChem* **2018**, *10* (7), 1512–1525.
(42) Decker, C. The Use of UV Irradiation in Polymerization. *Polym. Int.* **1998**, *45* (2), 133–141.
(43) Calvert, P.; Crockett, R. Chemical Solid Free-Form Fabrication: Making Shapes without Molds. *Chem. Mater.* **1997**, *9* (3), 650–663.
(44) Ligon-Auer, S. C.; Schwentenwein, M.; Gorsche, C.; Stampfl, J.; Liska, R. Toughening of Photo-Curable Polymer Networks: A Review. *Polym. Chem.* **2016**, *7* (2), 257–286.
(45) Stampfl, J.; Baudis, S.; Heller, C.; Liska, R.; Neumeister, A.; Kling, R.; Ostendorf, A.; Spitzbart, M. Photopolymers with Tunable Mechanical Properties Processed by Laser-Based High-Resolution Stereolithography. *J. Micromechanics Microengineering* **2008**, *18* (12), 1–9.
(46) Corcione, C. E.; Greco, A.; Maffezzoli, A. Photopolymerization Kinetics of an Epoxy-Based Resin for Stereolithography. *J. Appl. Polym. Sci.* **2004**, *92* (6), 3484–3491.
(47) Janusziewicz, R.; Tumbleston, J. R.; Quintanilla, A. L.; Mecham, S. J.; DeSimone, J. M. Layerless Fabrication with Continuous Liquid Interface Production. *Proc. Natl. Acad. Sci. U. S. A.* **2016**, *113* (42), 11703–11708.
(48) Decker, C.; Nguyen Thi Viet, T.; Decker, D.; Weber-Koehl, E. UV-Radiation Curing of Acrylate/Epoxide Systems. *Polymer (Guildf).* **2001**, *42* (13), 5531–5541.
(49) Konuray, O.; Fernández-Francos, X.; Ramis, X.; Serra, À. State of the Art in Dual-Curing Acrylate Systems. *Polymers (Basel).* **2018**, *10* (2).
(50) Kaur, M.; Srivastava, A. K. Photopolymerization: A Review. *J. Macromol. Sci. - Polym. Rev.* **2002**, *42* (4), 481–512.
(51) *Radiation Curing of Polymeric Materials*; Hoyle, C. E., Kinstle, J. F., Eds.; ACS Symposium Series; American Chemical Society: Washington, DC, 1990; Vol. 417.
(52) Stansbury, J. W. Curing Dental Resins and Composites by Photopolymerization. *J. Esthet. Dent.* **2000**, *12*, 300–308.
(53) Decker, C. Kinetic Study and New Applications of UV Radiation Curing. *Macromol. Rapid Commun.* **2002**, *23* (18), 1067–1093.
(54) Penterman, R.; Klink, S. I.; de Koning, H.; Nisato, G.; Broer, D. J. Single-Substrate Liquid-Crystal Displays by Photo-Enforced Stratification. *Nature* **2002**, *417* (6884), 55–58.
(55) Goss, B. Bonding Glass and Other Substrates with UV Curing Adhesives. *Int. J. Adhes. Adhes.* **2002**, *22* (5), 405–408.
(56) Hancock, A.; Lin, L. Challenges of UV Curable Ink-Jet Printing Inks - A Formulator's Perspective. *Pigment Resin Technol.* **2004**, *33* (5), 280–286.
(57) Decker, C. Light-Induced Crosslinking Polymerization. *Polym. Int.* **2002**, *51* (11), 1141–1150.
(58) Fouassier, J. P.; Allonas, X.; Burget, D. Photopolymerization Reactions under Visible Lights: Principle, Mechanisms and Examples of Applications. *Prog. Org. Coatings* **2003**, *47* (1), 16–36.
(59) Crivello, J. V.; Reichmanis, E. Photopolymer Materials and Processes for Advanced Technologies. *Chem. Mater.* **2014**, *26* (1), 533–548.
(60) Broer, D. J.; Haaren, J. A. M. M. Van; Lub, J. Liquid Crystal Polymers and Networks for Display Applications. In *Proceedings Volume 4107, Liquid Crystals IV*; 2000; Vol. 4107.
(61) Gruber, H. F. Photoinitiators for Free Radical Polymerization. *Prog. Polym. Sci.* **1992**, *17* (6), 953–1044.

(62) Pan, Y., Zhou, C.; Chen, Y. Rapid Manufacturing in Minutes: The Development of a Mask Projection Stereolithography Process for High-Speed Fabrication. In *Proceedings of the ASME 2012 International Manufacturing Science and Engineering Conferences MSEC2012*; 2012; pp 1–10.

(63) Odian, G. Radical Chain Polymerization. In *Principles of Polymerization*; John Wiley & Sons, Ltd, 2004; pp 198–349.

(64) Norrish, R. G. W.; Bamford, C. H. Photodecomposition of Aldehydes and Ketones. *Nature* **1936**, *138* (3502), 1016.

(65) Scaiano, J. C.; Stamplecoskie, K. G.; Hallett-Tapley, G. L. Photochemical Norrish Type i Reaction as a Tool for Metal Nanoparticle Synthesis: Importance of Proton Coupled Electron Transfer. *Chem. Commun.* **2012**, *48* (40), 4798–4808.

(66) Davidson, R. S.; Dias, A. A.; Illsley, D. A New Series of Type II (Benzophenone) Polymeric Photoinitiators. *J. Photochem. Photobiol. A Chem.* **1995**, *89* (1), 75–87.

(67) O'Brien, A. K.; Bowman, C. N. Impact of Oxygen on Photopolymerization Kinetics and Polyme Structure. *Macromolecules* **2006**, *39* (7), 2501–2506.

(68) Ligon, S. C.; Husár, B.; Wutzel, H.; Holman, R.; Liska, R. Strategies to Reduce Oxygen Inhibition in Photoinduced Polymerization. *Chem. Rev.* **2014**, *114* (1), 557–589.

(69) Andrzejewska, E. Photopolymerization Kinetics of Multifunctional Monomers. *Prog. Polym. Sci.* **2001**, *26* (4), 605–665.

(70) Decker, C. Photoinitiated Crosslinking Polymerisation. *Prog. Polym. Sci.* **1996**, *21* (4), 593–650.

(71) Fraga, I.; Montserrat, S.; Hutchinson, J. M. Vitrification during the Isothermal Cure of Thermosets : Part I. An Investigation Using TOPEM, a New Temperature Modulated Technique. *J. Therm. Anal. Calorim.* **2008**, *91* (3), 687–695.

(72) Cook, W. D.; Scott, T. F.; Quay-Thevenon, S.; Forsythe, J. S. Dynamic Mechanical Thermal Analysis of Thermally Stable and Thermally Reactive Network Polymers. *J. Appl. Polym. Sci.* **2004**, *93* (3), 1348–1359.

(73) Lecamp, L.; Youssef, B.; Bunel, C.; Lebaudy, P. Photoinitiated Polymerization of a Dimethacrylate Oligomer: 1. Influence of Photoinitiator Concentration, Temperature and Light Intensity. *Polymer (Guildf).* **1997**, *38* (25), 6089–6096.

(74) Lovell, L. G.; Lu, H.; Elliott, J. E.; Stansbury, J. W.; Bowman, C. N. The Effect of Cure Rate on the Mechanical Properties of Dental Resins. *Dent. Mater.* **2001**, *17* (6), 504–511.

(75) Baxter, R.; Hastings, N.; Law, A.; Glass, E. J. . *Stereolithography; Materials, Processes and Applications*; 2008; Vol. 39.

(76) Hoyle, C. E. Calorimetric Analysis of Photopolymerization. In *Radiation Curing: Science and Technology*; Pappas, S. P., Ed.; Springer US: Boston, MA, 1992; pp 57–133.

(77) Francis, L. F.; Mccormick, A. V; Vaessen, D. M.; Payne, J. A. Development and Measurement of Stress in Polymer Coatings. *J. Mater. Sci.* **2002**, *37* (22), 4717–4731.

(78) Karalekas, D.; Aggelopoulos, A. Study of Shrinkage Strains in a Stereolithography Cured Acrylic Photopolymer Resin. *J. Mater. Process. Technol.* **2003**, *136* (1–3), 146–150.

(79) Batsanov, S. *Van Der Waals Radii of Elements*; 2001; Vol. 37.

(80) Schneider, L. F. J.; Cavalcante, L. M.; Silikas, N. Shrinkage Stresses Generated during Resin-Composite Applications: A Review. *J. Dent. Biomech.* **2010**, *1* (1), 1–14.

(81) Rueggeberg, F.; Tamareselvy, K. Resin Cure Determination by Polymerization Shrinkage. *Dent. Mater.* **1995**, *11* (4), 265–268.

(82) Ringsberg, J. W.; Ulfvarson, A. Y. J. On Mechanical Interaction between Steel and Coating in Stressed and Strained Exposed Locations. *Mar. Struct.* **1998**, *11* (6), 231–250.

(83) Chen, H. Y.; Manhart, J.; Hickel, R.; Kunzelmann, K. H. Polymerization Contraction Stress in Light-Cured Packable Composite Resins. *Dent. Mater.* **2001**, *17* (3), 253–259.

(84) Munksgaard, E. C.; Hansen, E. K.; Kato, H. Wall-to-wall Polymerization Contraction of Composite Resins versus Filler Content. *Eur. J. Oral Sci.* **1987**, *95* (6), 526–531.

(85) Chunk, K. H.; Greener, E. H. Correlation between Degree of Conversion, Filler Concentration and Mechanical Properties of Posterior Composite Resins. *J. Oral Rehabil.* **1990**, *17* (5), 487–494.

(86) Torres-Filho, A.; Neckers, D. C. Mechanical Properties of Acrylate Networks Formed by Visible Laser-Induced Polymerization. 2. Control of the Mechanical Properties. *Chem. Mater.* **1995**, *7* (4), 744–753.

(87) Gonalves, F.; Azevedo, C. L. N.; Ferracane, J. L.; Braga, R. R. BisGMA/TEGDMA Ratio and Filler Content Effects on Shrinkage Stress. *Dent. Mater.* **2011**, *27* (6), 520–526.

(88) Kim, Y.; Kim, C. K.; Cho, B. H.; Son, H. H.; Um, C. M.; Kim, O. Y. A New Resin Matrix for Dental Composite Having Low Volumetric Shrinkage. *J. Biomed. Mater. Res. - Part B Appl. Biomater.* **2004**, *70* (1), 82–90.

(89) Loshaek, S.; Fox, T. G. Cross-Linked Polymers. I. Factors Influencing the Efficiency of Cross-Linking in Copolymers of Methyl Methacrylate and Glycol Dimethacrylates. *J. Am. Chem. Soc.* **1953**, *75* (14), 3544–3550.

(90) Trujillo-Lemon, M.; Ge, J.; Lu, H.; Tanaka, J.; Stansbury, J. W. Dimethacrylate Derivatives of Dimer Acid. *J. Polym. Sci. Part A Polym. Chem.* **2006**, *44* (12), 3921–3929.

(91) Kloxin, C. J.; Scott, T. F.; Adzima, B. J.; Bowman, C. N. Covalent Adaptable Networks (CANs): A Unique Paradigm in Cross-Linked Polymers. *Macromolecules* **2010**, *43* (6), 2643–2653.

(92) Kloxin, C. J.; Bowman, C. N. Covalent Adaptable Networks: Smart, Reconfigurable and Responsive Network Systems. *Chem. Soc. Rev.* **2013**, *42* (17), 7161–7173.

(93) Denissen, W.; Winne, J. M.; Du Prez, F. E. Vitrimers: Permanent Organic Networks with Glass-like Fluidity. *Chem. Sci.* **2015**, *7* (1), 30–38.

(94) Zou, W.; Dong, J.; Luo, Y.; Zhao, Q.; Xie, T. Dynamic Covalent Polymer Networks: From Old Chemistry to Modern Day Innovations. *Adv. Mater.* **2017**, *29* (14).

(95) Montarnal, D.; Capelot, M.; Tournilhac, F.; Leibler, L. Silica-like Malleable Materials from Permanent Organic Networks. *Science* **2011**, *334* (6058), 965–968.

(96) Denissen, W.; Rivero, G.; Nicolaÿ, R.; Leibler, L.; Winne, J. M.; Du Prez, F. E. Vinylogous Urethane Vitrimers. *Adv. Funct. Mater.* **2015**, *25* (16), 2451–2457.

(97) Chen, X. A Thermally Re-Mendable Cross-Linked Polymeric Material. *Science.* **2002**, *295* (5560), 1698–1702.

(98) Wydra, J. W.; Fenoli, C. R.; Cramer, N. B.; Stansbury, J. W.; Bowman, C. N. Influence of Small Amounts of Addition-Fragmentation Capable Monomers on Polymerization-Induced Shrinkage Stress. *J. Polym. Sci. Part A Polym. Chem.* **2014**, *52* (9), 1315–1321.

(99) Fenoli, C. R.; Wydra, J. W.; Bowman, C. N. Controllable Reversible Addition-Fragmentation Termination Monomers for Advances in Photochemically Controlled Covalent Adaptable Networks. *Macromolecules* **2014**, *47* (3), 907–915.

(100) Brutman, J. P.; Delgado, P. A.; Hillmyer, M. A. Polylactide Vitrimers. *ACS Macro Lett.* **2014**, *3* (7), 607–610.

(101) Chakma, P.; Konkolewicz, D. Dynamic Covalent Bonds in Polymeric Materials. *Angew. Chemie Int. Ed.* **2019**, No. 58, 9682–9695.

(102) Kuang, X.; Liu, G.; Dong, X.; Wang, D. Correlation between Stress Relaxation Dynamics and Thermochemistry for Covalent Adaptive Networks Polymers. *Mater. Chem. Front.* **2017**, *1* (1), 111–118.

(103) Scott, T. F. Photoinduced Plasticity in Cross-Linked Polymers. *Science.* **2005**, *308* (5728), 1615–1617.

(104) Zhang, B.; Kowsari, K.; Serjouei, A.; Dunn, M. L.; Ge, Q. Reprocessable Thermosets for Sustainable Three-Dimensional Printing. *Nat. Commun.* **2018**, *9* (1831).

Chapter 2

Stress relaxation via Diels-Alder reactions

Abstract: The use of thermally reversible Diels-Alder groups as a method to compensate for the shrinkage stress in UV curable acrylate monomers was investigated. For this purpose, a Diels-Alder containing monomer was synthesized and successfully incorporated in a polymer network. Upon heating the polymer above 150 °C, the Diels-Alder bonds open. The mechanical properties of the material after shrinkage compensation were investigated with tensile testing. The designed system performs better at the higher strain rates that are prevalent in load bearing applications.

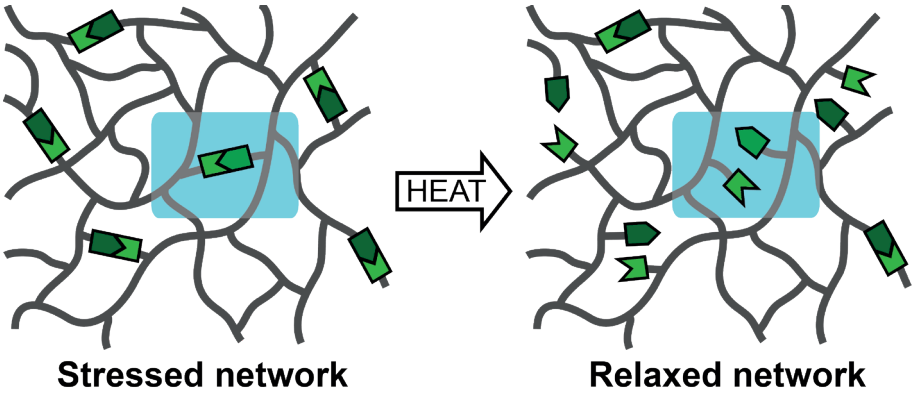

2.1 Introduction

A Diels-Alder reaction is a [4+2]-cycloaddition of an electron rich diene and an electron poor dienophile, yielding a cyclohexene adduct, Scheme 2.1.[1] Although the adduct is often more stable than the reactants, most Diels-Alder reactions are thermoreversible.[2] The substituents present on the diene and the dienophile strongly influence the speed of the reaction.[3] Since many reversible Diels-Alder reactions have a low activation energy, these reactions can be used as reversible crosslinks in polymeric materials without addition of a catalyst. As a thermal treatment is often part of the production process for photopolymers,[4] the Diels-Alder moieties will be activated at that stage.

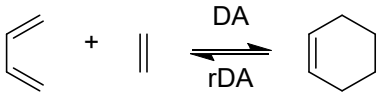

Scheme 2.1. The simplest possible (retro)Diels-Alder reaction of 1,3-butadiene and ethene.

Several examples of the use of Diels-Alder adducts in polymer chemistry can be found in literature,[5,6] with furan-maleimide adducts (Scheme 2.2) being among the most popular ones.[7,8] The electron withdrawing carbonyl substituents on the maleimide make the dienophile more electron-poor and therefore more reactive. The furan-maleimide adduct also has a relatively low (≥110 °C) dissociation temperature.[9] The kinetics of the system are well studied,[10–12] and many interesting applications such as self-healing or recyclability have been reported.

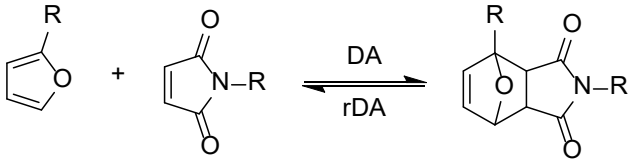

Scheme 2.2. The (retro)Diels-Alder reaction between of furan and maleimide.

One of the first examples of a self-healing material based on the furan-maleimide Diels-Alder reaction was by Wudl *et al*.[13] They used a monomer with four furan groups, and a monomer with three maleimide groups to form a highly crosslinked network. The resulting hard polymeric material was transparent, and showed reversibility for multiple bonding and debonding cycles. A fractured sample was healed by keeping the pieces in contact with each other at 150 °C for two hours, showing recovery of 57% of the original fracture strength. Healing could be repeated multiple times without any surface treatment.
A very similar system was applied by Terryn *et al*.[14] in the development of soft robotics. Using soft materials in robotics is key in the case of dynamic environments such as human interactions. A disadvantage of using soft materials is their susceptibility to damage. By using a material which is crosslinked with Diels-Alder bonds, the life span of soft robotic systems can be increased because cuts and perforations can be healed.

In the previously described self-healing systems, Diels-Alder monomers or oligomers are used to form a polymeric material. Another approach is to covalently crosslink existing polymer chains via Diels-Alder chemistry. This is schematically shown in Scheme 2.3, where

polymer chains with dangling furan groups are crosslinked using a bismaleimide. This crosslinking is reversible upon changing temperature, giving rise to a recyclable thermoset. Using this method, poly(styrene-block-butadiene-block-styrene) polymers with 8 times higher tensile strength could be obtained.[15] Due to the dynamic behavior it is also possible to remold these polymers. The same strategy was also used to create recyclable composites,[16] and recyclable rubbers.[17] Normally, these materials cannot be recycled due to the permanent crosslinks. Using Diels-Alder crosslinks the mechanical properties can be improved without loss of plastic remodeling.

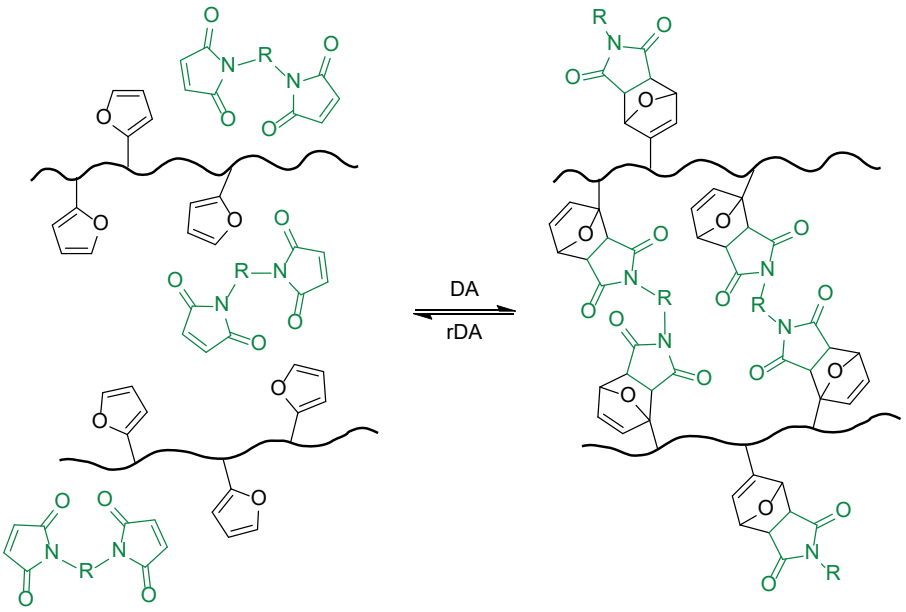

Scheme 2.3. The crosslinking and decrosslinking of polymers via (retro)Diels-Alder reaction of grafted furan groups with bismaleimide.

The use of Diels-Alder adducts to improve material properties has also found its way into 3D printing.[18] Poly(lactic acid), which is used as a bulk printing material for fused filament fabrication, was blended with 10 to 25 wt.% mending agent which contained Diels-Alder groups, prior to filament production. The use of this mending agent could improve the ultimate strength of the materials with 88% when using 10 wt.%. This is due to the fact that the Diels-Alder groups form reversible crosslinks between different printed layers, which strengthens the material.

While reversible Diels-Alder reactions have been used to create self-healing materials, and recyclable thermosets, they have, to the best of our knowledge, never been explored for stress relaxation. In this Chapter, diacrylate monomers containing furan-maleimide Diels-Alder adducts are produced. Polymeric networks containing these monomers are prepared, and the effect of opening of the Diels-Alder adduct on mechanical properties, in particular material lifetime, is studied.

2.2 Monomers

To study the effect of Diels-Alder containing monomers on the material properties, three different diacrylate monomers were used (Figure 2.1). Bisphenol A ethoxylate diacrylate (BPAda, **1**) was used as a benchmark system to characterize the behavior of a highly cured reference (co)polymer network. This monomer was further used in copolymerizations with two different comonomers in a 60:40 (w/w) ratio. First, with a non-reversible analog (NRM, **2**) to investigate the effect of copolymerization on the network properties, and then with the Diels-Alder-group containing monomer (DA, **3**) to investigate the effect of reversible Diels-Alder reactions.

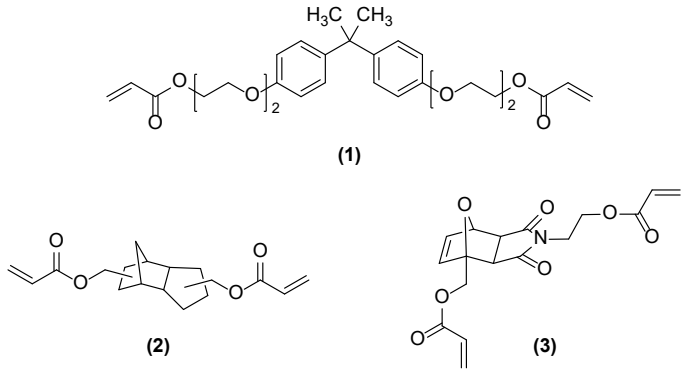

Figure 2.1. Chemical structure of the monomers used: (**1**) BPAda (**2**) NRM (**3**) DA.

The multistep synthetic approach towards the photopolymerizable diacrylate monomer containing a reversible Diels-Alder adduct is presented in Scheme 2.4.[19,20]

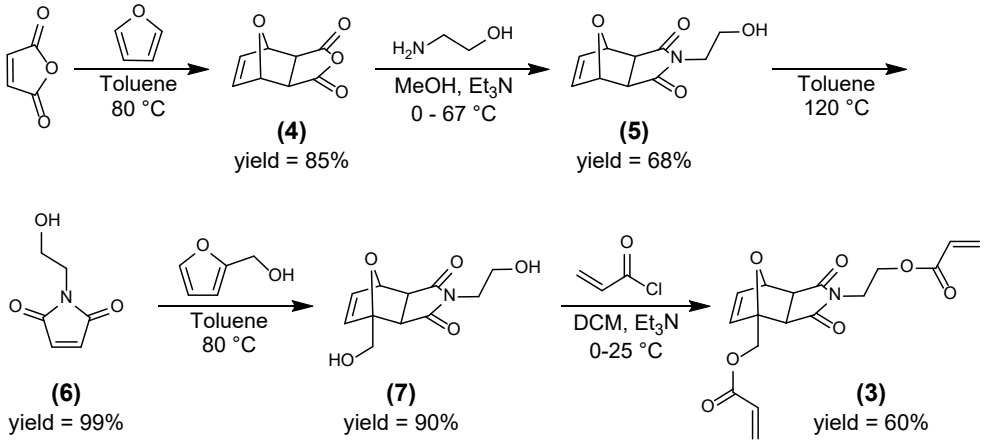

Scheme 2.4. Synthesis of the photopolymerizable monomer (DA) containing a reversible Diels-Alder group.

Maleic anhydride was protected via a Diels-Alder reaction with furan to form compound **4**. With the anhydride protected, amidation of the succinic anhydride was achieved via reaction with amino ethanol. By heating compound **5**, a retro Diels-Alder reaction occurred, and the deprotected maleimide **6** was obtained. This maleimide compound was coupled to furfuryl alcohol to yield compound **7**. In the final step, acrylate groups were attached by reaction with acryloyl chloride. Intermediates **4-7** were not purified. The final product **3** was obtained on a 5 g scale using column chromatography.

2.3 Polymerization

To simulate a single layer in a stereolithographic printer, thin polymer films were prepared via photopolymerization. In order to compare the samples, the UV dose should be kept constant, thus the layer thickness of the sample should be kept constant. Spin coating was used to create thin layers of monomeric resin with a homogeneous thickness. The layer thickness obtained by spin coating strongly depends on the viscosity of the mixture.[21] The viscosities were determined by rheology, the results are depicted in Figure 2.2 below. The resins show Newtonian behavior as the viscosity values are independent on the shear rate used. It is known from previous work that the spin coating process can be described as the coating of a Newtonian liquid on a rotating disk.[22] By assuming that the density of all monomeric solutions is the same, a correction for the viscosity was performed and the correct spin speed for each solution could be obtained.

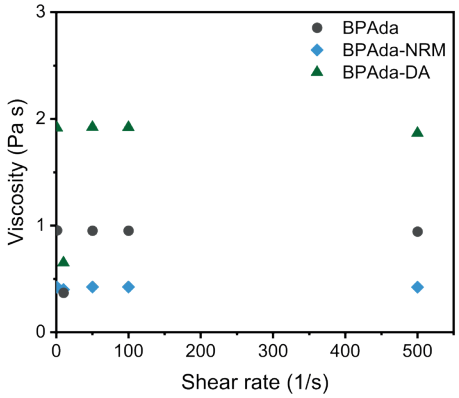

Figure 2.2. The viscosity of the three resins measured at different shear rates. The standard system BPAda (grey circles), reference BPAda-NRM (blue diamonds) and the reversible BPAda-DA (green triangles).

The polymerization conditions were optimized using the BPAda monomer. Samples with 3 wt.% photoinitiator were formulated, which was found to be the optimized amount of photoinitiator.[22] To ensure maximal curing after the photopolymerization, the conversion of the double bonds as a function of irradiation time was studied. The size of each sample was 3x3 cm and the film thickness was kept at ~80 µm. The conversion of the acrylate double bonds and T_g of these samples were determined via FTIR and DSC, respectively. For FTIR, the decrease of the narrow band of the acrylate CH=CH_2 twist vibration at 810 cm^{-1}

was used.[23] The results for the homopolymerization of BPAda are shown in Figure 2.3a. The conversion increased steeply in the first few seconds and reached a plateau after about 50 seconds, after which no further curing seemed to take place. The T_g values obtained from DSC measurements, however, increased more gradually and only seemed to level off after about 150 seconds. Therefore, in subsequent experiments, samples were cured for 200 seconds to ascertain that the plateau conversion was reached.

The effect of comonomers on the conversion rate was investigated with *in situ* FTIR experiments in which a small amount of monomer mixture was irradiated directly on the FTIR crystal (Figure 2.3b). The BPAda-NRM copolymer system showed similar curing behavior as pure BPAda with a plateau conversion of 72%, whereas for the mixture with Diels-Alder monomer the maximum conversion was considerably lower (61%). To increase the conversion and obtain similar values for all three systems, a thermal step was included in the curing protocol. After photo curing, samples were kept in an oven at 180 °C for one hour. For the BPAda and BPAda-NRM systems, the gains in conversion were minimal, from 74% to 79% and from 72% to 78%, respectively. However, the conversion of the BPAda-DA copolymer system increased from 61% to 77%. Thus, by combining 200 seconds of UV irradiation with thermal post curing a consistent and high level of conversion of 78±1% for all three systems was achieved.

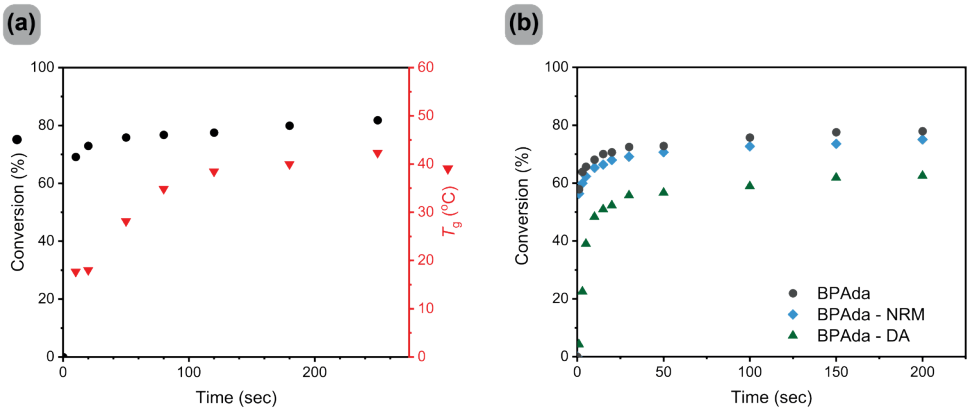

Figure 2.3. (a) Acrylate conversion (black circles) and T_g (red triangles) as a function of radiation time for the UV photopolymerization of BPAda. **(b)** Evolution of conversion over time measured by *in situ* FTIR for the three different resin compositions, the standard system BPAda (grey circles), reference BPAda-NRM (blue diamonds) and the reversible BPAda-DA (green triangles).

2.4 Opening of Diels-Alder groups

In addition to increasing the conversion, heating the polymer samples also activates the Diels-Alder bond in the samples containing DA monomer, as was shown with FTIR (Figure 2.4). A maleimide peak is absent in a UV cured sample, proving the Diels-Alder moieties are stable during the curing process. After the additional thermal treatment, appearance of a distinct maleimide band at 697 cm^{-1} indicates opening of Diels-Alder groups.[24]

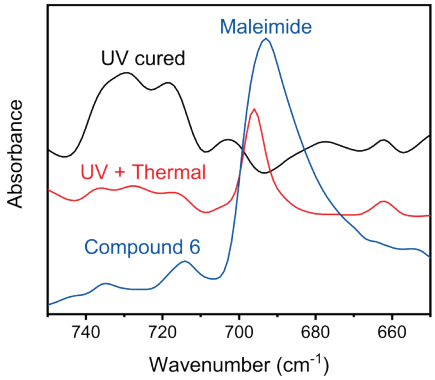

Figure 2.4. FTIR traces of a polymer sample containing DA monomer. A sample which is UV cured (black line), sample which is UV cured and thermally treated (red line). Compound **6** is shown as a reference for maleimide (blue line). The curves are shifted on the y axis for clarification.

Heat effects accompanying the retro Diels-Alder reaction were studied in more detail with DSC directly after the UV curing step (Figures 2.5a-c). In the DSC traces of all three compositions, a small endothermic peak around 50 °C was observed in the first heating cycle, corresponding to the enthalpy relaxation due to sample aging. Only in the DA containing sample (Figure 2.5c) an additional endothermic peak was found in the first heating cycle at ~ 150 °C, which is the temperature at which the retro Diels-Alder reaction of furan–maleimide adducts takes place.[25,26] This result is consistent with the appearance of a maleimide band in IR upon heating of the sample. In consecutive heating cycles, only a small bump was observed at the same temperature in the DSC traces, which hints at only partial Diels-Alder reformation during the cooling of the sample. Similar small peaks around 150 °C were also observed for a DA containing sample after the additional thermal treatment step following the UV curing (Figure 2.5d). The absence of a large endothermic peak, as was observed in the case of the sample before the thermal heating step (Figure 5c), is consistent with the previous results. From this it can be concluded that the heat treatment step following the UV curing leads to the opening of a significant number of Diels-Alder groups, which are only partially reformed during the cooling step of the sample.

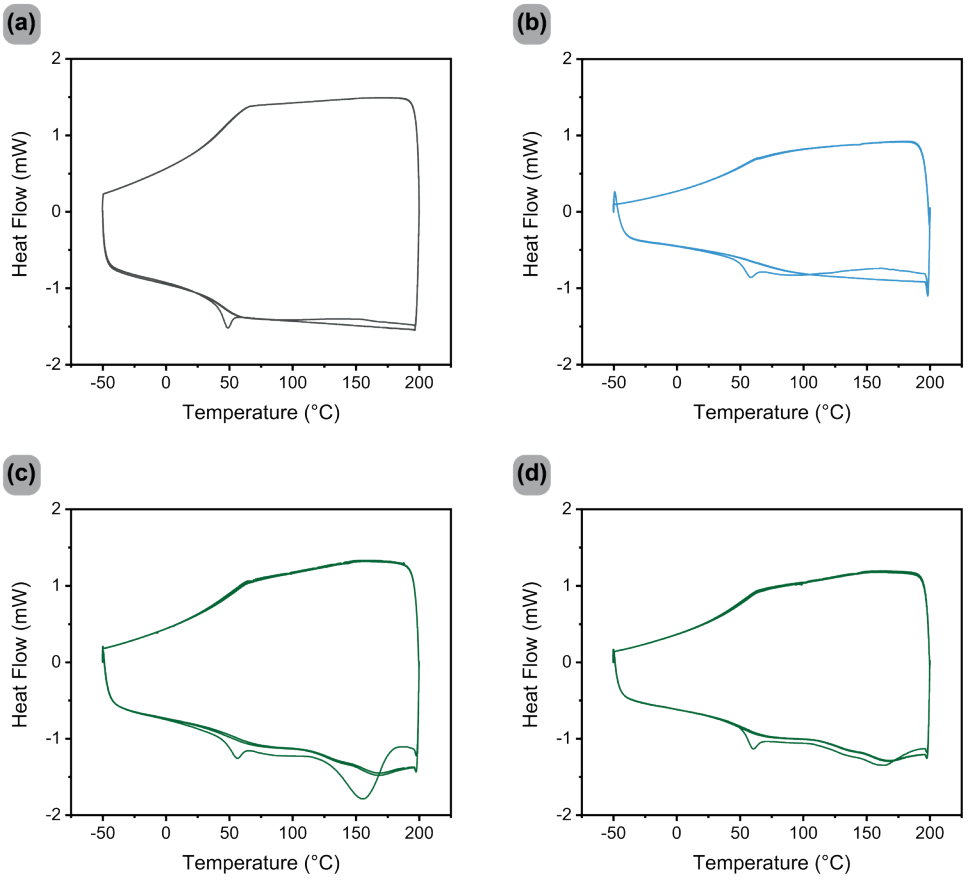

Figure 2.5. DSC data for polymer films after UV curing for 200s: **(a)** BPAda **(b)** BPAda-NRM **(c)** BPAda-DA and **(d)** BPAda-DA after an additional thermal treatment. Three heating/cooling cycles with a rate of 40 °C/min from -50 °C to 200 °C.

It was subsequently attempted to stimulate reformation of the Diels-Alder adduct by introducing annealing steps in the second cooling and fourth heating cycle in DSC measurement, where the temperature was changed at a very low rate between 80 °C and 100 °C (Figure 2.6a). In Figure 2.6b, the DSC traces of these experiments in the relevant temperature range are shown, and to clarify the graph the different cycles are shifted on the y-axis. The annealing steps did not increase the size of the endotherm as the second heating (before the annealing step) and third and fourth heating (after the annealing steps) have very similar peak sizes.

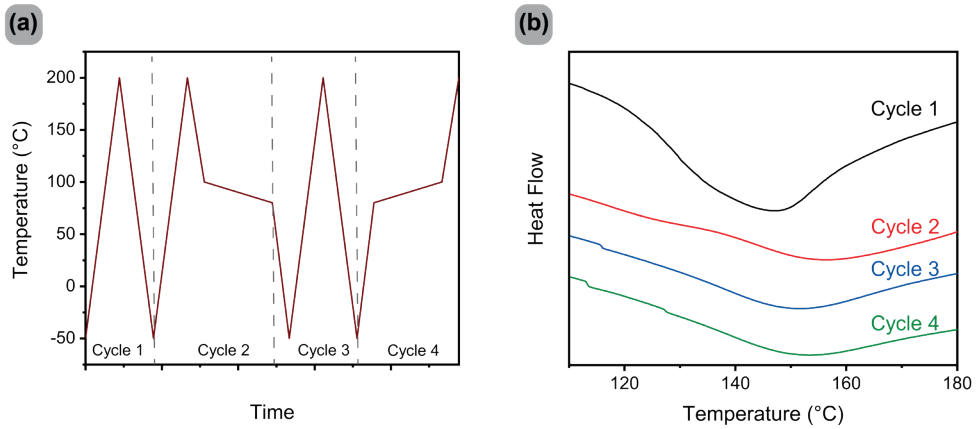

Figure 2.6. (a) The experimental procedure used in DSC to stimulate Diels-Alder reformation, 10 °C/min for the normal parts and 0.1 °C/min for the annealing steps between 80 °C and 100 °C which is the Diels-Alder formation temperature. **(b)** Relevant part of the DSC trace of consecutive heating runs shifted vertically.

2.5 Mechanical properties

The (thermo)mechanical properties of the films were studied by Dynamic Mechanical Thermal Analysis (DMTA) and tensile tests. In Figure 2.7, the DMTA results are shown for films after UV curing followed by a thermal post-curing step for all three compositions. It is clear that both copolymer films have a higher T_g than the BPAda homopolymer film. This result is easily explained by the fact that the NRM and DA monomers are more rigid building blocks than the BPAda monomer. It is also clear that the BPAda and reference BPAda-NRM systems have similar rubber plateaus with a storage modulus of 60 ± 5 MPa at 200 °C, whereas the rubber plateau of the BPAda-DA film at 200 °C is about 50% lower (Figure 2.6a). Since the modulus is directly related to the crosslink density of the material,[27] this result implies that the crosslink density of the BPAda-DA films is approximately 50% lower, consistent with quantitative opening of the Diels-Alder bonds.

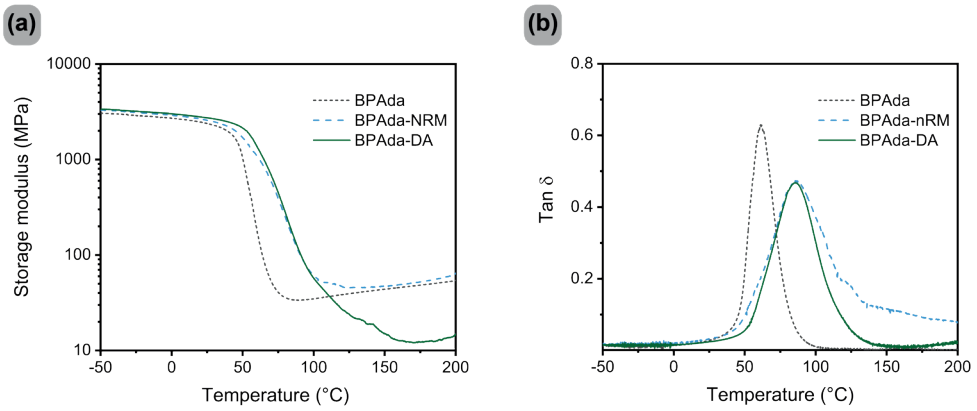

Figure 2.7. DMTA results for the three different sample compositions after UV curing for 200 seconds and thermal treatment for 1 hour at 180 °C. BPAda (grey dotted line) reference BPAda-NRM (blue dashed line) and BPAda-DA (green line). **(a)** The storage modulus used to determine the crosslink density **(b)** Tan δ peaks from which the T_g is obtained.

To test whether the opening of Diels-Alder bonds has an effect on the material properties, tensile tests were performed on thermally treated samples. As the Diels-Alder groups have already quantitatively opened, the network static during the measurements. The reference copolymer material (BPAda-NRM) was measured after identical thermal treatment. Both materials were tested at room temperature using different strain rates, the results are shown in Figure 2.8. Initially the materials display a linear elastic response. At higher stresses, the responses become non-linear and reach a maximum, *i.e.*, the yield point, after which plastic deformation occurs. Moreover, the deformation kinetics depend on the loading conditions. The higher the strain rate applied, the higher the yield stress observed.

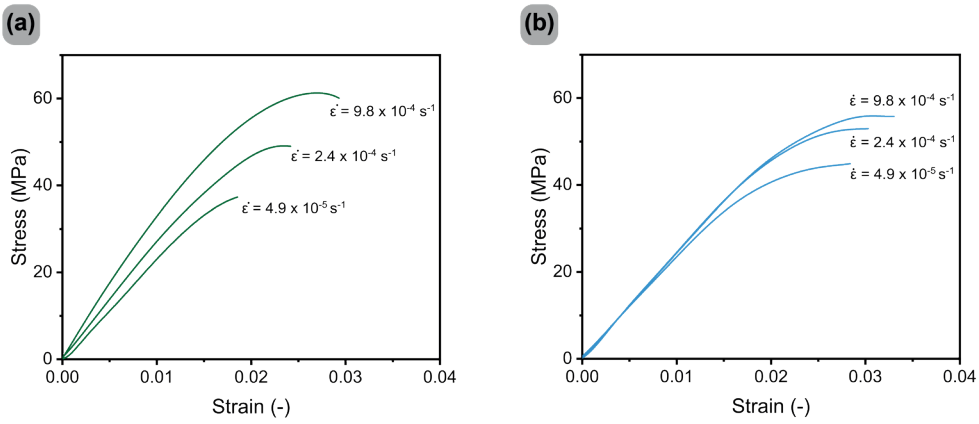

Figure 2.8. Tensile response at different strain rates ($4.9 \cdot 10^{-5}$, $2.4 \cdot 10^{-4}$ and $9.8 \cdot 10^{-4}$ s^{-1}) from which the yield point is determined. **(a)** BPAda-DA **(b)** BPAda-NRM.

In Figure 2.9, the rate dependence of the yield stresses for the BPAda-NRM and BPAda-DA samples is shown. For both systems we assume thermorheological simple behavior, as suggested by the tensile data. The yield stress is linearly dependent on the logarithm of the strain rate, with the BPAda-DA system displaying a higher slope than the BPAda-NRM system. It is known from extensive literature that the yield stress dependence of a polymer allows accurate estimates for the time-to-failure under constant stress.[28–30] The time-to-failure of a polymer scales predictably with the inverse slope of the yield stress.[31,32] The higher strain rate dependence for the BPAda-DA material implies there is more chain mobility. This is in accordance with the lower crosslink density observed in the DMTA experiment. As a consequence of this, it can be assumed that at higher applied stresses, the BPAda-DA material has a longer lifetime than the reference BPAda-NRM materials.

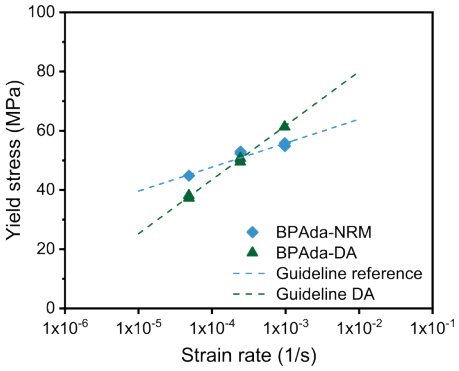

Figure 2.9. Yield stress versus applied strain rate for BPAda-NRM (blue diamonds) and BPAda-DA (green triangles) samples after UV and thermal curing.

2.6 Conclusions

A UV curable acrylate copolymer containing Diels-Alder crosslinks was successfully synthesized. It has been shown with DSC and FTIR that the Diels-Alder structure remains stable during UV curing at room temperature and that at elevated temperatures the retro Diels-Alder reaction occurs. DSC results also showed that there is only partial reformation of Diels-Alder moieties. The occurrence of retro Diels-Alder reactions was shown to significantly decrease the crosslink density of the materials, resulting in materials with a longer lifetime at high loadings.

2.7 Experimental details

Materials

The monomers used for this study, Bisphenol A ethoxylate diacrylate (BPAda), $M_n \approx 512$ g/mol and tricyclo[5.2.1.02,6]decane-dimethanol diacrylate (NRM) were used as received from Sigma Aldrich. Maleic anhydride was obtained from Acros Organics, acryloyl chloride was obtained from ABCR. All other chemicals for the synthesis were purchased from Sigma Aldrich and solvents from Biosolve. All chemicals and solvents were used without further purification unless otherwise noted.

Synthesis

Synthesis of 4,10-Dioxatricyclo[5,2,1,0]dec-8-ene-3,5-dione (compound 4):[19]

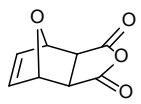

Maleic anhydride (50 g, 0.51 mol) and furan (55 mL, 1.5 eq.) were suspended in toluene. Upon heating, all substrates dissolved and a homogeneous slightly yellow liquid was obtained. The solution was heated to 80 °C, and left to react overnight. Some precipitation was observed and upon cooling to ambient temperature more product precipitated out of solution. The crystals were washed with diethyl ether and dried. The final product was obtained as white crystals (yield: 85%).

^{1}H NMR (400 MHz, $CDCl_3$): δ [ppm] = 6.58 (s, 2H), 5.46 (s, 2H), 3.18 (s, 2H).

^{13}C NMR (101 MHz, $CDCl_3$): δ [ppm] = 169.86, 136.97, 82.2, 48.71

Synthesis of 4-(2-Hydroxy-ethyl)-10-oxa-4-aza-tricyclo[5.2.1.02,6] dec-8-ene-3,5-dione (compound 5):[19]

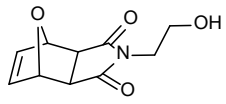

Compound 4 (60 g, 0.37 mol) and aminoethanol (27 mL, 1.2 eq.) are dissolved in methanol (400 mL, 0.09 M) and heated to 67 °C. The mixture was reacted overnight, yielding a dark yellow liquid. Solvents were evaporated and the resulting crude was extracted with water and chloroform. The organic layer was dried and the product ws obtained as a white solid (yield: 68%).

^{1}H NMR (399 MHz, $CDCl_3$): δ [ppm] = 6.53 (s, 2H), 5.28 (s, 2H), 3.81 – 3.67 (m, 4H) 2.9 (s, 2H).

^{13}C NMR (101 MHz, $CDCl_3$): δ [ppm] = 176.78, 136.52, 80.98, 60.30, 47.5, 41.78

Synthesis of 1-(2-hydroxyethyl)-1H-pyrrole-2,5-dione (compound 6):[19]

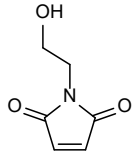

Compound 5 (49.16 g) was suspended in toluene and heated to 120 °C and reacted for two nights. The solvent was evaporated and the product was obtained as an off white solid (yield 99%).

^{1}H NMR (399 MHz, $CDCl_3$): δ [ppm] = 6.72 (s, 2H), 3.82 – 3.68 (m, 4H).

^{13}C NMR (101 MHz, $CDCl_3$): δ [ppm] = 171.10, 134.21, 60.81, 40.64

Synthesis of 1-(hydroxymethyl)-10-oxatricyclo[5.2.1.02,6]dec-8-ene-3,5-dione-2-Aminoethanol (compound 7):[19]

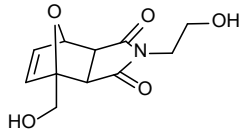

A mixture of compound 6 (30 g, 0.21 mol) and furfuryl alcohol (21 mL, 1.1 eq.) was heated to 80 °C in toluene (400 mL, 0.5 M). After overnight reaction, the product precipated as one big block. The mixture was filtered and the resulting solid was washed with fresh toluene, yielding the pure product with a yield of 90%.

^{1}H NMR (399 MHz, DMSO-d_6): δ [ppm] = 6.55 – 6.50 (m, 2H), 5.07 (d, *J* = 1.5 Hz, 1H), 4.93 (t, *J* = 5.8 Hz, 1H), 4.79 – 4.72 (m, 1H), 4.03 (dd, *J* = 12.5, 6.1 Hz, 1H), 3.72 – 3.65 (m, 1H), 3.33 (s, 4H), 3.04 (d, *J* = 6.5 Hz, 1H), 2.87 (d, *J* = 6.5 Hz, 1H).

^{13}C NMR (101 MHz, DMSO-d_6): δ [ppm] = 176.36, 174.93, 138.09, 136.43, 91.62, 80.16, 58.91, 57.25, 49.95, 47.76, 40.53

Synthesis of acrylic acid 2-(1-acryloyloxymethyl-3,5-dioxo-10-oxa-4-azatricyclo[5.2.1.02,6] dec-8-en-4-yl)-ethyl ester (compound 3):[20]

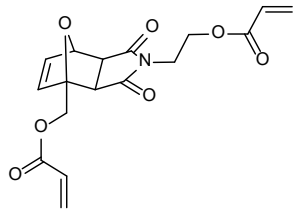

Diels-Alder-diol, compound 7 (6.5 g, 0.027 mol) was dissolved in a mixture of dry dichloromethane (150 mL, 0.14 M) and triethylamine (26.5 mL, 7 eq.). BHT was added as a stabilizer. Whilst stirring the solution at 0 °C, a mixture of acryloyl chloride in dichloromethane was added dropwise (5.8 mL, 2.6 eq. in 50 mL). After all the acryloyl chloride was added, the ice bath was removed and the reaction was stirred at room temperature for five hours. The mixture was quenched with 150 mL of water and an extraction was performed. The organic layer was dried over magnesium sulphate, dried and redissolved in chloroform. The crude product was purified using silica column chromatography with chloroform (A) - ethyl acetate (B). Gradient started at 100% (v/v) A, ramping up to 6% B over 6 column volumes, followed by isocratic separation with 15% B. After solvent evaporation the product was obtained as a yellow oil (yield 60%).

^{1}H NMR (400 MHz, $CDCl_3$): δ [ppm] = 6.59 – 6.34 (m, 4H), 6.22 – 6.01 (m, 2H), 5.91 – 5.81 (m, 2H), 5.28 (s, 1H), 5.04 (d, J = 16 Hz, 1H), 4.52 (d, J = 12 Hz, 1H), 4.31 (m, 2H), 3.82 (m, 2H), 2.98 (dd J = 8 Hz + 20 Hz, 2H).

^{13}C NMR (100 MHz, $CDCl_3$): δ [ppm] = 175.4, 173.9, 165.7, 165.6, 137.5, 137.1, 131.8, 131.5, 127.9, 127.7, 89.6, 81.1, 61.4, 60.7, 49.9, 48.4, 37.9

HRMS (MALDI-TOF): calcd for $C_{17}H_{17}NO_7$: 347.10; found, $[M + Na]^+$: 370.15

Preparation of films

A UV-curable resin was prepared by adding 3 wt.% of photoinitiator, 2,2-dimethoxy-2-phenylacetonphenone (Irgacure 651), to the (co)monomer mixture, followed by sonication in an ultrasonic bath to obtain a homogeneous solution. Approximately 3 g of this resin was cast onto a 4-inch silicon wafer, after which spin coating was used to spread the formulation on the substrate, and to obtain a homogeneous layer of approximately 80 µm thickness. A two-step process was used, the first step was the same for all resins, 10 seconds at 300 rpm. The required spin speed for the second step (30 seconds) depends on the viscosity of the mixture, for BPAda 500 rpm, NRM 325 rpm and DA 730 rpm. The resin layer was then flushed with nitrogen for 20 minutes to prevent oxygen inhibition. UV polymerization was

performed under nitrogen, using LED light (wavelength 365 nm, Honle Group, LED Cube 100 model, Germany). The light intensity at the sample position is uniform and equal to 7 mW/cm^2, as measured with a UV-meter.[22] After the polymerization the film was peeled from the wafer. From this film rectangular strips (*ca* 10.0 (length) x 5.3 (width) mm^2) or dog-bone shaped tensile bars (width 2.2 mm) were punched.

Characterization methods

Differential Scanning Calorimetric (DSC): The thermal behavior of the polymer films was measured on a Q2000 DSC (TA instruments) equipped with an RCS90 cooling accessory. Standard aluminum pans were used to maximize sample contact and approximately 10 mg of sample was used. The temperature range used for these materials was -50 °C to 200 °C. The general method consisted of three heating/cooling cycles with a rate of 40 °C min^{-1}. The glass transition temperature T_g was determined from the second heating run. The Universal Analysis TRIOS software was used for data acquisition and the midpoint at half height was used to determine T_g.

Dynamic Mechanical Thermal Analysis (DMTA): strips (ca 10.0 (length) x 5.3 (with) mm) were cut from the polymeric films. The thermomechanical properties were measured on a Q800 DMA (TA instruments) with film tension setup. The general used method applied a preload of 0.01 N, a frequency of 1 Hz and a strain of 0.1%. The temperature was equilibrated at -50 °C for 10 minutes after which it was increased at a heating rate of 3 °C min^{-1} to 200 °C.

Fourier-Transform Infrared spectroscopy (FTIR): spectra were recorded in Attenuated Reflection mode on a Spectrum One (Perkin Elmer) spectrometer at room temperature. 4 scans were performed from 4000 - 450 cm^{-1}. The conversion of the acrylate groups was determined using the sharp and distinct peak of the CH=CH$_2$ twist of the acrylate at 810 cm^{-1}.[23] To quantify the amount of monomer being consumed, a comparison with the uncured monomer mixture was made. As an internal standard, the aromatic peak at 829 cm^{-1} was used. To enhance separation of overlapping peaks, and to remove baseline errors, the second derivative spectroscopy method was used to determine the conversion, using equation 1.[33,34]

$$conversion\ [\%] = \left(1 - \frac{\left(\frac{A''_{810}}{A''_{829}}\right)_t}{\left(\frac{A''_{810}}{A''_{829}}\right)_{t=0}}\right) * 100\% \quad (1)$$

In this equation, A_{810}" and A_{829}" are the CH=CH$_2$ twist of the acrylate and aromatic ring at 810 and 829 cm^{-1}, respectively.

Nuclear magnetic resonance spectroscopy (NMR): ^{1}H and ^{13}C spectra were recorded on a 400 MHz Bruker Advance III HD (400 MHz for ^{1}H NMR) spectrometer. Chemical shifts (δ) are expressed in ppm with respect to tetramethylsilane (TMS, 0 ppm) as an internal standard. Coupling constants are reported as J-values in Hz.

Matrix assisted laser absorption/ionization-time of flight mass spectra (MALDI-TOF): Molecular mass of the synthesized small molecules were determined using a Bruker Autoflex Speed mass spectrometer using α-cyano-4- hydroxycinnamic acid (CHCA) or trans-2-[3-(4-tert-butylphenyl)-2-methyl-2-propenylidene]- malononitrile (DCBT) as a matrix.

Rheology: The viscosity of the resins was measured in plate-plate geometry using a MCR501Anton Paar rheometer, at 22 °C in a range of shear rates from 1 to 500 s^{-1}.
Tensile tests: dog-bone shaped tensile bars were punched from the polymeric films and thermally treated for 1 hour at 180 °C. Stress-Strain curves were measured using a micro tensile stage (TST350 Linkam Scientific) equipped with a load cell of 200 N. The tests were performed at room temperature and the load was recorded for constant strain rates of $4.9 \cdot 10^{-5}$, $2.4 \cdot 10^{-4}$ and $9.8 \cdot 10^{-4}$ s^{-1}.

2.8 References

(1) Diels, O.; Alder, K. Synthesen in Der Hydroaromatischen Reihe. *Justus Liebig's Ann. der Chemie* **1928**, *460* (1), 98–122.

(2) Solomons, G. T. W.; Fryhle, C. B. Conjugated Unsaturated Systems. In *Organic Chemistry*; 2004; pp 577–621.

(3) Qiu, Y. Substituent Effects in the Diels-Alder Reactions of Butadienes, Cyclopentadienes, Furans and Pyroles with Maleic Anhydride. *J. Phys. Org. Chem.* **2015**, *28* (5), 370–376.

(4) Kruth, J. P.; Leu, M. C.; Nakagawa, T. Progress in Additive Manufacturing and Rapid Prototyping. *CIRP Ann. - Manuf. Technol.* **1998**, *47* (2), 525–540.

(5) Omurtag, P. S.; Gunay, U. S.; Dag, A.; Durmaz, H.; Hizal, G.; Tunca, U. Diels-Alder Click Reaction for the Preparation of Polycarbonate Block Copolymers. *J. Polym. Sci. Part A Polym. Chem.* **2013**, *51* (10), 2252–2259.

(6) Inglis, A. J.; Sinnwell, S.; Stenzel, M. H.; Barner-Kowollik, C. Ultrafast Click Conjugation of Macromolecular Building Blocks at Ambient Temperature. *Angew. Chemie Int. Ed.* **2009**, *48* (13), 2411–2414.

(7) Chakma, P.; Konkolewicz, D. Dynamic Covalent Bonds in Polymeric Materials. *Angew. Chemie Int. Ed.* **2019**, No. 58, 9682–9695.

(8) Liu, Y. L.; Chuo, T. W. Self-Healing Polymers Based on Thermally Reversible Diels-Alder Chemistry. *Polym. Chem.* **2013**, *4* (7), 2194–2205.

(9) Gandini, A. The Furan/Maleimide Diels-Alder Reaction: A Versatile Click-Unclick Tool in Macromolecular Synthesis. *Prog. Polym. Sci.* **2013**, *38* (1), 1–29.

(10) Koehler, K. C.; Durackova, A.; Kloxin, C. J.; Bowman, C. N. Kinetic and Thermodynamic Measurements for the Facile Property Prediction of Diels–Alder-Conjugated Material Behavior. *AIChE J.* **2012**, *58* (11), 3545–3552.

(11) Froidevaux, V.; Borne, M.; Laborbe, E.; Auvergne, R.; Gandini, A.; Boutevin, B. Study of the Diels-Alder and Retro-Diels-Alder Reaction between Furan Derivatives and Maleimide for the Creation of New Materials. *RSC Adv.* **2015**, *5* (47), 37742–37754.

(12) Rulíšek, L.; Šebek, P.; Havlas, Z.; Hrabal, R.; Čapek, P.; Svatoš, A. An Experimental and Theoretical Study of Stereoselectivity of Furan-Maleic Anhydride and Furan-Maleimide Diels-Alder Reactions. *J. Org. Chem.* **2005**, *70* (16), 6295–6302.

(13) Chen, X.; Dam, M. A.; Ono, K.; Mal, A. A Thermally Re-Mendable Cross-Linked Polymeric Material. **2002**, *295* (March), 1698–1703.

(14) Terryn, S.; Brancart, J.; Lefeber, D.; Van Assche, G.; Vanderborght, B. Self-Healing Soft Pneumatic Robots. *Sci. Robot.* **2017**, *2* (9), 1–13.

(15) Bai, J.; Li, H.; Shi, Z.; Tian, M.; Yin, J. Dynamic Crosslinked Poly(Styrene-Block-Butadiene-Block-Styrene) via Diels-Alder Chemistry: An Ideal Method to Improve Solvent Resistance and Mechanical Properties without Losing Its Thermal Plastic Behavior. *RSC Adv.* **2015**, *5* (56), 45376–45383.

(16) Turkenburg, D. H.; Fischer, H. R. Diels-Alder Based, Thermo-Reversible Cross-Linked Epoxies for Use in Self-Healing Composites. *Polymer (Guildf).* **2015**, *79*, 187–194.

(17) Polgar, L. M.; Kingma, A.; Roelfs, M.; van Essen, M.; van Duin, M.; Picchioni, F. Kinetics of Cross-Linking and de-Cross-Linking of EPM Rubber with Thermoreversible Diels-Alder Chemistry. *Eur. Polym. J.* **2017**, *90*, 150–161.

(18) Davidson, J. R.; Appuhamillage, G. A.; Thompson, C. M.; Voit, W.; Smaldone, R. A. Design Paradigm Utilizing Reversible Diels-Alder Reactions to Enhance the Mechanical Properties of 3D Printed Materials. *ACS Appl. Mater. Interfaces* **2016**, *8* (26), 16961–16966.

(19) Syrett, J. A.; Mantovani, G.; Barton, W. R. S.; Price, D.; Haddleton, D. M. Self-Healing Polymers Prepared via Living Radical Polymerisation. *Polym. Chem.* **2010**, *1* (1), 102–106.

(20) Chen, Y.; Spiering, A. J. H.; Karthikeyan, S.; Peters, G. W. M.; Meijer, E. W.; Sijbesma, R. P. Mechanically Induced Chemiluminescence from Polymers Incorporating a 1,2-Dioxetane Unit in the Main Chain. *Nat. Chem.* **2012**, *4* (7), 559–562.

(21) Hall, D. B.; Underhill, P.; Torkelson, J. M. Spin Coating of Thin and Ultrathin Polymer Films. *Polym. Eng. Sci.* **1998**, *38* (12), 2039–2045.

(22) Anastasio, R.; Maassen, E. E. L.; Cardinaels, R.; Peters, G. W. M.; van Breemen, L. C. A. Thin Film Mechanical Characterization of UV-Curing Acrylate Systems. *Polymer (Guildf).* **2018**, *150*, 84–94.

(23) Decker, C.; Moussa, K. A New Method for Monitoring Ultra-Fast Photopolymerizations by Real-Time Infra-Red (RTIR) Spectroscopy. *Die Makromol. Chemie* **1988**, *189* (10), 2381–2394.

(24) Ke, X.; Liang, H.; Xiong, L.; Huang, S.; Zhu, M. Synthesis, Curing Process and Thermal Reversible Mechanism of UV Curable Polyurethane Based on Diels-Alder Structure. *Prog. Org. Coatings* **2016**, *100*, 63–69.

(25) Heo, Y.; Sodano, H. A. Self-Healing Polyurethanes with Shape Recovery. *Adv. Funct. Mater.* **2014**, *24* (33), 5261–5268.

(26) Min, Y.; Huang, S.; Wang, Y.; Zhang, Z.; Du, B.; Zhang, X.; Fan, Z. Sonochemical Transformation of Epoxy–Amine Thermoset into Soluble and Reusable Polymers. *Macromolecules* **2015**, *48* (2), 316–322.

(27) Kuang, X.; Liu, G.; Dong, X.; Wang, D. Correlation between Stress Relaxation Dynamics and Thermochemistry for Covalent Adaptive Networks Polymers. *Mater. Chem. Front.* **2017**, *1* (1), 111–118.

(28) Kanters, M. J. W.; Remerie, K.; Govaert, L. E. A New Protocol for Accelerated Screening of Long-Term Plasticity-Controlled Failure of Polyethylene Pipe Grades. *Polym. Eng. Sci.* **2016**, *56* (6), 676–688.

(29) Janssen, R. P. M.; Govaert, L. E.; Meijer, H. E. H. An Analytical Method to Predict Fatigue Life of Thermoplastics in Uniaxial Loading: Sensitivity to Wave Type, Frequency, and Stress Amplitude. *Macromolecules* **2008**, *41* (7), 2531–2540.

(30) Klompen, E. T. J.; Engels, T. A. P.; Van Breemen, L. C. A.; Schreurs, P. J. G.; Govaert, L. E.; Meijer, H. E. H. Quantitative Prediction of Long-Term Failure of Polycarbonate. *Macromolecules* **2005**, *38* (16), 7009–7017.

(31) Söntjens, S. H. M.; Engels, T. A. P.; Smit, T. H.; Govaert, L. E. Time-Dependent Failure of Amorphous Poly-d,l-Lactide: Influence of Molecular Weight. *J. Mech. Behav. Biomed. Mater.* **2012**, *13*, 69–77.

(32) Engels, T. A. P.; Breemen, L. C. A. V.; Govaert, L. E.; Meijer, H. E. H. Predicting the Long-Term Mechanical Performance of Polycarbonate from Thermal History during Injection Molding. *Macromol. Mater. Eng.* **2009**, *294* (12), 829–838.

(33) Saito, H.; Ando, I.; Tonelli, A. E.; Schilling, F. C.; Earl, W. L.; Vanderhart, D. L.; Lyerla, J. R.; Yannoni, C. S.; Fyfe, C. A.; Sheppard, N. J.; et al. Real-Time Kinetic Study of Laser-Induced Polymerization. *Annu. Rep. NMR Spectrosc* **1985**, *107* (28), 86.

(34) Durner, J.; Obermaier, J.; Draenert, M.; Ilie, N. Correlation of the Degree of Conversion with the Amount of Elutable Substances in Nano-Hybrid Dental Composites. *Dent. Mater.* **2012**, *28* (11), 1146–1153.

Chapter 3

Post curing of an acrylate network induced by oscillatory strain

Abstract: The mechanical properties and network structure of photocurable polymers are strongly dependent on processing conditions. Here we report that after UV and thermal curing, highly crosslinked Bisphenol A ethoxylate diacrylate undergoes unexpected additional curing during DMTA measurements, resulting in an increase in T_g and modulus. A detailed study of the conditions under which the change in properties takes place, unequivocally shows that a small (0.1%) oscillatory strain applied above T_g is responsible for the observed additional curing.

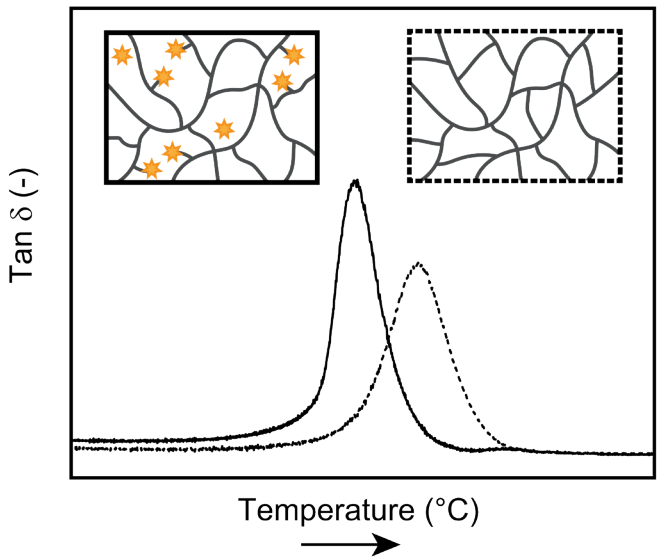

3.1 Introduction

The photopolymerization of multifunctional (meth)acrylic monomers occurs at room temperature,[1] giving rise to highly crosslinked polymer networks.[2] The T_g of the final material will strongly depend on the degree of crosslinking, and thus on the conversion.[3] If the material is cured below its T_g, reaching complete conversion of double bonds will be hindered by hardening, also called vitrification.[4,5] As the network is formed, the mobility of functional groups is strongly restricted until they are fully trapped in the glassy state.[6] Higher conversion and crosslink density can be obtained by heating during the photopolymerization, or addition of a thermal post curing step.[7,8] If the temperature is increased above T_g, the radicals and vinyl groups still present in the system regain their molecular mobility and polymerization can proceed.[9] This additional curing has a large impact on the final properties of the material, for example, it leads to a higher T_g.[10]

The preparation and thermo-mechanical properties of photo cured thermosets containing reversible Diels-Alder bonds were described in the previous chapter. In those materials, a thermal curing step led to an increase in double bond conversion for all three investigated monomer systems. The samples containing Diels-Alder bonds were subjected to consecutive heating cycles during a DMTA experiment, to study their thermal reversibility. In those experiments, an unexpectedly large shift in T_g from the first to the second heating cycle was observed. In this chapter, the origin of the increase in T_g is studied in detail.

3.2 Initial experiments

Films with a thickness of 80 µm containing 60 wt.% of bisphenol A ethoxylate diacrylate monomer (BPAda) and 40 wt.% of Diels-Alder (DA) monomer (Figure 3.1, see Chapter 2 for the synthesis), were UV cured for 200 seconds using 365 nm UV light with an intensity of 7 mW/cm^2.

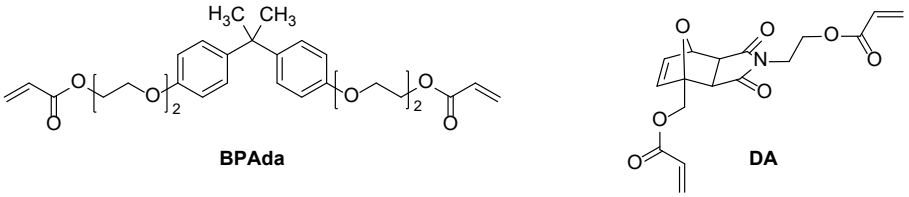

Figure 3.1. Chemical structure of the bisphenol A ethoxylate diacrylate (BPAda) and the Diels-Alder (DA) monomers used.

In order to study the effect of the thermally reversible Diels-Alder crosslinks on the storage modulus, DMTA tests with three heating cycles were performed. During these tests, a small oscillatory strain was applied while the sample was heated at a constant rate. All three cycles used the same heating and cooling rate of 3 °C/min. The modulus as a function of temperature for UV cured sample containing Diels-Alder monomer is shown in Figure 3.2a. The T_g of the UV cured material increased from 77 °C in the first cycle to 115 °C in the second, and 117 °C in the third cycle, an increase of roughly 40 °C. In Chapter 2, an increase in double bond conversion from 61% to 77% was reported upon thermal post curing for 1 hour at

180 °C. Such an increase in double bond conversion would indeed lead to a significant increase in T_g.[11] When the samples are heated to 200 °C during the DMTA experiment, the sample is above the initial T_g of 77 °C for 40 minutes during each cycle when using a heating rate of 3 °C/min. The elevated temperatures during such a DMTA experiment could induce a similar increase in conversion as during thermal curing.
For a sample which underwent additional thermal curing for 1 hour at 180 °C prior to DMTA experiments, (Figure 3.2b) the T_g increased to 85 °C. The 8 °C increase in T_g upon thermal curing explains only a fraction of the observed shift of 40 °C, and there still is a significant unexplained shift of 20 °C observed when the thermally cured sample is measured for multiple cycles. From the second to the third cycle, no significant change was observed, indicating maximum curing was reached after the first cycle. It was also shown in Chapter 2, that thermal treatment opens Diels-Alder moieties, and hereby the crosslink density is lowered, this can be seen here by a significantly lower rubber plateau for the thermally treated samples.

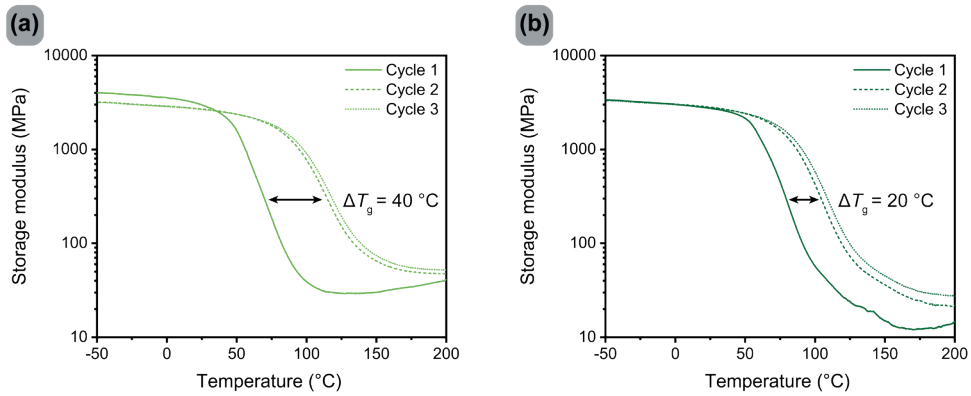

Figure 3.2. Storage moduli of three consecutive DMTA cycles on samples containing 60 wt.% BPAda and 40 wt.% DA monomer. **(a)** Only UV cured. **(b)** UV and thermally cured for 1 hour at 180 °C.

To exclude effects from reversible bonds, samples of the reference material, bisphenol A ethoxylate diacrylate (BPAda), were used for further study. The UV cured sample has a T_g of 53 °C in the first heating cycle (Figure 3.3a). The storage modulus increases around 150 °C. This is indicative of thermal curing during the DMTA measurement. A shift in T_g of 20 °C is observed in following cycles. Thermally treating the sample prior to DMTA measurements increased the T_g of the first cycle to 59 °C (Figure 3.3b). This increase of 6 °C can be attributed to the increase in double bond conversion from 74% to 79%. Still there is a significant difference of 5 °C between the first and consecutive cycles.

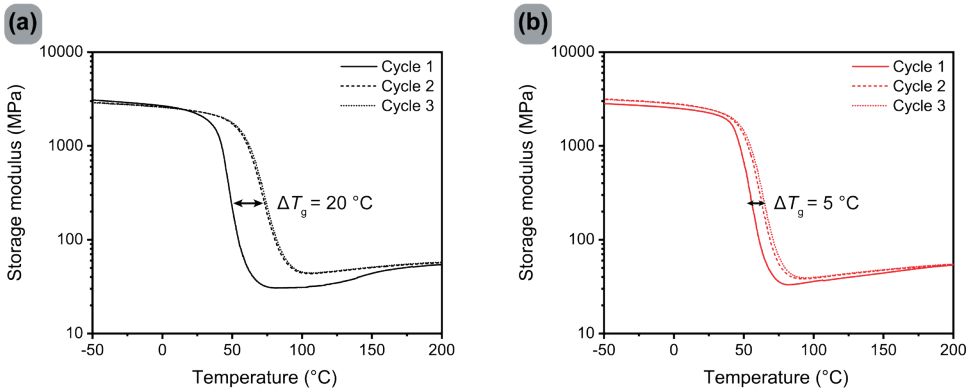

Figure 3.3. Storage moduli of three consecutive DMTA cycles on BPAda samples. **(a)** Only UV cured. **(b)** UV and thermally cured for 1 hour at 180 °C.

From these results it is clear that during DMTA measurements additional curing occurs, resulting in an increase in T_g. The additional curing is not caused by reversible bonds, as it was also observed in BPAda samples. Part of the additional curing is thermal curing, which can occur *in situ* during DMTA experiments, or prior to measurements by thermally post curing samples in an oven. In addition to the effect of 'normal' thermal curing, there is another factor with unknown origin that induces additional curing, both factors are investigated in more detail in this chapter.

3.3 Effect of thermal treatment

To study the contribution of a thermal curing in more detail, additional thin polymer films of BPAda were prepared via photopolymerization. Samples were cured for 200 seconds with UV light. After polymerization, the film was lifted from the wafer and part of the film was thermally treated at 180 °C for 1 hour after which DSC measurements were performed. DSC traces of both UV cured material and thermally post cured samples are shown in Figure 3.4. In both traces, a clear peak around 50 °C corresponds to enthalpy relaxation, which complicates accurate determination of the T_g.[12] The second cycle DSC data, however, cannot be used in this study, as the thermal history of the sample is of importance and initial differences in the samples are removed in the first cycle. Furthermore, in contrast to the DMTA measurements, the difference in T_g observed in DSC is small. Since DMTA is more sensitive, the curing effect was studied further by DMTA.[13]

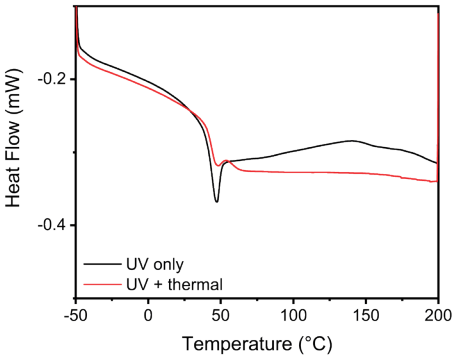

Figure 3.4. DSC data of the first heating cycle of BPAda polymer films measured from -50 °C to 200 °C with a rate of 10 °C/min. A sample which was UV cured for 200 seconds (black line), and a sample which was UV cured and thermally treated for 1 hour at 180 °C (red line).

By increasing the temperature above the T_g of the material, trapped radicals regain their mobility and further curing can take place. In the preliminary DMTA experiments, the material was heated to 200 °C and held for about 50 minutes above its T_g as a result of this. In further experiments with maximum temperatures of 150, 200 and 250 °C, all three traces of the first heating cycle nicely overlap and have a T_g of 53 °C (Figure 3.5a). In the second cycles (Figure 3.5b) T_g values were 65, 75, and 75 °C, respectively. Therefore, a maximum temperature of 250 °C provides no additional curing compared to a maximum temperature of 200 °C, and further experiments were performed with a maximum temperature of 200 °C.

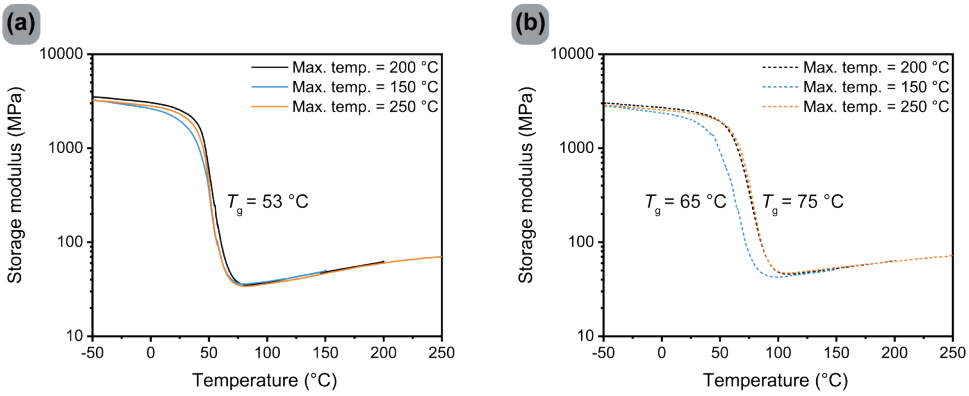

Figure 3.5. Storage moduli of BPAda samples measured in DMTA experiments with different maximum temperatures, the reference case of 200 °C in black, 150 °C in blue and 250 °C in orange. **(a)** First cycle. **(b)** Second cycle.

Upon heating, trapped radicals can react with unreacted vinyl groups or with other radicals. By reaction with vinyl groups, the conversion of double bonds will increase, and the resulting radical allows further reaction. If a trapped radical combines with another radical,

the active radical species are lost and there is no change in double bond conversion, but an additional crosslink is formed. By determining the double bond conversion with FTIR, the contribution of further polymerization to the curing was determined. The double bond conversions, T_g and plateau moduli of different samples are shown in Table 3.1. In all cases the reference material is a UV cured sample with a T_g of 53 °C, and a double bond conversion of 76%. Thermal curing for 1 hour at 180 °C increases the double bond conversion with 2% and increases T_g to 59 °C. Thermal curing during a DMTA experiment yields a much larger increase in double bond conversion of 10% with a concomitantly larger increase in T_g of 22 °C. When thermally post cured samples were treated in the DMTA, only a small increase in double bond conversion is observed which corresponds to a smaller change in T_g.

Table 3.1. Data of BPAda polymer samples after 1 and 2 DMTA cycles for both UV cured sample, and UV and thermally treated sample. The DMTA method used was -50 to 200 °C with a rate of 3 °C/min, FTIR was used to determine the double bond conversion.

Sample	Conversion [%]	T_g [°C]	G' 200 °C [MPa]
Reference (UV cured)	76	53	55
After 1 cycle	86	75	57
After 2 cycles	85	77	58
After thermal curing	78	59	54
After 1 cycle	80	65	54
After 2 cycles	79	67	55

When studying the changes in T_g for each sample in more detail, (Figure 3.6), there are a few important observations. The thermal treatment the sample automatically underwent during a DMTA experiment gives a significantly larger increase in T_g compared to a 'normal' thermal treatment in an oven, indicating more than just thermal curing occurs in the DMTA. The overall shift in T_g after multiple DMTA cycles is largest for the material which was only UV cured. This shows that the thermal history of the sample is important. It is possible that the thermal treatment destroys radicals still present in the system, but it is also possible that samples with higher initial conversion due to thermal post curing have less mobility of unreacted chain ends due to the higher crosslink density. Another important conclusion from this data is that there is a minimal change of only 1 °C or 2 °C observed if a sample which was already measured in DMTA, is ran for another cycle, so the main additional curing occurs in the first DMTA cycle.

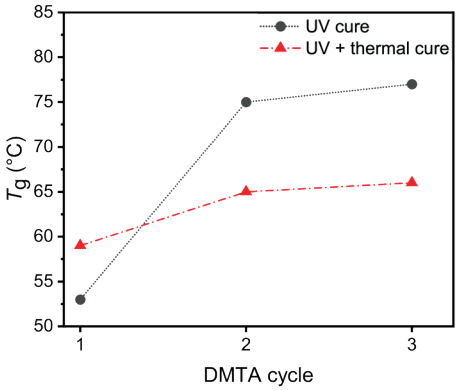

Figure 3.6. The values for T_g measured during a given DMTA cycle for UV cured material (black dots) and material after a thermal treatment of 1 hour at 180 °C (red triangles).

3.4 Effect of oscillatory stain

In addition to applying heat, the DMTA experiment also subjects the samples to oscillatory strain. The deformation may introduce additional chain mobility, and initiate further curing. To investigate the effect of cyclic straining, 10.0 x 5.3 mm sized strips of UV cured BPAda polymer were pre-strained in a DMTA at a constant temperature, prior to normal measurements. The strain used to pre-treat the samples is the same as used in normal DMTA measurements, 0.1%, which is within the linear viscoelastic region of the materials. UV cured samples were used because they display the largest shift in T_g. The oscillatory strain treatment was performed at 40 °C, which is below the materials initial T_g and at 180 °C, is well above the initial T_g. When strained at 40 °C, the T_g of the material increased from 53 °C to 61 °C, suggesting some additional curing occurred. But in the second cycle the T_g increased to 79 °C, which is comparable to the T_g values observed for samples which were not pre-strained (Table 3.1). The shift in conversion of this sample was 8%, which is also similar to the UV cured reference sample shown in Table 3.1. These results suggest that straining below the T_g of the material leads to limited additional curing. On the other hand, the sample strained at 180 °C, Figure 3.7b, shows almost no difference in T_g between the first and second cycle. Furthermore, the T_g of 76 °C in the first cycle is comparable to other values obtained for "two-cycle experiments". This demonstrates that oscillatory strain contributes to additional curing of the material, in particular when performed above T_g.

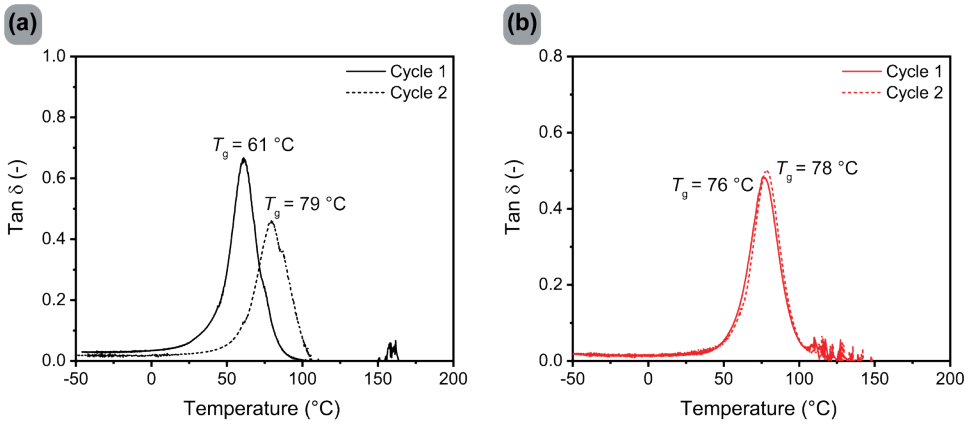

Figure 3.7. Tan δ curves for two consecutive DMTA cycles of UV-cured samples which were strained at 0.1% for 30 minutes prior to the measurements. **(a)** Strained at 40 °C. **(b)** Strained at 180 °C.

To verify the effect of strain-induced curing, samples were UV cured *in situ* in a rheometer. After UV curing, an oscillatory shear strain of 0.2% at a temperature of 150 °C was applied to induce further curing. The T_g of the UV cured sample, and of a rheologically strained sample after UV curing, were measured by DSC. The thermograms are shown in Figure 3.8. The T_g of the UV cured sample was 45 °C, while after the strain treatment at elevated temperature, a T_g of 52 °C was measured. It is important to note that the data used to determine the T_g, is the data of the second heating run in DSC. This means that both samples are thermally treated in the DSC during the first heating run. For the sample which was only UV cured, it is very likely that the T_g increased during this first heating run due to thermal curing. Although the absolute T_g of only UV cured sample cannot be determined, the shift of 7 °C due strain-induced post curing is still a significant increase. A shear strain at elevated temperatures yielded a material with a significantly higher T_g. These results confirm that the effects seen previously in DMTA are not an artifact of this measuring technique, but could be reproduced using another form of strain.

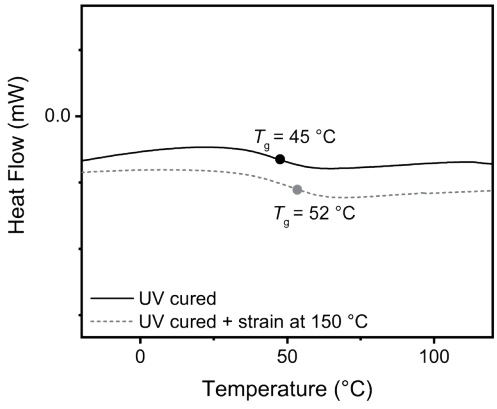

Figure 3.8. Second cycle DSC curves for samples cured in the rheometer, only UV curing (black solid line) and UV curing with additional oscillatory strain at 150 °C (grey dotted line).

3.5 Optical anisotropy

Applying a mechanical force on the polymer samples in one direction might cause an alignment of the chains. Such an alignment might also affect the material properties.
Alignment of the samples was studied using polarized optical microscopy (POM).[14] By placing the samples between crossed polarizers at an angle of 45°, presence of optical anisotropy can be determined. When the axes of two polarizers are crossed, the image is black, as no light which is polarized by the first polarized passes the second polarizer. If a sample which is placed in-between the polarizers is oriented, it is optically anisotropic and can act as a third polarizer that switches the polarization of the light. In this case we can observe birefringence. The effect of the anisotropy on the mechanical properties was studied using DMTA, the results are shown in Figure 3.9.

UV curing yielded isotropic samples without birefringence, (Figure 3.9a). Applying an oscillatory strain above the T_g during a DMTA experiment yielded a birefringent sample (Figure 3.9c), which means optical anisotropy is present. The most likely explanation for this optical anisotropy is the presence of an alignment along the direction of the force applied by the DMTA. The alignment is reversible as heating the anisotropic sample to 180 °C, which is above T_g, led to loss of the birefringence (Figure 3.9f).
The contribution of the alignment on the mechanical properties was determined by measuring samples for a second time in DMTA. Both an aligned sample (Figure 3.9c) and a sample after thermal alignment removal (Figure 3.8f) were tested. The T_g was 76 °C for both samples (Figure 3.9d, 3.9g), so the alignment does not contribute to the mechanical properties measured in DMTA. Although the alignment introduced during a DMTA experiment is reversible, the change in the material properties is permanent.

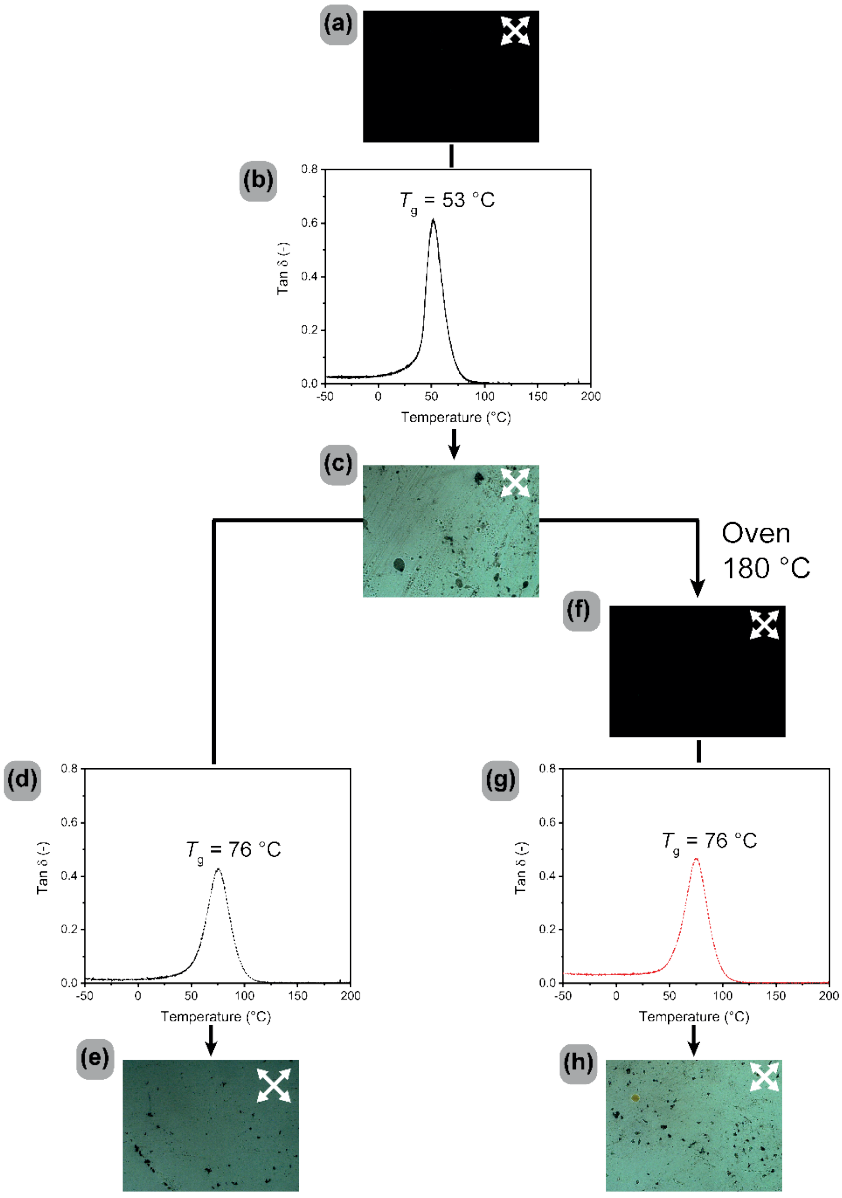

Figure 3.9. POM pictures under an angle of 45° between crossed polarizers to show optical anisotropy, and tan δ curves of DMTA measurement to obtain the T_g. **(a)** POM of UV cured sample. **(b)** DMTA of UV cured sample. **(c)** POM of UV cured materials after 1 DMTA cycle. **(d)** Second DMTA cycle. **(e)** POM after 2 DMTA cycles. **(f)** POM after thermal removal of alignment. **(g)** DMTA cycle after thermal removal of alignment. **(h)** POM after 2 DMTA cycles with removal of alignment in-between.

3.6 Conclusions

The additional curing of highly crosslinked polymer samples during a DMTA experiment was found to be a thermomechanical effect. Thermal post curing prior to DMTA measurements did lead to thermal curing but additional mechanical curing still occurred during the DMTA measurement. Mechanically deforming the samples below the T_g, prior to DMTA measurements yielded some additional curing, but there was still a significant additional increase in T_g during DMTA measurements. It was found that a small (0.1%) oscillatory strain applied above T_g was responsible for the additional curing. This was confirmed by shear induced curing above T_g, which showed similar trends.

The thermal history of the samples is important for the final mechanical properties. As for samples which were thermally post cured prior to DMTA measurements showed different properties as samples thermally treated during DMTA measurements.

By POM it was confirmed that applying an oscillatory strain above the T_g introduces an alignment in the samples. This alignment is reversible and does not contribute to the mechanical properties measured in DMTA. The observed alignment and its reversibility are indicative of chain mobility above T_g of these materials. It is this chain mobility that gives radicals still present in the polymer network a chance to form additional crosslinks, leading to the observed increase in T_g and modulus.

3.7 Experimental details

Materials and polymerization methods are identical to Chapter 2.

Materials

The monomer used for this study was bisphenol A ethoxylate diacrylate (EO/phenol 2, number average molecular weight M_n = 512 g/mol). 2,2-dimethoxy-2-phenylacetophenone is used as the photoinitiator. Both were obtained from Sigma-Aldrich and used without any purification.

Preparation of resin

A UV curable resin is prepared by mixing 3 wt.% of photo initiator (0.15 g) with the BPA diacrylate monomer (5 g). The mixture was sonicated for 2 hours at elevated temperatures (~ 60 °C) to homogeneously dissolve the initiator in the viscous monomer.

Preparation of films

Approximately 3 g of resin was cast on a 4-inch silicon wafer. Spin coating was used to dispense the formulation on the substrate, and to obtain a thin homogeneous layer. A first step was performed using a spinning speed of 300 rpm for 10 seconds. This was followed by a second step (500 rpm for 30 seconds) to obtain a homogeneous layer with thickness ~80 µm. The resin layer was then flushed with nitrogen for 20 minutes to remove oxygen. UV polymerization was performed under nitrogen using LED light (wavelength 365 nm,

Honle Group, LED Cube 100 model, Germany). The light intensity at the sample position was uniform and equal to 7 mW/cm^2, as measured with a UV-meter. After polymerization the film was lifted from the wafer without damage.
In the case of thermal curing, the films were put in an oven at 180 °C for 1 hour.

Characterization methods
Differential Scanning Calorimetry (DSC): T_g of the polymer films was measured using a TA Instruments Q2000 differential scanning calorimeter equipped with an RCS90 cooling accessory. Standard aluminium pans were used to maximize sample contact and approximately 10 mg of sample was used. The general method consisted of four cycles in which a sample was measured from -50 to 200 °C, the heating and cooling rate of cycle 1 and 2 was 10 °C min^{-1}, the 3th 20 °C min^{-1} and the last 40 °C min^{-1}.
The T_g of samples produced in the rheometer were determined using a DSC823e (Mettler Toledo). Approximately 7 mg of sample was placed in a pan and heated in a temperature range from -50 ˚C to 150 ˚C with a heating rate of 10 ˚C min^{-1} for two cycles. The glass-transition temperature was then evaluated from the second heating curve.
Dynamic Mechanical Thermal Analysis (DMTA): strips (ca 10.0 (length) x 5.3 (with) mm) were cut from the polymeric films. The mechanical properties were measured on a TA instruments Q800 DMA with film tension setup. The general method used a frequency of 1 Hz and an amplitude of 10 µm corresponding to 0.1%. The temperature was equilibrated at -50 °C for 10 minutes after which it was increased at a heating rate of 3 °C min^{-1} to 200 °C. After reaching the maximum temperature, the sample was cooled at the same rate. In a three-cycle experiment, three of these heat-cool cycles were performed.
A dynamic thermal treatment was performed using a DMA Q850 (TA instruments). UV cured samples were kept at a constant temperature, 150 °C, for 30 minutes during which an oscillatory strain is applied (0.1% strain with a frequency of 1 Hz).
Fourier-Transform Infrared spectroscopy (FT-IR): Spectra were recorded on a Perkin Elmer Spectrum One spectrometer at room temperature. 4 scans were performed from 4000 - 450 cm^{-1}. The sharp and distinct peak of the CH=CH$_2$ twist of the acrylate at 810 cm^{-1} was used to determine the double bond conversion,[15] quantifying the amount of reacted acrylic double bonds. To enhance separation of overlapping peaks, and to remove baseline errors, the second derivative spectroscopy method is used.[16]
Polarized Optical Microscopy (POM): anisotropy was studied by a Leica DM2700M microscope equipped with a Leica DFC320C camera. Samples are placed at an angle of 45 degrees between crossed polarizers.
Rheology: the effect of strain-induced post-curing was studied with a MCR 50 (Anton Paar-Physica), using plate-plate geometry equipped with a custom-made UV curing setup. The bottom plate is made of quartz, allowing the resin to be irradiated with UV light (bluepoint LED eco, Honle Group with wavelength of 365 nm), while the top geometry is a disposable plate with a diameter of 25 mm. A Peltier temperature-controlled hood (H-PTD 200) is used to thermally cure the sample while performing a rheological test. The resin was placed on the quartz plate and the gap set between the plates is 0.2 mm. The resin was then flushed with nitrogen for 10 minutes and UV cured for 200 seconds with light intensity of 8 mW/cm^2. The UV cured sample was heated by using the temperature-controlled hood and an oscillatory test is performed when the temperature is 150 ˚C. The sample was deformed at

a frequency of 1 Hz with a strain of 0.2%, which is in the linear viscoelastic regime. The samples were carefully removed from the quartz plate to perform DSC analysis.
Thermogravimetric analysis: Thermal stability studies were performed in a TA instruments TGA Q500 machine. Samples were heated under nitrogen conditions (flow 60 mL min^{-1}) from 26 to 600 °C with a heating rate of 10 °C min^{-1}.

3.8 References

(1) Fouassier, J. P.; Allonas, X.; Burget, D. Photopolymerization Reactions under Visible Lights: Principle, Mechanisms and Examples of Applications. *Prog. Org. Coatings* **2003**, *47* (1), 16–36.

(2) Andrews, M.; Tamboukou, M. Handbook of Thermoset Plastics 2nd Ed - S. Goodman (Noyes, 1998) WW.Pdf. **2013**, 0–26.

(3) Ratna, D. *Handbook of Thermoset Resins*; Smithers, 2009.

(4) Fraga, I.; Montserrat, S.; Hutchinson, J. M. Vitrification during the Isothermal Cure of Thermosets : Part I. An Investigation Using TOPEM, a New Temperature Modulated Technique. *J. Therm. Anal. Calorim.* **2008**, *91* (3), 687–695.

(5) Pascault, J. P.; Williams, R. J. J. Overview of Thermosets: Present and Future. In *Thermosets: Structure, Properties, and Applications: Second Edition*; Elsevier Ltd, 2017; pp 3–34.

(6) Cook, W. D.; Scott, T. F.; Quay-Thevenon, S.; Forsythe, J. S. Dynamic Mechanical Thermal Analysis of Thermally Stable and Thermally Reactive Network Polymers. *J. Appl. Polym. Sci.* **2004**, *93* (3), 1348–1359.

(7) Kruth, J. P.; Leu, M. C.; Nakagawa, T. Progress in Additive Manufacturing and Rapid Prototyping. *CIRP Ann. - Manuf. Technol.* **1998**, *47* (2), 525–540.

(8) Jorge Bártolo, P. Stereolithographic Processes. In *Stereolithography: Materials, Processes and Applications*; Jorge Bártolo, P., Ed.; Springer New York, 2011; pp 1–36.

(9) Lecamp, L.; Youssef, B.; Bunel, C.; Lebaudy, P. Photoinitiated Polymerization of a Dimethacrylate Oligomer: 1. Influence of Photoinitiator Concentration, Temperature and Light Intensity. *Polymer (Guildf).* **1997**, *38* (25), 6089–6096.

(10) Lovell, L. G.; Lu, H.; Elliott, J. E.; Stansbury, J. W.; Bowman, C. N. The Effect of Cure Rate on the Mechanical Properties of Dental Resins. *Dent. Mater.* **2001**, *17* (6), 504–511.

(11) Pascault, J. P.; Williams, R. J. J. Glass Transition Temperature versus Conversion Relationships for Thermosetting Polymers. *J. Polym. Sci. Part B Polym. Phys.* **1990**, *28* (1), 85–95.

(12) Sartor, G.; Mayer, E.; Johari, G. P. Thermal History and Enthalpy Relaxation of an Interpenetrating Network Polymer with Exceptionally Broad Relaxation Time Distribution. *J. Polym. Sci. Part B Polym. Phys.* **1994**, *32* (4), 683–689.

(13) Domínguez, J. C. Rheology and Curing Process of Thermosets. In *Thermosets: Structure, Properties, and Applications: Second Edition*; Guo, Q., Ed.; Elsevier, 2017; pp 115–146.

(14) Gåsvik, K. J. Photoelasticity and Polarized Light. In *Optical Metrology*; 2002; pp 217–247.

(15) Decker, C.; Moussa, K. A New Method for Monitoring Ultra-Fast Photopolymerizations by Real-Time Infra-Red (RTIR) Spectroscopy. *Die Makromol. Chemie* **1988**, *189* (10), 2381–2394.

(16) Rieppo, L.; Saarakkala, S.; Närhi, T.; Helminen, H. J.; Jurvelin, J. S.; Rieppo, J. Application of Second Derivative Spectroscopy for Increasing Molecular Specificity of Fourier Transform Infrared Spectroscopic Imaging of Articular Cartilage. *Osteoarthr. Cartil.* **2012**, *20* (5), 451–459.

Chapter 4

Stress relaxation via transalkylation chemistry

Abstract: A reversible crosslinker based on transalkylation chemistry was developed. The kinetics of the exchange reaction of benzyl bromide with DABCO was studied in detail by varying molar ratios and temperature. The system showed efficient exchange without addition of a catalyst. Reversibility in a polymer was studied by crosslinking of a linear, benzylic bromide functionalized polyacrylate with DABCO. The resulting network polymer was insoluble, but it readily dissolved in the presence of DABCO. Rheological measurements showed that the crosslinks are dynamic, with efficient stress relaxation at 120 °C.

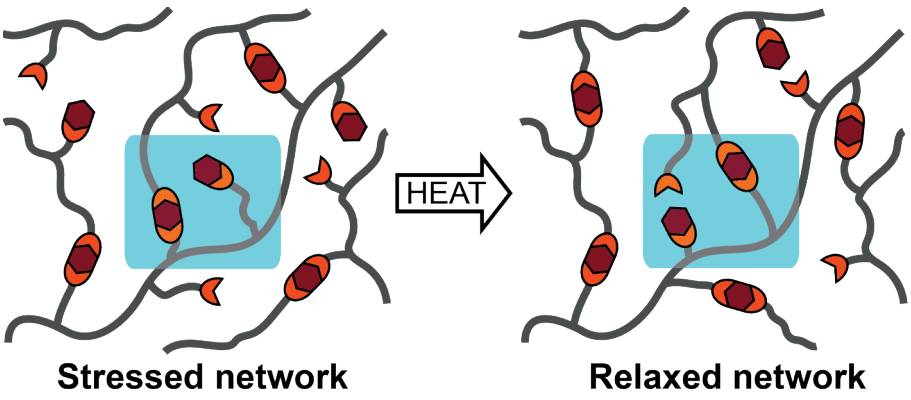

4.1 Introduction

Diels-Alder chemistry, as discussed in Chapter 2, has been investigated extensively for applications in dynamically crosslinked polymers. Alternative exchange reactions are gaining increasing interest.[1] An example of such an alternative approach are S_N2 type nucleophilic substitution reactions, such as transalkylation. S_N2 nucleophilic substitution reactions are ubiquitous in organic chemistry. In such reactions, shown in Scheme 4.1, an electron rich nucleophile reacts with an electrophilic substrate, resulting in the departure of a substituent, the leaving group.[2] The nucleophile is typically negatively charged, whereas the substrate is typically neutral or positively charged.

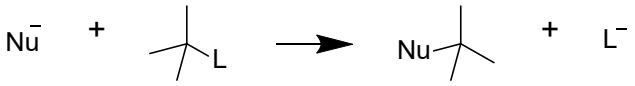

Scheme 4.1. A nucleophilic substitution reaction. The nucleophile donates an electron pair to the electrophile, forming a bond. Upon this new bond formation, the leaving group L departs with an electron pair.

The reversibility of some nucleophilic substitution reactions has been known for years, yet only recently it is gaining interest as a dynamic covalent bond.[3,4] Lehn *et al.* performed extensive kinetic studies, showing that S_N2 type nucleophilic substitution reactions of quaternary ammonium salts show great potential for the development of dynamic covalent chemistry.[5]

Drockenmuller *et al.* were the first to report a dynamic polymeric network based on transalkylation.[6] Thermal polymerization of an α-azide-ω-alkyne monomer yielded linear chains containing 1,2,3-triazole groups. By addition of 1,6-dibromohexane as a bifunctional quaternizing agent, 1,2,3-triazolium salts are formed with subsequent formation of reversible crosslinks. This is shown in Scheme 4.2. The polymerization process was a simple one-pot reaction which required no catalyst or solvent, allowing the formation of objects with various shapes and sizes. The network could be recycled by compression molding of ground material for 1 hour at 160 °C with a pressure of 20 bar. After two recycling cycles, samples with an extension at break similar to the starting material were obtained, indicating efficient network reformation. Furthermore, efficient stress relaxation was observed in rheological experiments. At a temperature of 200 °C, the characteristic relaxation time τ was only a few seconds.

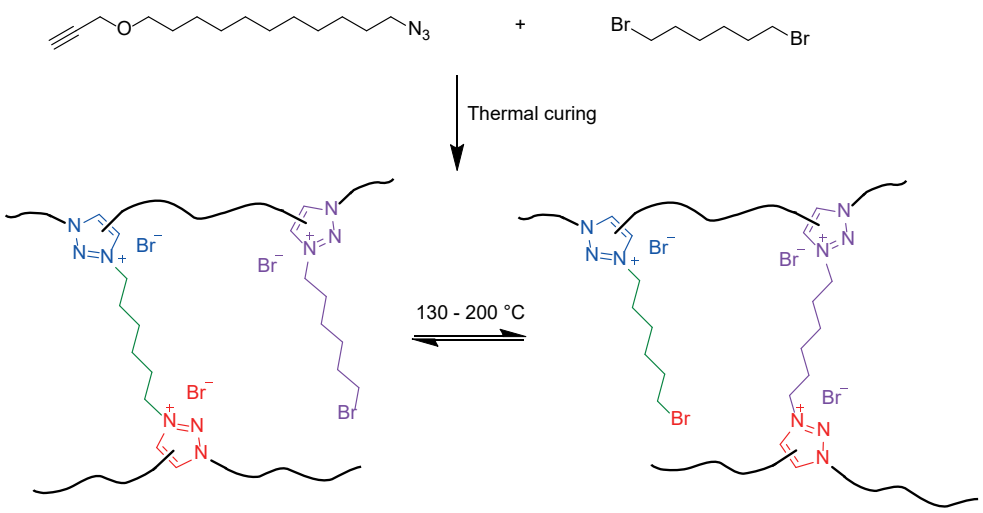

Scheme 4.2. Homopolymerization of α-azide-ω-alkyne monomer in the presence of 1,6-dibromohexane as a difunctional crosslinker yielded an ion conduction reversible network.[6]

Followed by this work, Du Prez *et al.* developed a reversible network via transalkylation of trialkylsulfonium salts.[1] These networks were prepared in a two-step procedure in which first a static network is formed, to which exchangeable bonds are later introduced. Photopolymerization of multifunctional monomers using a thiol-ene Michael addition reaction yielded a crosslinked material.[7] Kinetic studies showed that alkylbrosylates are efficient transalkylation agents to form trialkylsulfonium salts. Alkylbrosylates proved to be stable during the photopolymerization, allowing physical incorporation in the static network. By additional thermal treatment, reversible trialkylsulfonium salts are formed via the alkylation of the thioethers present in the network, see Scheme 4.3. The dynamic nature of this system was studied by stress relaxation experiments and recycling. Complete relaxation at elevated temperatures was observed in rheological stress relaxation experiments, and remolding by compression molding yielded defect free samples. Recycled samples showed no significant change in mechanical properties when measured in DMTA and tensile tests.

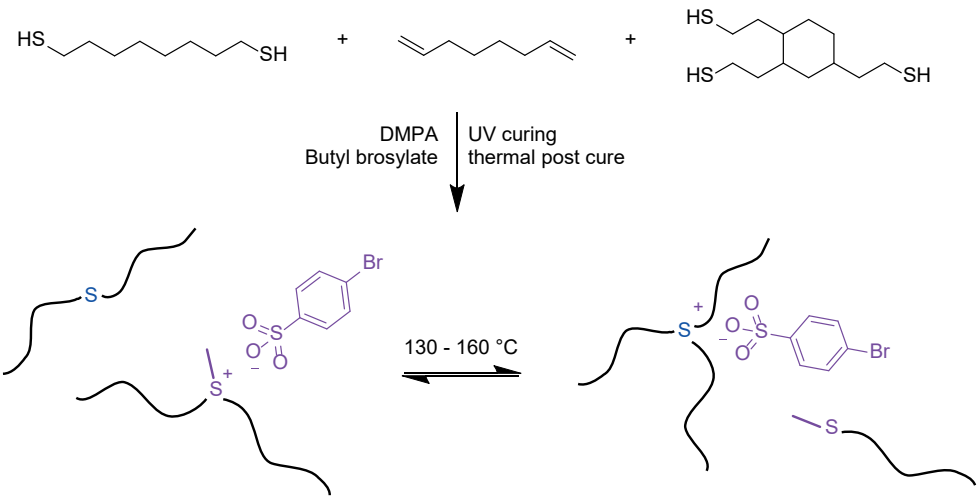

Scheme 4.3. Thiol-ene photopolymerization of octanedithiol, octadiene and trithiol with dimethylol propionic acid (DMPA) as a catalyst yielded a static network. By thermal post curing physically incorporated alkyl brosylates, alkylation of the network was achieved and exchangeable bonds were introduced yielding a reversible network.[1]

Inspired by these systems, we aimed to develop a transalkylation system which can be implemented in (meth)acrylate polymers. A number of tertiary amines were considered for quaternization. The thermal formation of 1,2,3-triazole groups as used by Drockenmuller *et al.* is not compatible with acrylic moieties. Lehn *et al.* found that imidazolium salts are too stable to undergo exchange reactions. However, pyridinium salts (see Figure 4.1) do show potential. By additional literature study, 1,4-diazabicyclo[2.2.2]octane (DABCO) was selected as the most promising candidate for fast exchange reactions.[8] Compared to the popular nucleophilic catalyst DMAP, a pyridine derivate, the bicyclic aliphatic amine DABCO is a significantly better nucleophile, yet also a much better leaving group (by a factor of 10^3 and 10^6 respectively).[8] This means that DABCO will give much faster exchange than pyridine salts. An additional advantage is that one DABCO molecule can form a crosslink between two polymer chains, because it contains two tertiary amine functional groups. Finally, DABCO can easily be alkylated at low temperatures, making the alkylation process compatible with (meth)acrylates.[9]

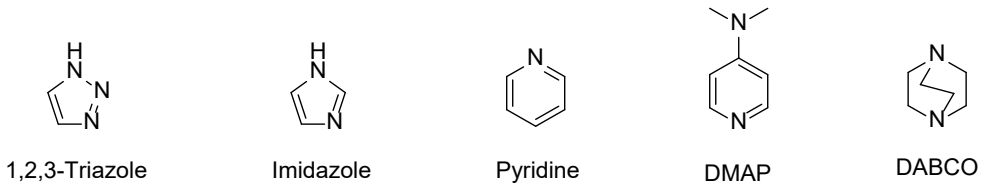

Figure 4.1. Five quaternizable amines.

In this chapter, the potential of DABCO in transalkylation reactions is first evaluated using low molecular weight model compounds. Benzyl bromide was selected as the alkylating agent, as the aromatic ring stabilizes the positive charge in the transition state of the alkylation. After model studies showed that DABCO is efficiently transalkylated, the DABCO unit was tested as a crosslinker for a linear polymer with benzylic bromide side groups. The strategy for network formation is shown in Scheme 4.4. Stress relaxation behavior of the networks is studied with rheological experiments.

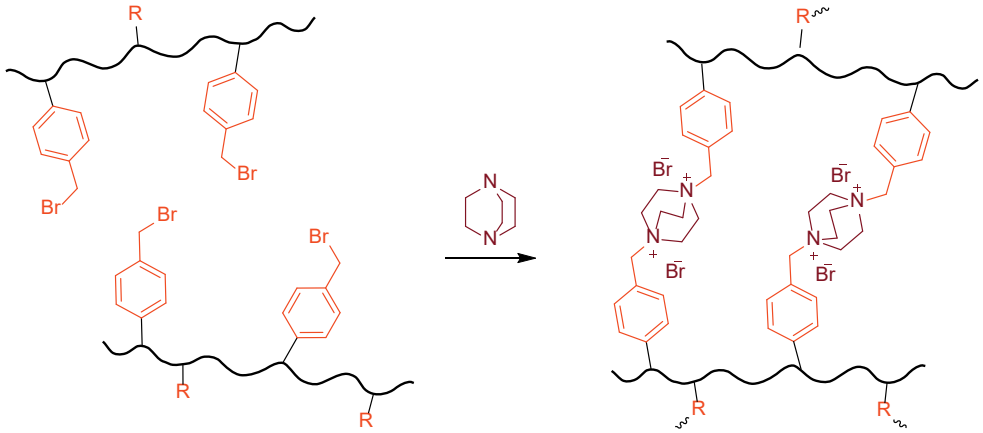

Scheme 4.4. Crosslinking of linear chains with alkylating side groups, by DABCO.

4.2 Small molecule kinetics

To evaluate the potential of DABCO in reversible transalkylation chemistry, a model study on simple small molecules was performed. First a model compound, bisbenzyl-DABCO, was prepared by alkylation of DABCO with benzyl bromide. To get more insight in the reaction mechanism the exchange kinetics of the resulting bisbenzyl-DABCO were investigated with free DABCO, single substituted DABCO and an excess of the alkylating agent, benzyl bromide. A recent article from the group of Lehn investigates the use of nucleophilic substitution reactions with amines in dynamic covalent networks, and describes two possible pathways for S_N2 exchange.[5] The pathways are illustrated for quaternized DABCO derivatives in Scheme 4.5. The indirect pathway is a dissociative mechanism in which the bisbenzyl-DABCO dissociates by nucleophilic attack of a bromide anion. The resulting products are a monobenzyl-DABCO and a benzylbromide. The benzylbromide can react with another tertiary amino group of monobenzyl-DABCO to form a new crosslink. This reaction occurs without the presence of DABCO. The direct pathway is associative, and requires the presence of a free amine. The DABCO will react directly with the bisbenzyl-DABCO substrate, resulting in the formation of two monobenzyl-DABCO products.

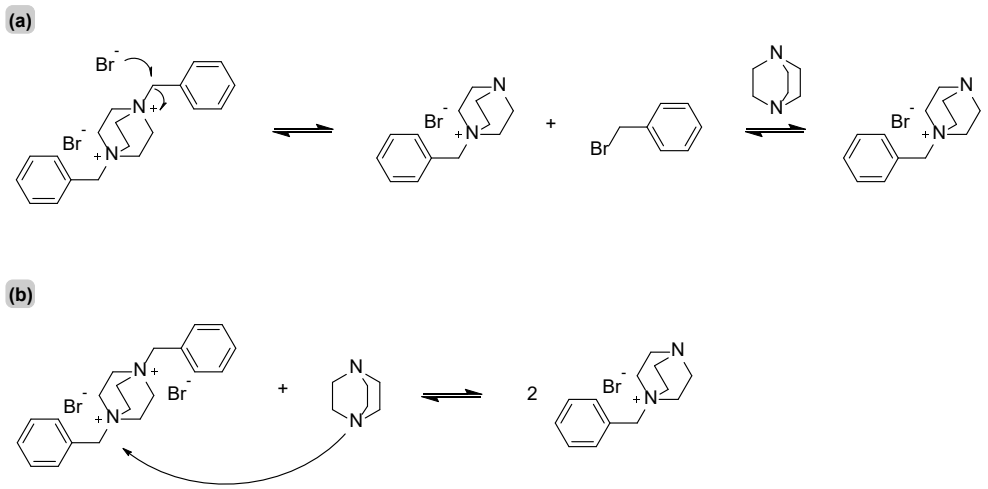

Scheme 4.5. S_N2 exchange pathways proposed by Lehn *et al.* illustrated for DABCO. **(a)** Indirect pathway, initiated by nucleophilic attack of the bromide anion on the benzylic carbon of the quaternary ammonium salt. **(b)** Direct pathway with nucleophilic attack of the amine on the benzylic carbon of the quaternary ammonium salt.[5]

Free DABCO

For the exchange experiments (see Figure 4.2a), bisbenzyl-DABCO (S) and DABCO (D) were dissolved in deuterated DMSO and heated in an NMR spectrometer. ^{1}H NMR spectra were measured *in situ* at different time intervals to monitor the concentration of monobenzyl-DABCO (P). In Figures 4.2b and 4.2c, the concentrations of the monobenzyl-DABCO, [P], are plotted as a function of reaction time for a range of initial concentrations at a temperature of 60 °C (Figure 4.2b), and at a range of temperatures for equimolar initial concentrations (Figure 4.2c).

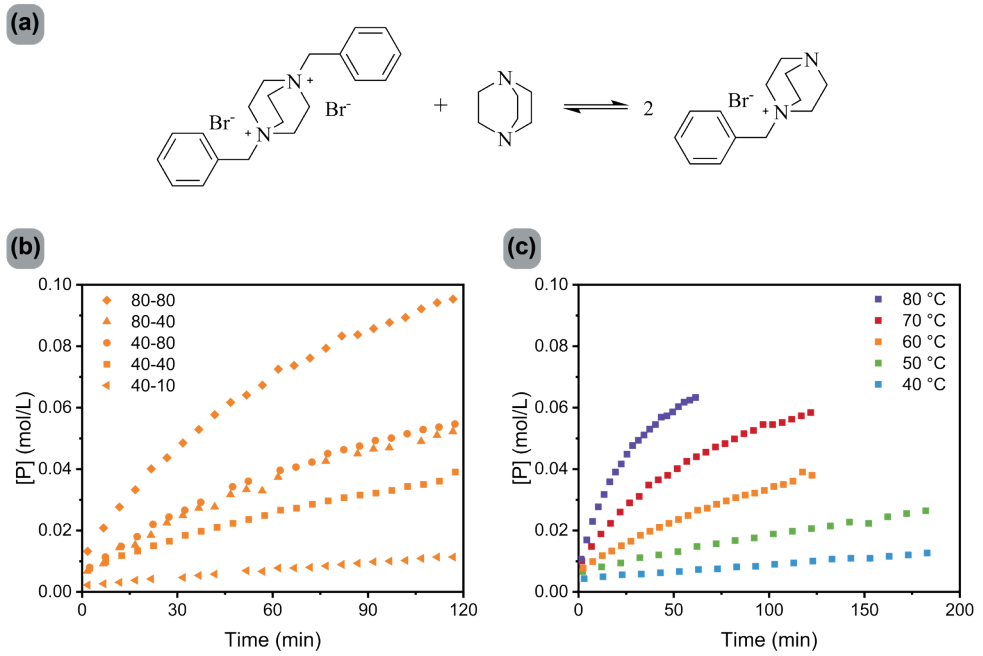

Figure 4.2. (a) Small molecule exchange reaction of bisbenzyl-DABCO (S) and free DABCO (D) for kinetic study. **(b)** Formation of monobenzyl-DABCO for a range of different starting concentrations at 60 °C. **(c)** Temperature dependence of the formation of monobenzyl-DABCO (P) using starting concentrations $[S]_0 = [D]_0 = 40$ mM.

The results shown in Figure 4.2b are consistent with a reaction rate that is first-order in both reactant concentrations (the initial slopes are proportional to $[S]_0 \times [D]_0$), which leads to the following rate equation for the forward (batch) reaction,

$$-\frac{d[S]}{dt} = -\frac{d[D]}{dt} = \frac{1}{2}\frac{d[P]}{dt} = k[S][D] \quad (1)$$

which in turn leads to the integrated rate equation (2a) in the case of equimolar starting concentrations $[S]_0 = [D]_0$ and (2b) in the case of $[S]_0 = [D]_0 + e$, where e is an excess amount of DABCO.

$$\frac{1}{[S]} = k \cdot t + \frac{1}{[S]_0} \quad (2a)$$

$$\frac{1}{e}\ln\left(\frac{e+[S]}{[S]}\right) = k \cdot t + \text{constant} \quad (2b)$$

All kinetic experiments were analyzed using equation 2b (except for those that exactly corresponded to $e = 0$) and in Figure 4.3a, a representative selection of the analyses is shown. The slopes of these plots correspond to the second order rate coefficient k, and in

Figure 4.3b the corresponding Arrhenius plot of the rate coefficients is shown. Regression of the data in Figure 4.3b yields an activation energy $E_a \approx 93$ kJ·mol^{-1} and frequency factor $A \approx 7 \cdot 10^{11}$ L·mol^{-1}·s^{-1}.

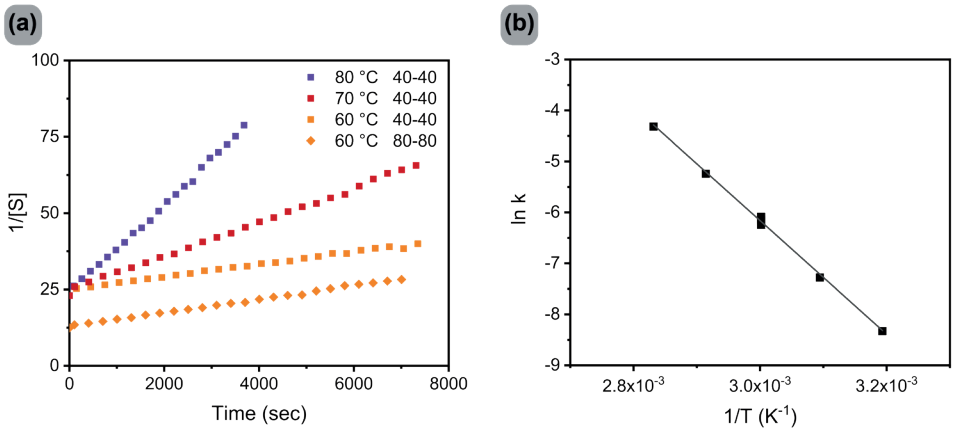

Figure 4.3b. (a) Representative second-order kinetic plots for a range of temperatures and starting concentrations. **(b)** Arrhenius plot of the kinetic study with free DABCO used to determine the activation energy.

Monosubstituted DABCO

In a dynamic polymer network, the nucleophile in the exchange reaction is not DABCO, but a dangling DABCO group that is quaternized on one of the nitrogen atoms. Since the positive charge may be expected to reduce the nucleophilicity of the second nitrogen atom through electrostatic repulsion, it was relevant to investigate the reactivity of a monosubstituted DABCO with bisbenzyl-DABCO, Figure 4.4a. The exchange reaction was monitored *in situ* with ^{1}H NMR. Equimolar initial concentrations of 40 mM and a temperature of 70 °C were used. In Figure 4.4b, the concentrations of the bisbenzyl-DABCO substrate as a function of reaction time are plotted for both unsubstituted and substituted DABCO. The data show that the initial rate of bisbenzyl-DABCO disappearance is a factor of 5 - 10 slower with monosubstituted DABCO than with DABCO itself. Taking into account the presence of a single amino group in benzyl DABCO instead of two, the amino group in benzyl DABCO is a factor of 3 - 5 less reactive than those in DABCO.

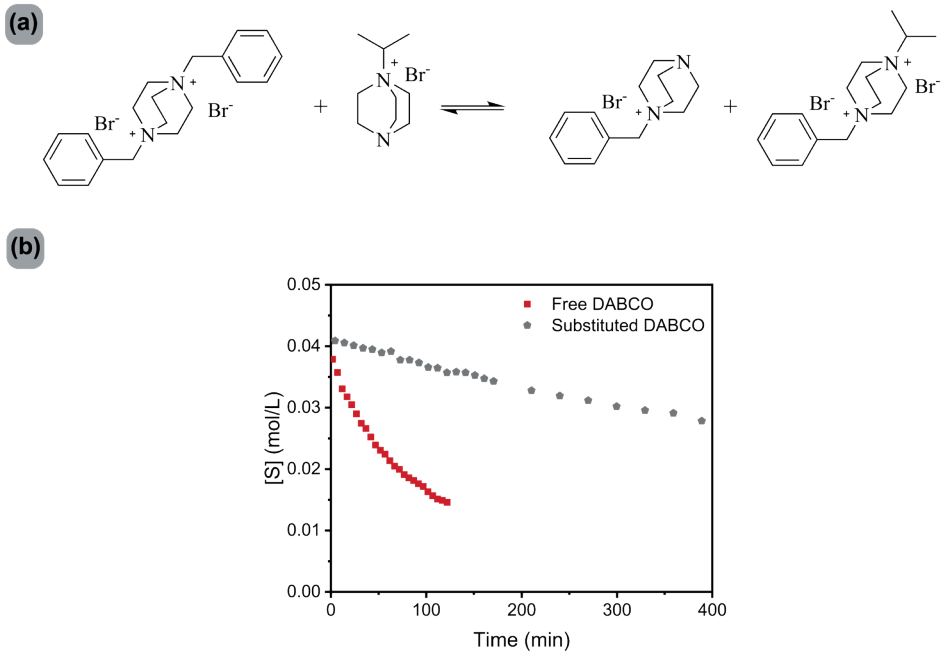

Figure 4.4. (a) Model exchange reaction of bisbenzyl-DABCO and substituted DABCO. **(b)** Decrease of bisbenzyl-DABCO upon exchange with substituted DABCO. The reaction with free DABCO is plotted as a reference. Both experiments are conducted at 70 °C with a concentration of 0.04 M for both reactants.

Excess benzylbromide

To investigate the rate of the reaction in the absence of free DABCO, a reaction with excess alkylating agent, 4-methylbenzyl bromide, was performed, Scheme 4.6. In order to minimize competing hydrolysis to benzyl alcohol, the reaction was performed in the presence of molecular sieves, but this made it difficult to do NMR measurements *in situ*. Therefore, conversion was only determined for one reaction time (2 h) at 70 °C. The reaction mixture contained 5 mM of the reaction product and 3 mM of hydrolysis product. This means that the product formation is slower than that for the reaction with free amine, but exchange still occurs.

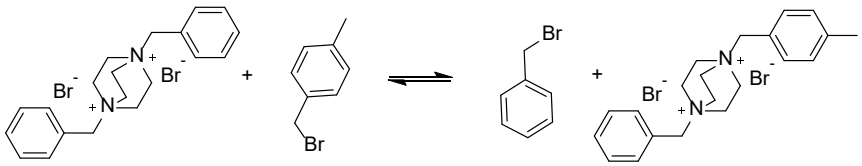

Scheme 4.6. Model exchange reaction of bisbenzyl-DABCO and 4-methylbenzyl bromide.

The kinetic experiments show that in the absence of free amine, the reaction occurs, but the reaction in the presence of free amine is faster. This observation suggests that both the associative and dissociative pathway occur.

4.3 Reversible crosslinking of linear chains

A monomer containing benzyl bromide side groups was synthesized via an esterification reaction of 4-(bromomethyl)benzoic acid and 2-hydroxyethylmethacrylate. This self-synthesized BrEMA monomer was copolymerized with butyl methacrylate (BMA). The copolymerization of these monomers in a free radical polymerization yielded a linear polymer with benzyl bromine side groups (Figure 4.5a). The ratio of the two monomers in the final product was one BrEMA on nine BMA units as determined by NMR. Butyl methacrylate was selected as the comonomer as this yielded a polymer with a low T_g, see figure 4.5c, to facilitate chain mobility necessary for the exchange. The polymer showed excellent thermal stability in TGA, Figure 4.5d.

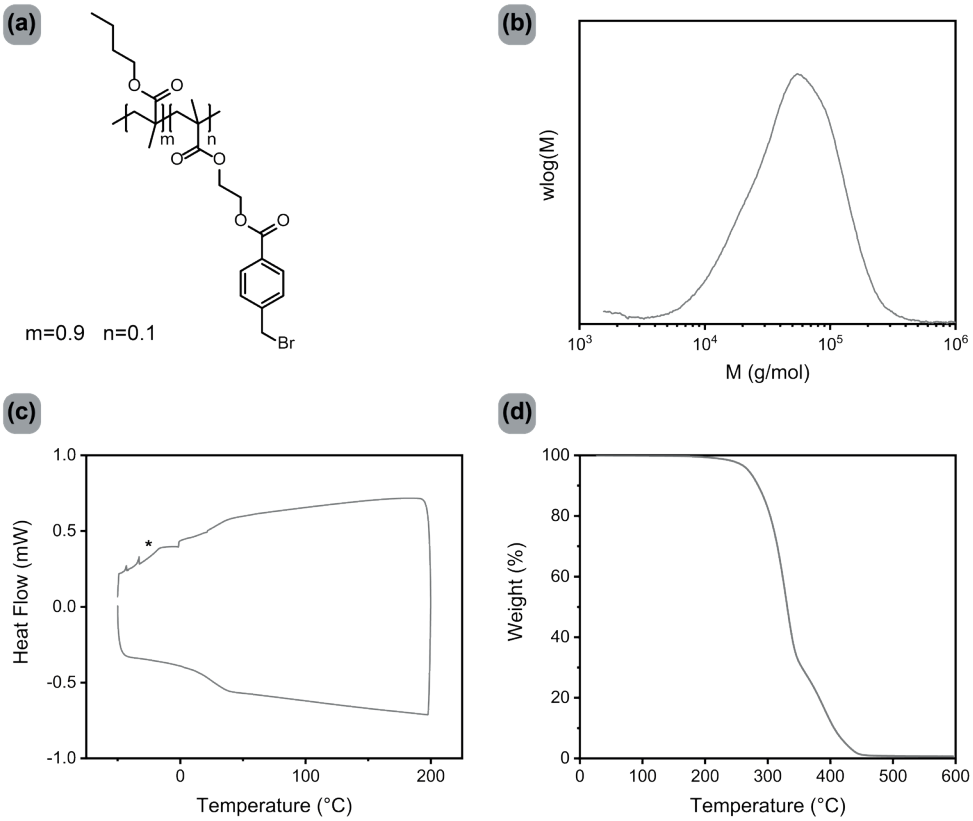

Figure 4.5. Properties of the linear polymer with benzylbromide side groups. **(a)** The molecular structure. **(b)** The molecular weight determined by SEC. **(c)** The T_g by DSC measured from -50 °C to 200 °C with a rate of 20 °C/min. **(d)** The thermal stability via TGA measured under N_2 with a heating rate of 10 °C/min. * is an artifact related to the cooling rate programmed for the experiment.

The linear polymer was crosslinked in THF solution with 0.6 equivalents of DABCO (with respect to benzyl bromide groups) for 1 hour at 60 °C. The resulting organogel was dried, yielding a solid polymer. After crosslinking, the dynamic nature of the crosslinks allowed reprocessing via compression molding at elevated temperatures, which did not affect the thermal properties or thermal stability of the material which were studied using DSC and TGA (Figure 4.6).

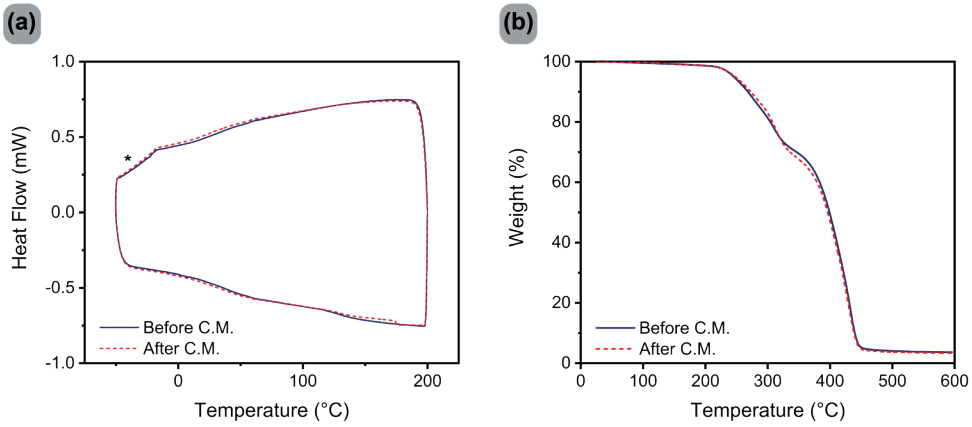

Figure 4.6. The properties of the crosslinked material before and after compression molding. **(a)** The T_g by DSC measured from -50 °C to 200 °C with a rate of 20 °C/min. **(b)** The thermal stability via TGA measured under N_2 with a heating rate of 10 °C/min.
* is an artifact related to the cooling rate programmed for the experiment.

When compression molded samples were heated to 100 °C, a clear difference between the linear polymer and the crosslinked polymer could be observed, Figure 4.7a. The non-crosslinked polymer flowed, while the crosslinked samples maintained their shape even when heated to 250 °C. Some yellowing occurred when heating samples above 200 °C. The sol-gel content of the crosslinked polymer was determined by stirring a bar-shaped sample of approximately 250 mg for 75 hours in 10 mL of THF. The polymer bar could be taken out of the solvent in one piece and the soluble fraction was determined to be about 1.5 wt.%. Together with the observed thermal stability, this indicates the presence of a highly crosslinked network. To show the reversibility of the network, a bar of polymer was heated in a solution with excess DABCO in THF, resulting in full dissolution (Figure 4.7b).

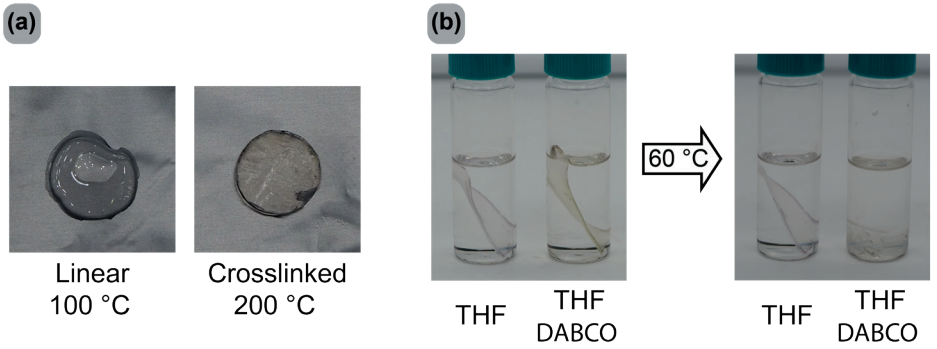

Figure 4.7. (a) When the crosslinked samples were heated to 100 °C no flow was observed, while the linear polymer flows. **(b)** A bar of crosslinked polymer did not dissolve when heated, whilst in the presence of excess DABCO de-crosslinked occurred, yielding a soluble polymer.

4.4 Stress relaxation

Networks with 0.4 and 0.6 equivalents of DABCO crosslinker were prepared from the same linear functional polymer, Figure 4.8. With 0.4 equivalents of DABCO benzylbromide groups are in excess, while with 0.6 equivalents of DABCO the amine is in excess.

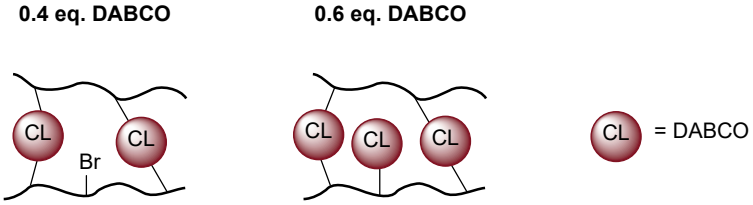

Figure 4.8. Schematic representation of the two different networks synthesized. The system with 0.4 eq. of DABCO still contains free bromine groups, the system with 0.6 eq. of DABCO contains free amine.

For a quantitative study on the reversibility of these systems, stress relaxation experiments were performed in a rheometer. The experiments were performed in the linear viscoelastic regime at 1% strain. The normalized stress relaxation moduli, G(t)/G(0) are shown in Figure 4.9 with 0.4 and 0.6 eq. of DABCO at four different temperatures. Both systems show efficient stress relaxation with a rate that increases with temperature, relaxation being well over 50% complete within a minute at 140 °C. In accordance with the small molecule kinetic studies discussed in section 4.2, the system with excess amine is faster than the system with excess benzyl bromide groups.

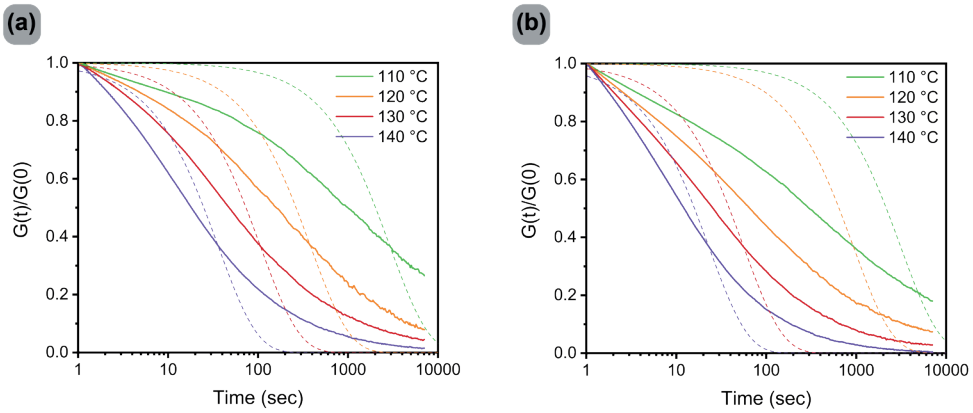

Figure 4.9. Stress relaxation data at various temperatures using 1% strain. The dashed lines are predications for an exponential decay using the experimentally determined τ_{app}. **(a)** System with 0.4. eq. of DABCO. **(b)** System with 0.6 eq of DABCO.

It is also clear that the stress relaxation modulus cannot be adequately described by a simple Maxwell model. However, realizing that the results would not have a clear physical meaning, we did use the Maxwell model to get an estimate for the temperature-dependence, and determined the time at which the stress relaxation modules had decreased to ~ 37% (= 1/e) of its original value for a range of different temperatures. In Figure 4.10, Arrhenius plots of these apparent relaxation times, τ_{app}, are shown and result in activation energies of 231±33 and 191±18 kJ/mol for the system with excess amine and the system with excess benzyl bromide, respectively. These activation energies are significantly higher than the activation energy obtained from the small molecule kinetics. This difference is likely due to a difference in polarity, as the small molecule kinetics are performed in DMSO which is a polar medium and will lower the activation energy of the reaction.

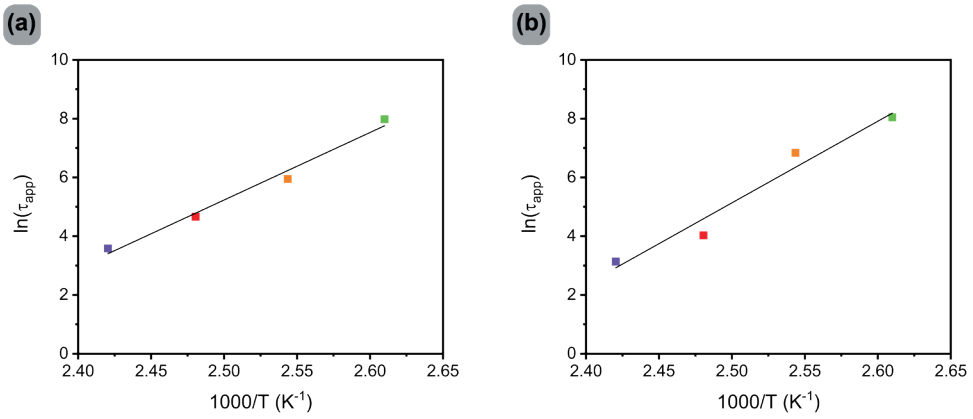

Figure 4.10. Arrhenius relationships from which the activation energies were calculated. **(a)** System with 0.4 eq. of DABCO. **(b)** System with 0.6 eq. of DABCO.

4.5 Conclusions

It was demonstrated that the alkylation of benzyl bromide with DABCO forms a dynamic bond which exchanges at elevated temperatures. Kinetic experiments showed efficient exchange with both excess of amine and excess of bromine, indication the presence of both a dissociative and an associative reaction pathway.

A linear polymer with benzyl bromide side groups was successfully synthesized and crosslinked using DABCO as a divalent crosslinker. The crosslinking reaction occurred very fast at 60 °C without addition of a catalyst. Solubility experiments showed the formation of a network which could be de-crosslinking by addition of excess DABCO.

The network polymer shows efficient stress relaxation in both a system with excess benzylbromide and an excess DABCO. Faster relaxation in the material with excess amino groups is in agreement with the small molecule kinetic studies. The fast relaxation combined with a high activation energy of the system in a polymer matrix are very beneficial for vitrimers. This gives stable materials at low temperatures, with effective relaxation at high temperatures. Since the networks are made from easily accessible chemicals and the exchange reaction is efficient at relatively low temperatures, this system offers a simple route towards moldable, recyclable network polymers.

4.6 Experimental details

Materials

All commercial chemicals and solvents were used as received, unless stated otherwise. 4-(Bromomethyl)benzoic Acid and 2-Hydroxyethyl Methacrylate were obtained from TCI EUROPE. All other chemicals for the synthesis were purchased from Sigma Aldrich. All solvents were obtained from Biosolve.

Synthesis

Synthesis of 1,4-Dibenzyl-1,4-diazabicyclo[2.2.2]octane-1,4-diium dibromide:[10]

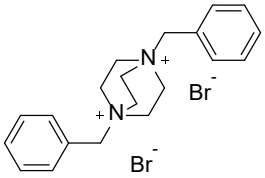

Benzyl bromide (0.48 mL, 2.1 eq.) was dissolved in methanol (20 mL, 0.3 M). Subsequently, DABCO (224 mg, 1.0 eq.) was added to the solution. The reaction mixture was stirred overnight at room temperature. The reaction mixture was then precipitated in diethyl ether. The obtained product was filtered, washed three times with diethyl ether and dried under high vacuum. The final product was obtained as a white solid (yield: 73.8%).

^{1}H NMR (400 MHz, DMSO-d_6): δ [ppm] = 7.61 – 7.47 (m, 10H), 4.85 (s, 4H), 3.89 (s, 12H).

^{13}C NMR (101 MHz, DMSO-d_6): δ [ppm] = 133.5, 131.18, 129.6, 126.9, 66. 8, 50.6

HRMS (MALDI-TOF): calcd for $C_{20}H_{26}N_2^{2+}$: 294.21; found, [M + Br]: 375.18

Synthesis of 1-benzyl-1,4-diazabicyclo[2.2.2]octan-1-ium bromide:

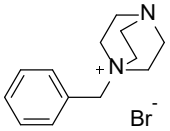

DABCO (0.5 g, 1 eq.) was dissolved in methanol (50 mL, 0.09 M) yielding a colorless solution. Benzyl bromide (1 eq.) was added dropwise under vigorous stirring. The reaction mixture was stirred overnight at room temperature. The reaction mixture was concentrated in vacuo and dried under high vacuum. The final product was obtained together with 10 mol% disubstituted DABCO as a byproduct, (yield: 98.8%).

^{1}H NMR (400 MHz, DMSO-d_6): δ [ppm] = 7.53 (s, 5H), 4.55 (s, 2H), 3.32 (t, J = 6.9 Hz, 6H), 3.02 (t, J = 6.9, Hz, 6H). About 10 mol % of bisbenzylDABCO was formed as a byproduct.

Synthesis of 1-benzyl-4-(4-methylbenzyl)-1,4-diazabicyclo [2.2.2]octane-1,4-diium dibromide:

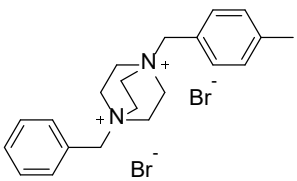

A solution of 1-benzyl-1,4-diazabicyclo[2.2.2]octan-1-ium bromide in DMSO-d_6 (51 mg in 0.5 mL, 0.36 M), and a solution of 4-methylbenzylbromide (67 mg in 1 mL in DMSO-d_6, 0.36M) are prepared. The solutions are combined in a 1:1 ratio and left to react overnight at room temperature. Product was not isolated, so no yield was obtained, but an NMR reference spectrum of the compound was obtained.

^{1}H NMR (400 MHz, DMSO-d_6): δ [ppm] = 7.61 – 7.49 (m, 5H), 7.37 (dd, J = 8.0 Hz and 19.9 Hz, 4H), 4.85 (s, 2H), 4.80 (s, 2H), 3.87 (s, 12H), 2.35 (s, 3H). Some 4-methylbenzylbromide is still present in the product.

Synthesis of 1-isopropyl-1,4-diazabicyclo[2.2.2]octan-1-ium bromide:[11]

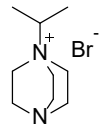

DABCO (1 g, 1 eq.) was dissolved in acetone (45 mL, 0.2 M) and 2-bromopropane (1 eq.) was added dropwise under magnetic stirring. The reaction mixture was stirred for 3 nights at room temperature. The formed white precipitate was filtered, washed with ethyl acetate, and dried under high vacuum. The final product was obtained as a white solid (yield: 25,2%).

^{1}H NMR (400 MHz, DMSO-d_6): δ [ppm] = 3.53 – 3.47 (m, 1H), 3.26 (t, J = 7.3 Hz, 6H), 3.02 (t, J = 7.3 Hz, 6H), 1.28 (dt, J = 6.6, 1.8 Hz, 6H).

^{13}C NMR (101 MHz, DMSO-d_6): δ [ppm] = 65.5, 49.1, 45.2, 16.2.

Synthesis of 2-(Methacryloyloxy)ethyl 4-(bromomethyl) benzoate:[12]

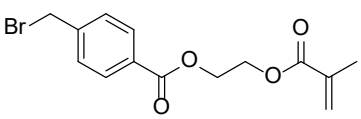

4-(Bromomethyl)benzoic acid (31.2 g, 1.1 eq.) was suspended in chloroform (500 mL, 0.3 M) and 2-hydroxyethylmethacrylate (16.1 mL, 1 eq.), N,N'-Dicyclohexylcarbodiimide (DCC, 1.5 eq.) and 4-(Dimethyl-amino)pyridinium 4-toluene-sulfonate (DPTS, 0.25 eq.) added. The mixture was stirred for 3 nights before filtration over a glass filter. The solvent was evaporated and crude was taken in methylene chloride to impregnate on silica. Column chromatography with Ethyl acetate - Heptane 80:20 was used to purify the mixture. Some sticky polymeric material was obtained, and the product was precipitated in methanol to remove any present homopolymer formed during the workup. (White solid, yield: 38%).

^{1}H NMR (400 MHz, DMSO-d_6): δ [ppm] = 7.94 (d, J = 8.3 Hz, 2H), 7.60 (d, J = 8.3 Hz, 2H), 6.03 (s, 1H), 5.69 (s, 1H), 4.76 (s, 2H), 4.62 – 4.49 (m, 2H), 4.49 – 4.38 (m, 2H), 1.87 (s, 3H).
^{13}C NMR (101 MHz, DMSO-d_6): δ [ppm] = 166.9, 165.6, 144.0, 136.1, 130.1, 130.0, 129.6, 126.6, 63.2, 62.8, 33.6, 18.4.
GPC analysis of the resulting final product showed no presence of polymer.

Synthesis of poly(butyl methacrylate-co-2-(methacryloyloxy) ethyl 4-(bromomethyl)benzoate):

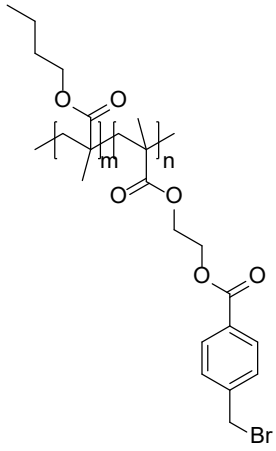

Inhibitor was removed from BMA monomer by filtration over basic alumina. BMA (22 mL, 9.0 eq.) and 2-(Methacryloyloxy)ethyl 4-(bromomethyl)benzoate (5g, 1.0 eq.) were dissolved in THF (58 mL, 70 wt.%). 1-decanethiol (0.008 M) and AIBN (0.015 M) were added to the solution. The solution was cooled to 0 °C and degassed by purging with argon for 20 minutes. Still under argon conditions, the reaction mixture was heated to 50 °C to start the polymerization. After 18 hours of reaction, the conversion determined via NMR was 82% and the viscosity was greatly increased. The reaction was stopped by addition of hydroquinone. The mixture was precipitated in 7-fold v/v cold methanol, yielding a white sticky solid. The precipitate was filtered and dried in a vacuum oven at 50 °C for a period of 16 h. The final product was obtained as a white solid.
^{1}H-NMR (400 MHz, DMSO-d_6): δ [ppm] = 8.08 (s, Ar<u>H</u>), 7.60 (s, Ar<u>H</u>), 4.69 (s, ArC<u>H</u>$_2$Br), 4.53 (s, OC<u>H</u>$_2$CH$_2$O), 4.30 (s, OCH$_2$C<u>H</u>$_2$O), 3.96 (s, COOC<u>H</u>$_2$(CH$_2$)$_3$), 2.14 – 1.79 (multiple C<u>H</u>$_2$ main chain peaks), 1.61 (br s, COOCH$_2$C<u>H</u>$_2$CH$_2$CH$_3$), 1.42 (br s, COOCH$_2$CH$_2$C<u>H</u>$_2$CH$_3$), 1.01 – 0.82 (multiple C<u>H</u>$_3$ peaks)
GPC analysis showed a single broad polymer peak with a M_w of ~33000 g/mol and a PDI of 1.7 with respect to polystyrene standards.

Network synthesis:
The linear poly(butyl methacrylate-co-2-(methacryloyloxy)ethyl 4-(bromomethyl)benzoate) (7 g) was dissolved in 70 mL tetrahydrofuran using sonication. The desired amount of DABCO (0.46 mg for ratio 0.6) was added and sonicated for 2 minutes, to ensure homogeneous mixing. The liquid mixture is heated for 1 hour at 60 °C resulting in the formation of an organogel. The gel was transferred to aluminum molds, and solvent was removed using a vacuum oven at 70 °C overnight.

Sample preparation:
The crosslinked polymer was compression molded into disk or bar shaped samples using a Collin Press 300 G with an operating temperature of 140 °C, pressure of 100 bar for 20 minutes and subsequently cooled with water. To remove any thermal history prior to rheology experiments, the samples were thermally treated by placing them into an oven overnight at 120 °C.

Characterization methods

Differential Scanning Calorimetry (DSC): T_g of the polymers was measured using a TA Instruments Q2000 differential scanning calorimeter equipped with an RCS90 cooling accessory using aluminum hermetic pans. 5-10 mg of sample was used per measurement. The general method consisted of four cycles where a sample was measured from -50 to 200 °C with heating and cooling rates of 10 °C min^{-1} (cycle 1 and 2), 20 °C min^{-1} and 40 °C min^{-1}. The first heating run was discarded. Universal Analysis TRIOS software was used for data acquisition, midpoint at half height was used to determine T_g.

Matrix assisted laser absorption/ionization-time of flight mass spectra (MALDI-TOF): Molecular mass of the synthesized small molecules were determined using a Bruker Autoflex Speed mass spectrometer using α-cyano-4- hydroxycinnamic acid (CHCA) or trans-2-[3-(4-tert-butylphenyl)-2-methyl-2-propenylidene]- malononitrile (DCBT) as a matrix.

Nuclear magnetic resonance spectroscopy (NMR): ^{1}H and ^{13}C spectra were recorded on a 400 MHz Bruker Advance III HD (400 MHz for ^{1}H NMR) spectrometer. ^{1}H *In situ* NMR spectra were recorded using a Varian Inova 500 MHz spectrometer. Chemical shifts (δ) are expressed in ppm with respect to tetramethylsilane (TMS, 0 ppm) as an internal standard. Coupling constants are reported as J-values in Hz.

Rheology: The mechanical properties and stress relaxation behavior of disk-shaped samples were determined using a stress-controlled AR-G2 rheometer (TA instruments) using 8 mm parallel plate geometry. Time sweeps at constant temperature were performed before and after relaxation experiments using a strain of 1% with a frequency of 1 Hz. Stress relaxation experiments were performed at a temperature range between 110 °C and 140 °C with a strain of 1% using a constant normal force of 10 N to ensure contact. The used strain of 1% is within the linear viscoelastic regime. For G(t)/G(0) the G(0) is taken after 1 second to ensure a stable signal.

Size exclusion chromatography (SEC): Molecular mass of the linear polymers was measured on a Shimadzu Prominence-I LC-2030C 3D equipped with two Agilent columns (mixed C and mixed D) with a combined range of 200-2000000 g/mol. The used eluent was THF with a flow of 1 mL min^{-1} at 40 °C. The molecular weight is determined based on narrow dispersity polystyrene standards purchased from Agilent.

Sol/Gel fraction: The mass fraction of the crosslinked part of the material is defined as the gel fraction. A bar of crosslinked material (~250 mg) was weighed and immersed for 75 hours in THF at room temperature. The samples were filtered and dried in a vacuum oven at 60 °C in a vacuum oven. The gel fraction was determined using equation 3a:

$$\text{Gel fraction} = \frac{m_{dry}}{m_{initial}} \quad (3a)$$

Where m_{dry} is the mass of the sample after extraction and subsequent drying.

The soluble fraction was determined by concentration of the extraction liquid by rotary evaporation. The equation modified to equation 3b:

$$\text{Sol fraction} = \frac{m_{residue}}{m_{initial}} \quad (3b)$$

Where $m_{residue}$ is the mass of the soluble part of the material present in the solvent.

Thermogravimetric analysis: Thermal stability studies were performed in a TA instruments TGA Q500 machine. Samples were heated under nitrogen conditions (flow 60 mL min^{-1}) from 26 °C to 600 °C with a heating rate of 10 °C min^{-1}.

4.7 References

(1) Hendriks, B.; Waelkens, J.; Winne, J. M.; Du Prez, F. E. Poly(Thioether) Vitrimers via Transalkylation of Trialkylsulfonium Salts. *ACS Macro Lett.* **2017**, *6* (9), 930–934.

(2) Solomons, G. T. W.; Fryhle, C. B. Ionic Reactions - Nucleophilic Substitution and Elimination Reactions of Alkyl Halides. In *Organic Chemistry*; 2004; pp 238–286.

(3) Hughes, E. D.; Juliusburger, F.; Masterman, S.; Topley, B.; Weiss, J. Aliphatic Substitution and the Walden Inversion. *J. Chem. Soc.* **1935**, No. 0, 1525–1529.

(4) Chakma, P.; Konkolewicz, D. Dynamic Covalent Bonds in Polymeric Materials. *Angew. Chemie Int. Ed.* **2019**, No. 58, 9682–9695.

(5) Kulchat, S.; Lehn, J. M. Dynamic Covalent Chemistry of Nucleophilic Substitution Component Exchange of Quaternary Ammonium Salts. *Chem. - An Asian J.* **2015**, *10* (11), 2484–2496.

(6) Obadia, M. M.; Mudraboyina, B. P.; Serghei, A.; Montarnal, D.; Drockenmuller, E. Reprocessing and Recycling of Highly Cross-Linked Ion-Conducting Networks through Transalkylation Exchanges of C-N Bonds. *J. Am. Chem. Soc.* **2015**, *137* (18), 6078–6083.

(7) Fox, M. A.; Whitesell, J. K. Substitition Alpha to Carbonyl Groups. In *Organic Chemistry*; 2003; pp 638–677.

(8) Baidya, M.; Kobayashi, S.; Brotzel, F.; Schmidhammer, U.; Riedle, E.; Mayr, H. DABCO and DMAP - Why Are They Different in Organocatalysis? *Angew. Chemie - Int. Ed.* **2007**, *46* (32), 6176–6179.

(9) Zhang, K.; Drummey, K. J.; Moon, N. G.; Chiang, W. D.; Long, T. E. Styrenic DABCO Salt-Containing Monomers for the Synthesis of Novel Charged Polymers. *Polym. Chem.* **2016**, *7* (20), 3370–3374.

(10) Albrecht, M.; Yi, H.; Köksal, O.; Raabe, G.; Pan, F.; Valkonen, A.; Rissanen, K. CF3: An Electron-Withdrawing Substituent for Aromatic Anion Acceptors? “Side-On” versus “on-Top” Binding of Halides. *Chem. - A Eur. J.* **2016**, *22* (20), 6956–6963.

(11) Liu, W.; Zhu, K.; Teat, S. J.; Dey, G.; Shen, Z.; Wang, L.; O’Carroll, D. M.; Li, J. All-in-One: Achieving Robust, Strongly Luminescent and Highly Dispersible Hybrid Materials by Combining Ionic and Coordinate Bonds in Molecular Crystals. *J. Am. Chem. Soc.* **2017**, *139* (27), 9281–9290.

(12) Moore, J. S.; Stupp, S. I. Room Temperature Polyesterification. *Macromolecules* **1990**, *23* (1), 65–70.

Chapter 5

Stress relaxation via internally catalyzed transesterification reactions

Abstract: A rapid one-step method for the formation of dynamic crosslinks in polymers containing hydroxyl groups is reported. By using dianhydrides to form ester crosslinks, intrinsic carboxylic acid catalysts are formed simultaneously. The produced network can be processed by compression molding at elevated temperatures without requiring any external catalysts. Stress relaxation experiments showed the effectiveness of the internal carboxylic acid catalyst. However, thermally induced fixed crosslinks prevent full stress relaxation. Surprisingly, a system without excess free hydroxyl groups also showed efficient stress relaxation, suggesting a contribution of an anhydride intermediate in the transesterification reaction mechanism.

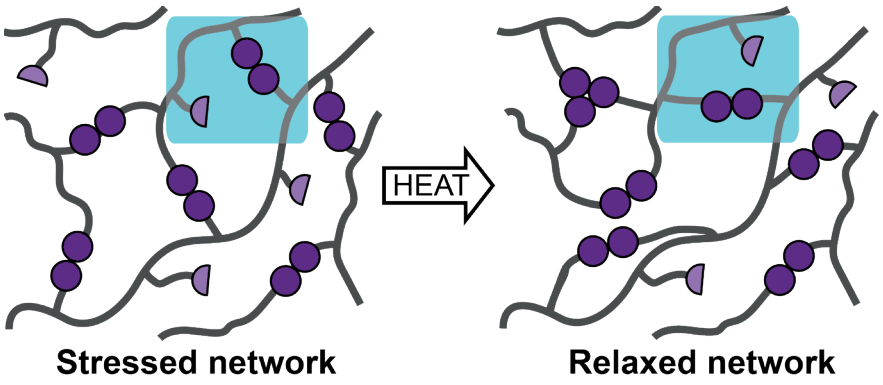

5.1 Introduction

Two approaches towards dynamic networks have been described In Chapters 2 and 4 of this thesis. In Chapter 2, networks containing Diels-Alder moieties were prepared and Chapter 4 describes the formation of a crosslinked network via transalkylation chemistry. Another well-known and broadly used approach towards reversible networks is the use of transesterification reactions,[1] a number of which have been presented in Section 1.5. In a transesterification reaction, one carboxylic acid ester is converted into another by reaction with an acid, hydroxyl group or a second ester.[2] In Scheme 5.1 the reaction with an alcohol is shown as an example. Transesterifications are equilibrium reactions, which can be accelerated by addition of a catalyst.[3] They are used both on a laboratory scale and in industry for the preparation of esters.[4] Examples of industrial applications are the production of biodiesel and the production of poly(ethylene terephthalate) (PET).[5,6]

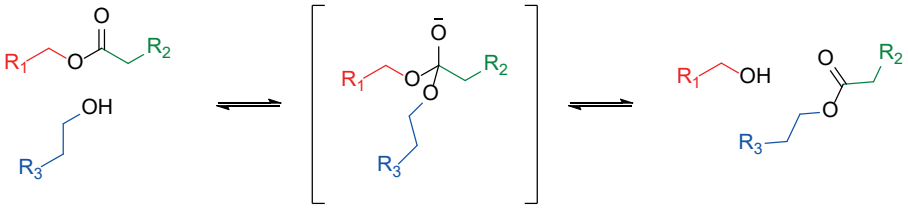

Scheme 5.1. The general transesterification reaction of an alcohol and an ester.

In 2011, the group of Leibler used transesterification reactions to develop permanently crosslinked materials which can be recycled and remolded at elevated temperatures.[7] They named this new class of materials 'vitrimers'. The epoxy polymer used to demonstrate this concept contained hydroxyl and ester groups, which undergo exchange reactions when heated. A zinc catalyst was added to accelerate the transesterification reaction and obtain efficient bond exchange.[8] By tuning the nature and the amount of catalyst added to the system, the temperature range of the exchange reaction can be tuned.[9] The reversible exchange reaction in the system of Leibler and coworkers is an associative process in which first a new bond is formed before the old bond is broken.[10] This reaction sequence ensures a constant crosslink density in the system which makes the material insoluble, even when heated in a solvent for prolonged times.[7]

Since the introduction of vitrimers by Leibler and coworkers, many interesting applications have been developed, such as engineering plastics with high melt strength,[11] recyclable rubbers,[12,13] or shape memory polymers.[14,15] An example of the use of vitrimers in additive manufacturing was reported by Zhang and coworkers, who produced reversible materials via stereolithographic printing of an acrylate resin.[16] The resin consisted of 95 mol% monoacrylate which formed linear chains. By addition of 5 mol% of a diacrylate monomer, crosslinks were formed resulting in a polymer network. By using a 1:1 molar ratio of ester and hydroxyl functionalities, and addition of 5 mol% zinc catalyst, they were able to obtain ≥80% stress relaxation after 40 minutes at 220 °C. They also demonstrated that the printed products can be repaired very efficiently. Repaired samples recovered 93% of their strength measured in uniaxial tensile tests after a heat treatment. The thermally induced

network rearrangements resulted in formation of covalent bonds which adhered the newly printed layers to the damaged part.
The systems discussed above use a dispersed catalyst to tune the exchange kinetics. Metal salts and strong bases are popular catalysts for this purpose, and are typically used at concentrations of 1-10 mol% with respect to the hydroxyl groups.[9] Most of these catalysts are toxic, which prevents their use in certain applications.[17] There are additional disadvantages associated with the use of dispersed or dissolved catalysts. Over time, they can leach from the material, reducing the network's ability to exchange.[18] For some catalysts, the solubility in organic compounds is low, which makes high catalyst loading impossible.[19,20]

Altuna *et al.* were able to form a network that is able to undergo transesterification without addition of an extrinsic catalyst.[21] By epoxy-acid reactions with a polycarboxylic acid, ester crosslinks and free hydroxyl groups were formed, Scheme 5.2. By tuning the amount of acid added to the system they were able to control the crosslink density of the network and the amount of free acid. They found that residual carboxylic acids present in the system catalyzed the transesterification reaction of the esters and hydroxyl groups, enabling self-healing and stress relaxation of the material. Since the catalyst is covalently attached, this prevents leaking and enables the use of high catalyst loadings.

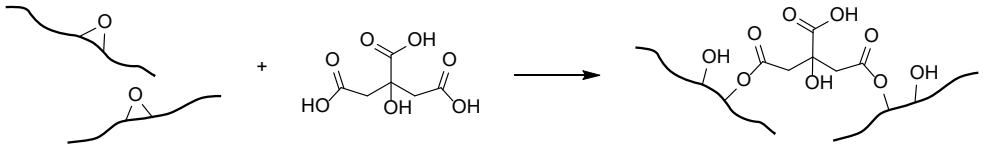

Scheme 5.2. The crosslinking via epoxy-acid reactions with citric acid.

The approach by Altuna *et al.* required the epoxidation of double bonds in the monomer to prepare for the crosslinking reaction.[21] An alternative approach to the synthesis of esters is the reaction of an acid anhydride with an an alcohol.[22] This reaction also produces one carboxylic acid group (Scheme 5.3) and thus constitutes a facile one-step route towards the formation of an ester crosslink and a carboxylic acid catalyst.

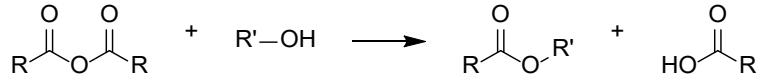

Scheme 5.3. Reaction of an acid anhydride with an alcohol to form an ester and a carboxylic acid.

Ongoing research in our group with polyester networks has shown that incorporation of carboxylic acid groups via pyromellitic dianhydride leads to efficient stress relaxation. The group of Du Prez is exploring the use of pyromellitic dianhydride in dynamic networks as well, and they found that the mechanism for exchange is most likely dissociative, in contrast to the vitrimers studied by Leibler which are associative.[7] In a detailed study on the participation of neighboring carboxylic acids in the hydrolysis reaction of phthalate esters, Bruice *et al*. propose several mechanisms.[23] They found that the mechanism is dependent on the leaving group and conclude that for poor leaving groups, the most likely pathway is an associative mechanism.

In this chapter, an easy two-step procedure for the formation of internally catalyzed dynamic networks is explored. In order to prepare these networks, the formation of the polymer backbone and the crosslinking reaction are decoupled. First a linear polymer with hydroxyl side groups is synthesized. The hydroxyl functionalities on this polymer are reacted with pyromellitic dianhydride, forming a crosslinked network.[24] This is schematically represented in Scheme 5.4. The formed network can undergo transesterification reactions upon heating.

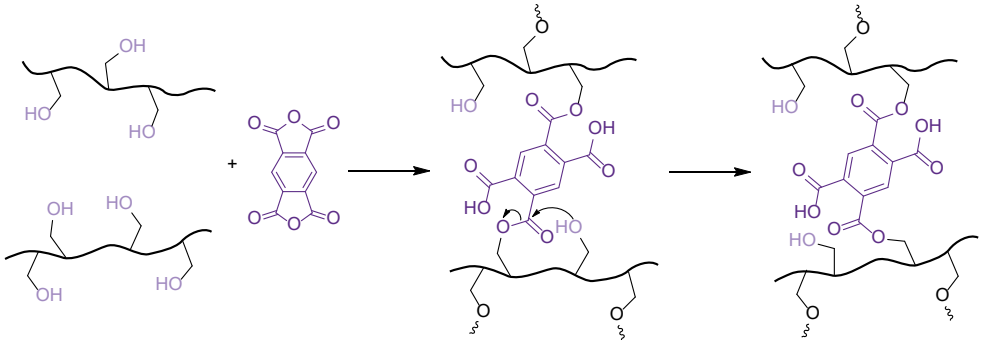

Scheme 5.4. The crosslinking of linear polymer via reaction of pyromellitic dianhydride and hydroxyl side groups, followed by a transesterification rearrangement.

Leibler and coworkers found that the concentration of hydroxyl groups present is an important parameter in controlling the reaction kinetics.[8] In the designed system, the concentration of free hydroxyl groups is varied by tuning the amount of pyromellitic dianhydride added to the system. Higher amounts of pyromellitic dianhydride will consume more free hydroxyl groups and lead to a higher crosslink density. To gain more information about the exchange mechanism for these self-catalyzed systems, networks with and without abundant free hydroxyl groups are prepared. The reversibility of both systems is evaluated by stress relaxation experiments.

5.2 Network synthesis

First, a linear copolymer of methyl methacrylate (MMA), butyl methacrylate (BMA) and hydroxyethyl methacrylate (HEMA), Figure 5.1a, was synthesized in solution using free radical polymerization. The molar ratios of the obtained copolymer were 0.4 eq. methyl methacrylate, 0.51 eq. butyl methacrylate and 0.09 eq. hydroxyethyl methacrylate as determined by NMR spectroscopy. The use of HEMA yielded free hydroxyl side groups which could later be used for crosslinking. The combination of monomers yielded a material with a T_g of 57 °C (Figure 5.1c), which facilitates the analysis of exchange reactions at a temperature above 100 °C.[25] The polymer showed excellent thermal stability in TGA, only 1% of weight loss at 250 °C, Figure 5.1d.

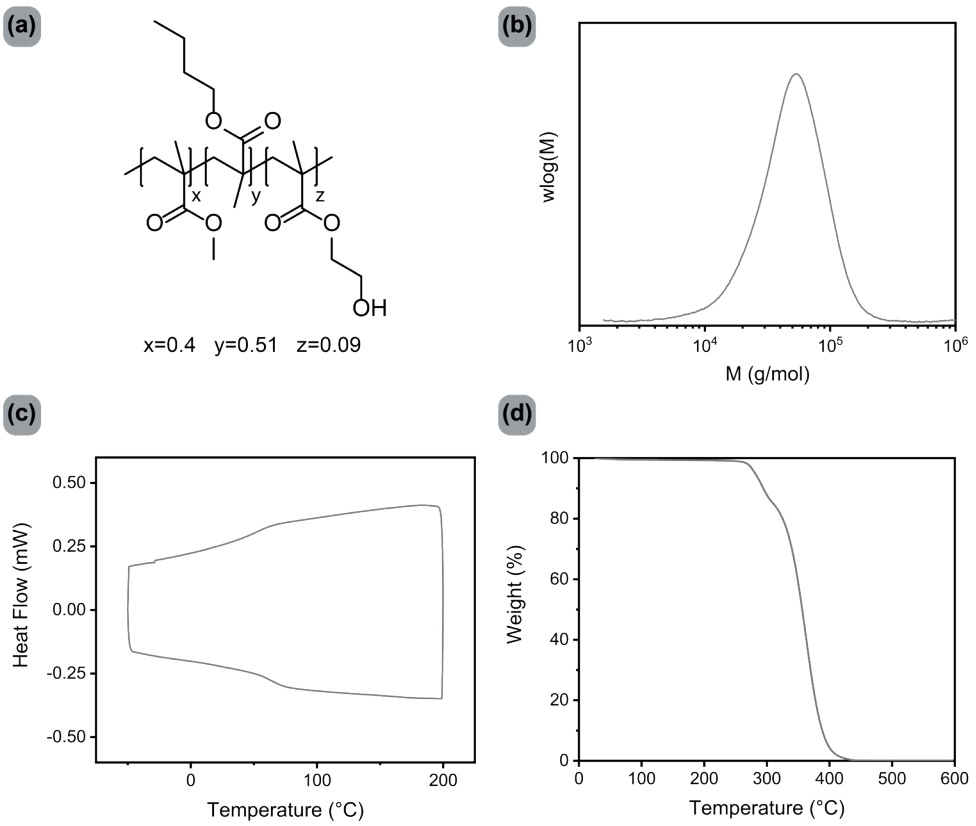

Figure 5.1. Properties of the linear polymer with hydroxyl side groups. **(a)** The molecular structure with the monomer ratio as determined by NMR. **(b)** The molecular weight determined by SEC. **(c)** The T_g by DSC measured from -50 °C to 200 °C with a rate of 20 °C/min. **(d)** The thermal stability via TGA measured under N_2 with a heating rate of 10 °C/min.

Pyromellitic dianhydride was used as a divalent crosslinker, in which each formation of an ester crosslink subsequently leads to the formation of an internal carboxylic acid catalyst as well. By adjusting the amount of pyromellitic dianhydride crosslinker, two networks with different concentrations of free hydroxyl groups were obtained (Figure 5.2). In system A, half an equivalent of anhydride with respect to free hydroxyl groups was added. This yielded a network with a 1:1 ratio of ester crosslinks to free hydroxyl groups. In system B, an equimolar amount of anhydride groups was added, which means all hydroxyl groups can form a crosslink, yielding a maximally cured network. The crosslinking reactions were performed in toluene at 110 °C and yielded an organogel for both systems. After removal of the solvent, the resulting polymer networks were processed by compression molding using 100 bar at 180 °C for 30 minutes. Using this crosslinking method, there could still be some residual free hydroxyl groups in system B due to hydrolysis of the anhydride or uncomplete conversion. However, the amount of hydroxyl groups should be significantly lower than in system A.

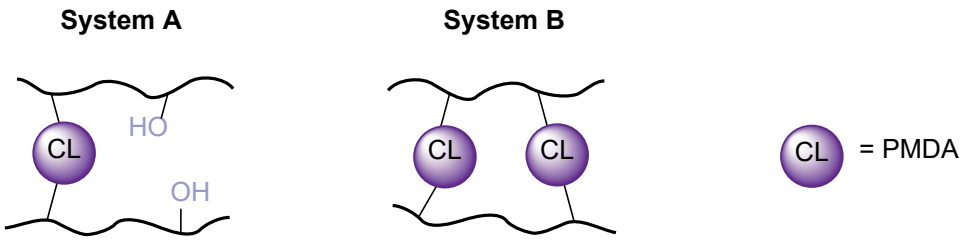

Figure 5.2. Schematic representation of the two different networks synthesized. System A had equal amounts of ester crosslinks and free hydroxyl groups, where in system B all hydroxyl groups have been converted to ester crosslinks.

The thermal properties and stability of both systems were determined by DSC and TGA before and after compression molding (Figure 5.3). The T_g for system A was 70 °C and for system B it was 78 °C.

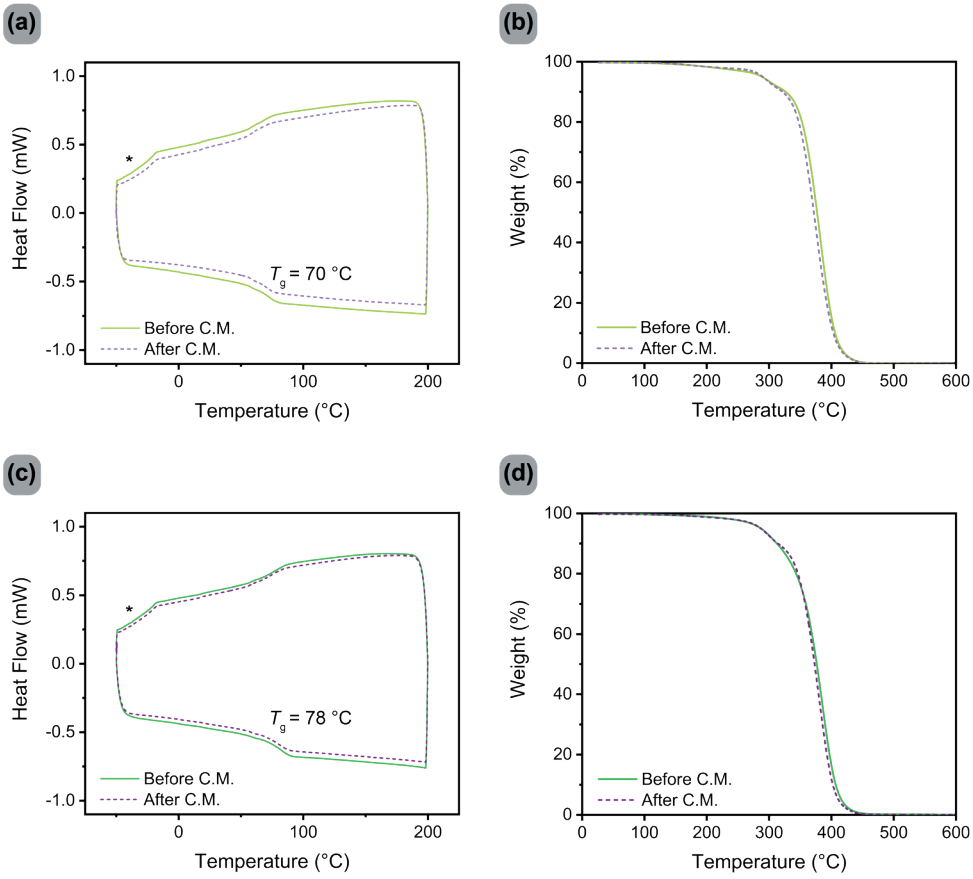

Figure 5.3. Effect of compression molding (C.M.) on the thermal properties (DSC) and thermal stability (TGA) of crosslinked polymers **(a,b)** System A. **(c,d)** System B.
* is an artifact related to the cooling rate programmed for the experiment.

Compression molding of the polymers did not lead to significant changes in the DSC traces (Figure 5.3 a, c). From TGA, it is clear that the temperature used for compression molding was sufficiently low to avoid any thermal degradation (Figure 5.3 b, d), and no significant changes occurred due to the compression molding. The thermal stability of the networks was similar to that of the linear polymer.
The solubility of the compression molded samples (approximately 250 mg each) was determined by stirring them in tetrahydrofuran for 3 days. The high gel content of ≥ 90% confirmed the formation of a polymer network, as the linear polymer was fully soluble in tetrahydrofuran.

5.3 System A: with free hydroxyl groups

The time and temperature dependent stress relaxation properties of the system with free hydroxyl groups, system A, were studied. Prior to the stress relaxation experiment, samples were subjected to an oscillatory shear for 30 minutes to determine the modulus, and subsequently equilibrate the sample at the desired temperature. After the relaxation experiment another 30-minute oscillatory shear experiment was performed to check for changes in the material properties. The experiments were performed in the linear viscoelastic regime at 3% strain. The normalized stress relaxation moduli, G(t)/G(0) are shown in Figure 5.4a for three different temperatures. At all three temperatures, relaxation is observed, which proves the effectivity of the intrinsic carboxylic acid catalyst. The system shows a clear temperature dependence, where higher temperatures lead to faster relaxation. However, at none of the probed temperatures full relaxation of the applied stress was observed which is indicative of thermoset behavior. To better compare the plateau stresses, the time was normalized to t/t_{ref} (Figure 5.4b), where t_{ref} is a reference time, here taken as the time to reach 37% of the initial applied stress. (this would have corresponded to the characteristic relaxation time, τ, if the data had followed a Maxwel model).[7] Normalizing the time shows that at all three probed temperatures, a minimum stress of ~20% of the initial stress was reached.

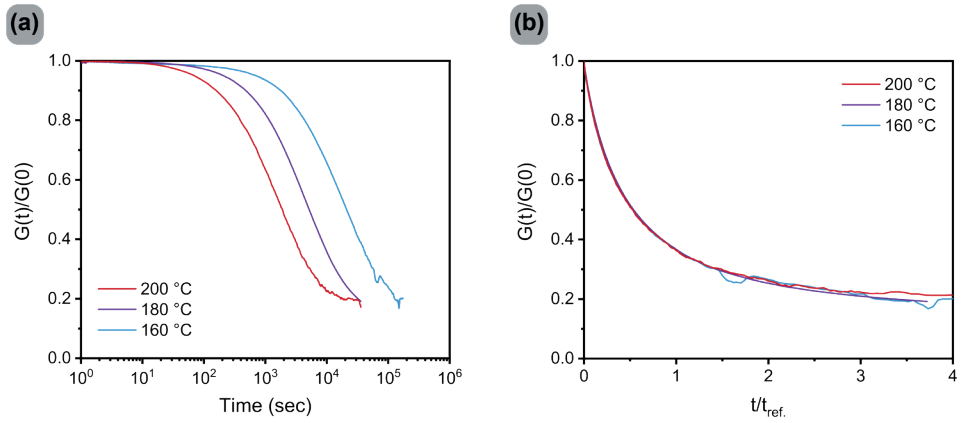

Figure 5.4. Stress relaxation experiments of polymer with excess hydroxyl groups. **(a)** Normalized stress relaxation curves at 160, 180 and 200 °C. **(b)** Time-normalized stress relaxation curves with respect to t/t_{ref} where t_{ref} is taken as 37%.

It is clear from the data above that the use of a Maxwell model for the estimation of an activation energy of the stress relaxation is not appropriate and a more complex model is required. Here, a simple extension of the Maxwell model was made by putting a second spring in parallel (representing the permanent crosslinks),[26] which results in the following equation for the normalized relaxation modulus:

$$\frac{G(t)}{(G)(0)} = \left(\frac{G(t)}{G(0)}\right)_{\infty} + e^{-\frac{t}{\tau}} \quad (1)$$

where the first term on the right-hand side of the equation is the plateau value in the curve, which in all cases of Figure 5.4a was set equal to 0.20. The fit results of using equation 1 to fit the data in Figure 5.4a are shown in Figure 5.5a. Considering the simplicity of the model (and the assumption of a chemically unchanging material), a remarkable agreement between model fit and experimental data is observed. In Figure 5.5b, the values for the relaxation times, τ, are shown as an Arrhenius plot and an activation energy of ~99 kJ/mol was obtained, which is lower than what is typically observed in Zn^{2+} catalyzed polyester vitrimers,[9,11,16] but close to what was found in on-going studies on PMDA crosslinked polyesters in our group.

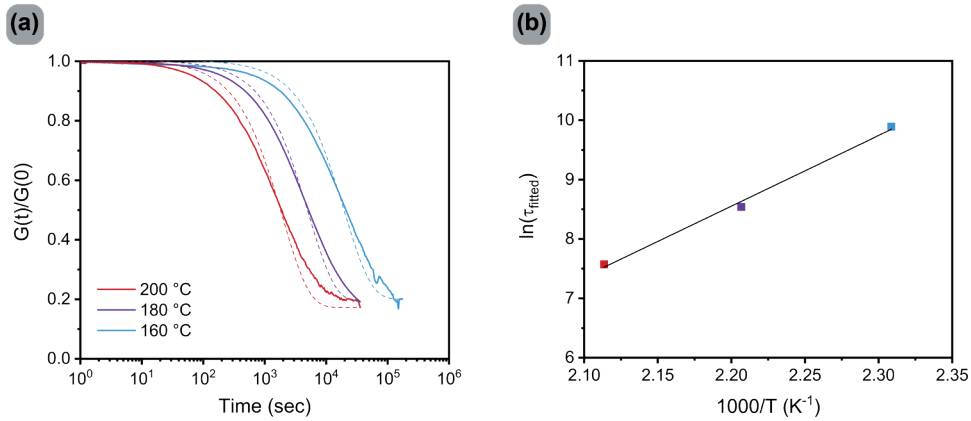

Figure 5.5. Stress relaxation experiments of polymer with excess hydroxyl groups. **(a)** Normalized stress relaxation curves at 160, 180 and 200 °C with the modified Maxwell fits (equation 1) as dotted lines. **(b)** Arrhenius relationship used to determine the activation energy, where τ_{fitted} were obtained by fitting equation 1 to the data in Figure 5.4a.

An indication for the origin of the residual stress was found in the moduli obtained before and after relaxation experiments (Table 5.1). For the sample measured at 200 °C, the initial modulus of the material was 0.22 MPa, while after stress relaxation experiments a storage modulus of around 0.9 MPa was measured. The moduli for samples measured at 180 °C and 160 °C also strongly increased.

Table 5.1. Moduli before and after stress relaxation experiments at different temperatures, determined from oscillatory shear experiments with a strain of 3% and a frequency of 1 Hz.

Measuring temperature [°C]	Initial G' [MPa]	Final G' [MPa]	Residual stress [%]
160	0.27	0.81	19
180	0.24	0.67	19
200	0.22	0.90	20

The observed increase in modulus indicates that additional curing takes place during the relaxation experiment. To determine the contribution of thermal curing to the observed modulus increase, a sample was kept in an oven at 200 °C for 10 hours, the same time period as used for the relaxation experiment at 200 °C. The storage modulus at 200 °C of this thermally post cured sample increased from 0.23 to 0.47 MPa. This is a strong increase yet not quite as high as the 0.85 MPa measured after relaxation experiments. However, as shown in Chapter 3, oscillatory forces applied during heating may lead to additional curing. To check whether shear contributed to curing in the current material, a sample was subjected to oscillatory strain for 10 h at 200 °C. During this experiment, the modulus increased from 0.22 MPa to 0.86 MPa (Figure 5.6), comparable to the value obtained after the stress relaxation experiments at the same temperature.

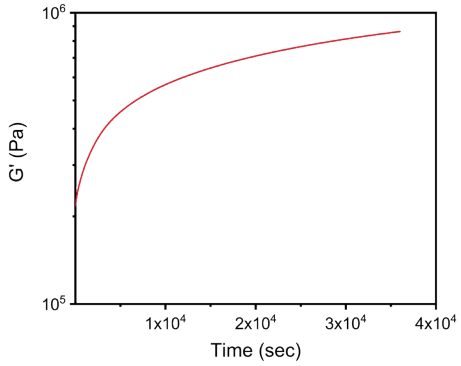

Figure 5.6. Time dependence of the storage modulus at 200 °C under an oscillatory strain of 3%.

Reaction of residual anhydrides present in the material would create additional crosslinks and increase the modulus. Such additional crosslinks would still be reversible and do not explain the observed residual stress of 20%. Therefore, it is very likely that part of the additional curing is caused by a reaction of hydroxyl groups with the two free carboxylic acid groups in the PMDA diester to form an additional ester crosslink (Scheme 5.5).[27] This reaction can occur without addition of a catalyst, but acids are known to catalyze these reactions.[28] If crosslinks are formed via esterification of the carboxylic acid, the effect is two-fold. First, the crosslink density and modulus increase. Secondly, a carboxylic acid is consumed which reduces the catalytic activity and thus slows down relaxation.

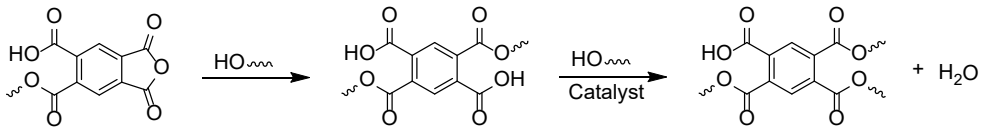

Scheme 5.5. The proposed reaction of carboxylic acid and hydroxyl groups forming a second ester bond, causing the additional curing in the system.

TGA data of a sample after a stress relaxation experiment at 200 °C showed a slight increase in thermal stability (Figure 5.7). This is an indication of additional crosslinking reactions caused by the prolonged thermal treatment. The increase in the number of crosslinks is likely to improve the thermal stability, and any acid catalyzed degradation is reduced.

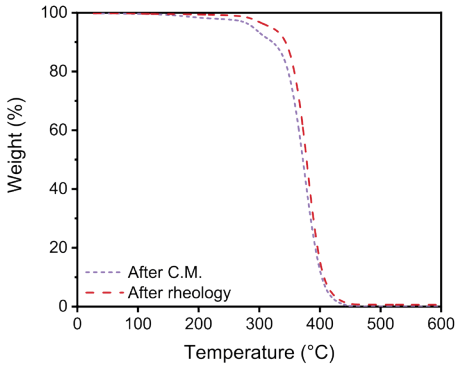

Figure 5.7. Thermal stability of a sample after compression molding (C.M.) at 180 °C, and a sample after a stress relaxation experiment at 200 °C.

5.4 System B: without free hydroxyl groups

The reaction mechanism applicable to the systems reported by Leibler *et al.* requires the presence of free hydroxyl groups for an efficient exchange reaction.[7,8] The alcohol will act as a nucleophile, attacking the ester carbon and forming a tetrahedral intermediate. This addition is followed by elimination of an alcohol, which reforms again an ester and an alcohol. Work in our group with pyromellitic dianhydride indicated that another reaction mechanism might be possible for our system. To elucidate the dynamic nature of networks without free hydroxyl groups (system B), the stress relaxation behavior was studied at different temperatures. Prior to stress relaxation and immediately after, a time sweep with an oscillatory force was performed to determine the modulus of the material. All experiments were performed in the linear viscoelastic regime (using 3% strain). The normalized stress relaxation moduli, G(t)/G(0) at different temperatures are shown in Figure 5.8a, and the relaxation moduli normalized to t/t_{ref} are shown in Figure 5.8b.

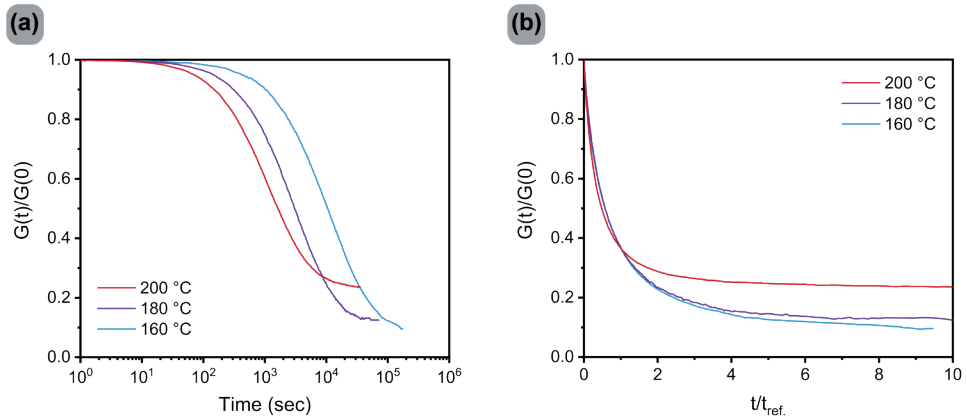

Figure 5.8. Stress relaxation experiments of polymer with equimolar amount of crosslinker. **(a)** Normalized stress relaxation curves at 160, 180 and 200 °C. **(b)** Time-normalized stress relaxation curves with respect to t/t_{ref} where t_{ref} is taken as 37%.

The system showed efficient stress relaxation, although there are minimal to no free hydroxyl groups present in the network. The relaxation rates for this system are very similar to those observed in system A, and fitting the data to equation 1 results in an estimated activation energy of ~95 kJ/mol, which is very close to the value obtained for system A.

These results indicate that the relaxation rate for this system is not dependent on the concentration of free hydroxyl groups and that the rate determining step is not the attack of the alcohol of the ester carbon (Scheme 5.1). If the carboxylic acid is able to catalyze the reformation of the anhydride, this would also reform a free hydroxyl group (Scheme 5.6). At elevated temperatures, the ring opening of anhydrides occurs very fast in the presence of alcohols and via this route relaxation could occur. Similar observations were also reported by Hillmyer *et al.* and Altuna and coworkers with different polymer systems.[29,30] Both these systems showed relaxation without significant concentrations of free hydroxyl groups.

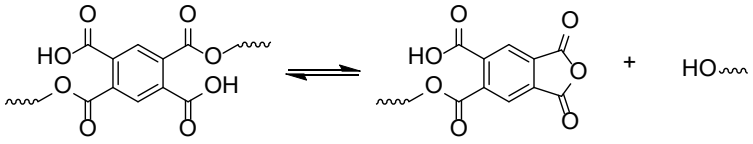

Scheme 5.6. The proposed reversible reaction which would enable exchange without presence of ample hydroxyl groups.

From Figure 5.8 it is also clear that no full relaxation occurs and that the residual stress after relaxation is dependent on the temperature at which the relaxation experiment is performed, Figure 5.8b. The sample measured at 200 °C reached a plateau stress of 24% of the initial applied stress, where the samples measured at 180 °C and 160 °C reached 13% and 10%, respectively. With system A, the residual stress was attributed to thermally induced side reactions between carboxylic acids and hydroxyl groups. If the exchange

reaction were to follow an associative pathway, only residual unreacted hydroxyl groups would be able to participate in the side reaction. In the case of a dissociative mechanism, there is reformation of free hydroxyl groups which can then participate in the side reaction with carboxylic acid. Therefore, the temperature dependent minimal stress is another indication of a dissociative mechanism. If the temperature is increased, more molecules will be dissociated resulting in more curing due to side reactions and thus less relaxation.

It was hypothesized that the residual stress in the system was due to formation of additional non reversible crosslinks during the stress relaxation experiment. This curing was studied with oscillatory time sweep experiments. In Figure 5.9, the modulus over time for was plotted at 160 °C and 200 °C. When a sample was measured for 10 hours at 200 °C, the modulus increased from 0.40 MPa to 1.26 MPa, while the same experiment at 160 °C only increased the storage modulus from 0.42MPa to 0.8 MPa. So, a lower temperature during the measurement led to lower additional curing and a higher amount of stress relaxation. This corresponds with the stress relaxation data, where the systems which showed less additional curing also showed more stress relaxation.

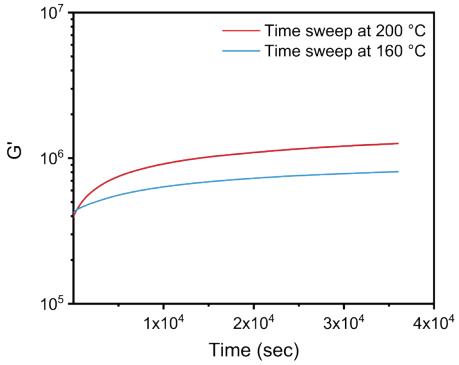

Figure 5.9. Time dependence of the storage modulus measured using oscillatory strain of 3% at 200 °C (red curve) and at 160 °C (blue curve).

5.5 Conclusions

A linear polymer with hydroxyl side groups was successfully crosslinked using pyromellitic dianhydride as a crosslinker. Solubility experiments showed the formation of a network. The crosslinking reaction occurred at elevated temperatures without addition of a catalyst. Formation of each ester crosslink is accompanied with the formation of a carboxylic acid.

Stress relaxation data of system A with a 1:1 ratio of ester and hydroxyl functionalities show the effectiveness of the carboxylic acid as internal catalysts. Unfortunately, no full relaxation of the initial stress was observed. A strong increase in the modulus during oscillatory strain experiments indicated thermal curing. The residual stress combined with increased thermal stability hints at thermally induced side reactions of the free hydroxyl

groups, forming additional crosslinks with the free carboxylic acid groups, and reducing the catalytic activity.

Surprisingly, a system without excess free hydroxyl groups also showed efficient relaxation of an applied stress. The relaxation rate of this system is comparable to the system with excess free hydroxyl groups, which indicated the rate of relaxation for these systems is independent on the concentration of free hydroxyl groups. This can be explained when the exchange takes place via a dissociative mechanism. The rate of exchange is then determined by the formation of an anhydride intermediate. Supporting the hypothesis for this anhydride intermediate is the temperature dependent residual stress. It was hypothesized that the residual stress is a result of acid-alcohol esterification and thus if only a minimal number of free hydroxyl groups is present in the system, then the amount of side reaction and thus residual stress will also be minimal. In the case of a dissociative mechanism, formation of an anhydride intermediate would also lead to formation of free hydroxyl groups which can participate in the proposed side reaction.

5.6 Experimental details

Materials

All commercial chemicals and solvents were used as received, unless stated otherwise. pyromellitic dianhydride and 2-hydroxyethyl methacrylate were obtained from TCI EUROPE. All other chemicals for the synthesis were purchased from Sigma Aldrich. All solvents were obtained from Biosolve.

Synthesis of poly(methyl-co- butyl -co- (hydroxyethyl) methacrylate):

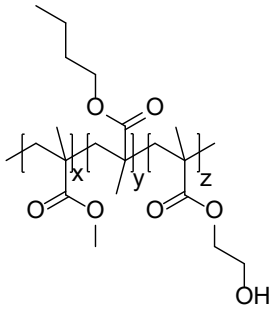

Inhibitor was removed from MMA, BMA and HEMA monomers by filtration over basic alumina. MMA (12.9 mL, 4.5 eq.) BMA (19 mL, 4.5 eq.) and HEMA (3.3 mL, 1.0 eq.) were dissolved in THF (150 mL). The solution was cooled to 0 °C and degassed by purging with argon for 30 minutes. 1-decanethiol (0.01 M) and AIBN (0.005 M) were added to the solution. Still under argon conditions, the reaction mixture was heated to 60 °C to start the polymerization. After 19 hours, the monomer conversion was found to be 74% via NMR. The reaction was stopped by addition of hydroquinone. The mixture was precipitated in 10-fold v/v cold methanol, yielding a white sticky solid. The precipitate was filtered and dried in a vacuum oven at 70 °C for a period of 16 h. The final product (8.6 g) was obtained as a white solid. The yield was low due to precipitation because low molecular weight polymer was still in the methanol.

^{1}H NMR (400 MHz, $CDCl_3$): δ [ppm] = 4.12 (br. s, $OC\underline{H}_2CH_2OH$), 3.95 (s, $OC\underline{H}_2(CH_2)_2CH_3$), 3.84 (br. s, $OCH_2C\underline{H}_2OH$), 3.60 (s, $COOC\underline{H}_3$), 2.13 – 1.71 (multiple $C\underline{H}_2$ main chain peaks), 1.61 (br s, $COOCH_2C\underline{H}_2CH_2CH_3$), 1.4 (br s, $COOCH_2CH_2C\underline{H}_2CH_3$), 1.15 – 0.60 (multiple $C\underline{H}_3$ peaks)

GPC analysis showed a single broad polymer peak with a M_w of ~48000 g/mol, with respect to polystyrene standards, PDI ≈ 1.4.

Network synthesis:
The linear poly(methyl-co- butyl -co- (hydroxyethyl) methacrylate) (7 g) was dissolved in 20 mL toluene. The desired amount of pyromellitic dianhydride (0.16 mg for ratio 0.25 and 0.32 mg for ratio 0.5). The suspension was heated for five days at 110 °C resulting in an organogel. The gel was transferred to aluminum molds, and solvent was removed using a vacuum oven at 80 °C for two nights.

Rheology sample preparation:
The crosslinked polymer was compression molded into disk or bar shaped samples, using a Collin Press 300 G with an operating temperature of 180 °C, pressure of 100 bar for 30 minutes and subsequently cooled with water.

Characterization methods
Differential Scanning Calorimetry (DSC): T_g of the polymers was measured using a TA Instruments Q2000 differential scanning calorimeter equipped with an RCS90 cooling accessory using aluminum hermetic pans. 5-10 mg of sample was used per measurement. The general method consisted of four cycles were a sample was measured from -50 to 200 °C with heating and cooling rates of 10 °C min^{-1} (cycle 1 and 2), 20 °C min^{-1} and 40 °C min^{-1}, for clarification only cycle 2 is shown. TRIOS software was used for data acquisition, midpoint at half height was used to determine T_g.
Gel fraction: The mass fraction of the crosslinked part of the material is defined as the gel fraction. A bar of crosslinked material (~250 mg) was weighed and immersed for 70 hours in 10 mL THF at room temperature. The samples were filtered and dried in a vacuum oven at 60 °C in a vacuum oven. The gel fraction was determined using equation 2:[31]

$$\text{Gel fraction} = \frac{m_{extracted}}{m_{initial}} \quad (2)$$

Where $m_{extracted}$ is the mass of the sample after extraction and subsequent drying, and $m_{initial}$ the original weight of the sample.
Nuclear magnetic resonance spectroscopy (NMR): ^{1}H NMR spectra were recorded on a 400 MHz Bruker Advance III HD (400 MHz for ^{1}H NMR) spectrometer. Chemical shifts (δ) are expressed in ppm with respect to tetramethylsilane (TMS, 0 ppm) as an internal standard.
Rheology: The mechanical properties and stress relaxation behavior of disk-shaped samples were determined using a stress-controlled AR-G2 rheometer (TA instruments) using 8 mm parallel plate geometry. Time sweeps at constant temperature were performed using a strain of 3% with a frequency of 1 Hz. Stress relaxation experiments were performed at a temperature range between 160 °C and 200 °C with a strain of 3% using a constant normal force of 15 N to ensure contact. The used strain of 3% is within the linear viscoelastic regime.
Size exclusion chromatography (SEC): Molecular mass of the linear polymers was measured on a Shimadzu Prominence-I LC-2030C 3D equipped with two Agilent columns (mixed C and mixed D) with a combined range of 200-2000000 g/mol. The used eluent was THF with a flow rate of 1 mL min^{-1} at 40 °C. The molecular weight is determined based on narrow dispersity polystyrene standards purchased from Agilent.

Thermogravimetric analysis: Thermal stability studies were performed in a TA instruments TGA Q500 machine. Samples were heated under nitrogen conditions (flow 60 mL min^{-1}) from 26 °C to 600 °C with a heating rate of 10 °C min^{-1}.

5.7 References

(1) Denissen, W.; Winne, J. M.; Du Prez, F. E. Vitrimers: Permanent Organic Networks with Glass-like Fluidity. *Chem. Sci.* **2015**, *7* (1), 30–38.

(2) Fox, M. A.; Whitesell, J. K. Nucleophilic Addition and Substitution at Carbonyl Groups. In *Organic Chemistry*; 2003; pp 570–637.

(3) Otera, J. Transesterification. *Chem. Rev.* **1993**, *93* (4), 1449–1470.

(4) Solomons, G. T. W.; Fryhle, C. B. Carboxylic Acids and Their Derivatives. Nucleophilic Addition - Elimination at the Acyl Carbon. In *Organic Chemistry*; 2004; pp 811–866.

(5) Ji, L. N. Study on Preparation Process and Properties of Polyethylene Terephthalate (PET). *Appl. Mech. Mater.* **2013**, *312*, 406–410.

(6) Fukuda, H.; Kond, A.; Noda, H. Biodiesel Fuel Production by Transesterification of Oils. *J. Biosci. Bioeng.* **2001**, *92* (405–416).

(7) Montarnal, D.; Capelot, M.; Tournilhac, F.; Leibler, L. Silica-like Malleable Materials from Permanent Organic Networks. *Science* **2011**, *334* (6058), 965–968.

(8) Capelot, M.; Montarnal, D.; Tournilhac, F.; Leibler, L. Metal-Catalyzed Transesterification for Healing and Assembling of Thermosets. *J. Am. Chem. Soc.* **2012**, *134* (18), 7664–7667.

(9) Capelot, M.; Unterlass, M. M.; Tournilhac, F.; Leibler, L. Catalytic Control of the Vitrimer Glass Transition. *ACS Macro Lett.* **2012**, *1* (7), 789–792.

(10) Kloxin, C. J.; Bowman, C. N. Covalent Adaptable Networks: Smart, Reconfigurable and Responsive Network Systems. *Chem. Soc. Rev.* **2013**, *42* (17), 7161–7173.

(11) Zhou, Y.; Groote, R.; Goossens, J. G. P.; Sijbesma, R. P.; Heuts, J. P. A. Tuning PBT Vitrimer Properties by Controlling the Dynamics of the Adaptable Network. *Polym. Chem.* **2019**, *10* (1), 136–144.

(12) Imbernon, L.; Norvez, S. From Landfilling to Vitrimer Chemistry in Rubber Life Cycle. *Eur. Polym. J.* **2016**, *82*.

(13) Cao, L.; Fan, J.; Huang, J.; Chen, Y. A Robust and Stretchable Cross-Linked Rubber Network with Recyclable and Self-Healable Capabilities Based on Dynamic Covalent Bonds. *J. Mater. Chem. A* **2019**, *7* (9), 4922–4933.

(14) Yang, Z.; Wang, Q.; Wang, T. Dual-Triggered and Thermally Reconfigurable Shape Memory Graphene-Vitrimer Composites. *ACS Appl. Mater. Interfaces* **2016**, *8* (33), 21691–21699.

(15) Pei, Z.; Yang, Y.; Chen, Q.; Wei, Y.; Ji, Y. Regional Shape Control of Strategically Assembled Multishape Memory Vitrimers. *Adv. Mater.* **2016**, *28* (1), 156–160.

(16) Zhang, B.; Kowsari, K.; Serjouei, A.; Dunn, M. L.; Ge, Q. Reprocessable Thermosets for Sustainable Three-Dimensional Printing. *Nat. Commun.* **2018**, *9* (1831).

(17) Nakatake, D.; Yokote, Y.; Matsushima, Y.; Yazaki, R.; Ohshima, T. A Highly Stable but Highly Reactive Zinc Catalyst for Transesterification Supported by a Bis(Imidazole) Ligand. *Green Chem.* **2016**, *18* (6), 1524–1530.

(18) Lessard, J. J.; Garcia, L. F.; Easterling, C. P.; Sims, M. B.; Bentz, K. C.; Arencibia, S.; Savin, D. A.; Sumerlin, B. S. Catalyst-Free Vitrimers from Vinyl Polymers. *Macromolecules* **2019**, *52* (5), 2105–2111.

(19) Han, J.; Liu, T.; Hao, C.; Zhang, S.; Guo, B.; Zhang, J. A Catalyst-Free Epoxy Vitrimer System Based on Multifunctional Hyperbranched Polymer. *Macromolecules* **2018**, *51* (17), 6789–6799.

(20) Chabert, E.; Vial, J.; Cauchois, J.-P.; Mihaluta, M.; Tournilhac, F. Multiple Welding of Long Fiber Epoxy Vitrimer Composites. *Soft Matter* **2016**, *12* (21), 4838–4845.

(21) Altuna, F. I.; Pettarin, V.; Williams, R. J. J. Self-Healable Polymer Networks Based on the Cross-Linking of Epoxidised Soybean Oil by an Aqueous Citric Acid Solution. *Green Chem.* **2013**, *15* (12), 3360–3366.

(22) Esterification. *Van Nostrand's Scientific Encyclopedia*. April 14, 2006.

(23) Thanassi, J. W.; Bruice, T. C. Neighboring Carboxyl Group Participation in the Hydrolysis of Monoesters of Phthalic Acid. The Dependence of Mechanisms on Leaving Group Tendencies. *J. Am. Chem. Soc.* **1966**, *88* (4), 747–752.

(24) Tao, B.; Xia, H.; Huang, C.-X.; Li, X.-W. Hydrolytic Ring Opening Reactions of Pyromellitic Dianhydride for Divalent Transition Metal Carboxylate Complexes. *Zeitschrift für Anorg. und Allg. Chemie* **2011**, *637* (6), 703–707.

(25) Polymer Properties Database. Glass Transition Temperatures http://polymerdatabase.com/polymer physics/Polymer Tg.html (accessed Feb 5, 2019).

(26) David Roylance. Engineering Viscoelasticity. *Eng. Viscoelasticity* **2014**, 1–37.

(27) Otera, J.; Nishikido, J. Reaction of Alcohols with Carboxylic Acids and Their Derivatives. In *Esterification: Methods, Reactions, and Applications*; 2010; pp 5–158.

(28) Thorat, T. S.; Yadav, V. M.; Yadav, G. D. Esterification of Phthalic Anhydride with 2-Ethylhexanol by Solid Superacidic Catalysts. *Top. Catal.* **1992**, *90* (2), 73–96.

(29) Brutman, J. P.; Delgado, P. A.; Hillmyer, M. A. Polylactide Vitrimers. *ACS Macro Lett.* **2014**, *3* (7), 607–610.

(30) Zhao, Q.; Zou, W.; Luo, Y.; Xie, T. Shape Memory Polymer Network with Thermally Distinct Elasticity and Plasticity. *Sci. Adv.* **2016**, *2* (1), e1501297.

(31) Chauvet, J.; Asua, J. M.; Leiza, J. R. Independent Control of Sol Molar Mass and Gel Content in Acrylate Polymer/Latexes. *Polymer (Guildf).* **2005**, *46* (23), 9555–9561.

Chapter 6

Epilogue

6.1 Introduction

The work presented in this thesis reports the development of thermally triggered dynamic covalent polymers. It was envisaged that these polymers aid in the production of commercially viable products produced via stereolithography. Stereolithography is a very popular and widely used 3D printing technique which allows the production of customized acrylic products within minutes.[1,2] Stress development due to polymerization induced volumetric shrinkage is the largest shortcoming of this technique.[3] Introduction of dynamic covalent bonds offers unique opportunities to reduce this stress by efficient bond exchange. An additional advantage of using dynamic covalent polymers is the possibility to improve layer to layer adhesion. As each layer of the product is polymerized separately, the interactions within two different layers is often weaker than the interaction within a single layer.[4] By bond exchange a covalent connection can be formed between separately printed layers, Figure 6.1.

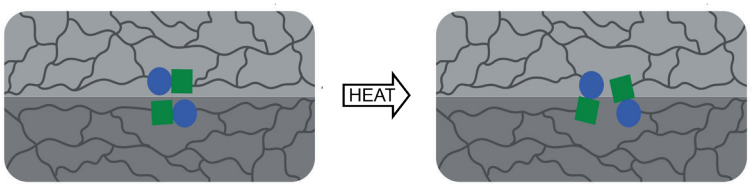

Figure 6.1 Schematic representation of the formation of covalent bonds between two printed layers.

To achieve a high crosslink density, the resins for stereolithography often contain high amounts of multifunctional monomers.[5] Another important requirement for the resin used for printing is a low viscosity. In order to ensure efficient layer recoating a viscosity below 5 Pa·s is required.[6] The final mechanical properties of a product can be tuned by using a mixture of monomers.[7] By incorporating exchangeable bonds in photopolymerizable monomers, dynamic covalent polymer products can be printed without any changes in the production process. A general design of photopolymerizable monomers for dynamic crosslinking is shown in Figure 6.2. The reversible group is in the center of the molecule, and via a spacer, two polymerizable groups are attached, in the example acrylate groups are shown. At high monomer conversions, both sides of the reversible group will be connected to the polymer. This will prevent leaching of reversible groups after opening has occurred.

Figure 6.2. The general design for photopolymerizable reversible monomers.

In this thesis, three chemical strategies towards exchangeable bonds have been investigated, namely Diels-Alder, transalkylation and transesterification chemistry. The mechanical properties of polymeric materials containing these exchangeable bonds were described. Here, a short recap of some of the conclusions are given, followed by strategies for incorporation in stereolithography. Some other future applications are proposed as well, and finally a general conclusion of the work is presented.

6.2 Overview of results

A photopolymerizable di-acrylic monomer containing Diels-Alder moieties was successfully synthesized (Figure 6.3). The viscosity of the obtained monomer was 1.9 Pa·s, which is well within the range for stereolithography. The monomer was successfully incorporated into a highly crosslinked polymer network using photopolymerization. It was shown by DSC and FTIR that the Diels-Alder structure remains stable during UV curing.

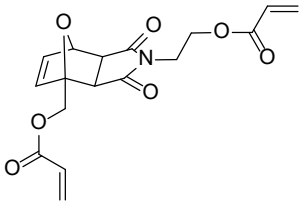

Figure 6.3. Chemical structure of the diacrylate monomer containing a Diels-Alder group.

Quantitative opening of the furan-maleimide Diels-Alder bonds was achieved by thermally treating the material. The reformation reaction proved to be less efficient and only minimal reformation was achieved by thermal annealing. It is known that the formation of furan-maleimide Diels-Alder bonds requires longer reaction times.[8] Reported reaction times in polymeric materials vary from several minutes to several hours depending on conditions such as concentration and temperature.[9,10] An additional factor which might inhibit the reformation, is the high crosslink density of the system which hinders the mobility of the reactive groups.

Another well-known type of reversible chemistry is the use of transesterification reactions, which are dependent on added catalysts for sufficient rate.[11] Here it was shown that by crosslinking linear chains containing free hydroxyl groups with pyromellitic dianhydride, a dynamic network polymer was obtained. The system did not require a dispersed catalyst, as the carboxylic acids formed during the network preparation were able to catalyze the exchange reaction. Remarkably, the concentration of free hydroxyl groups did not strongly affect the exchange rate. This indicated the contribution of a mechanism with an anhydride intermediate.

The previously described Diels-Alder and transesterification chemistries have been investigated extensively for applications in reversible materials. Alternative exchange reactions are also beginning to gain interest.[12] An example of such an alternative approach is the use of nucleophilic substitution reactions such as transalkylations. Kinetic studies on model reactions presented in this thesis show that DABCO quaternized with benzyl bromide is efficiently transalkylated with both DABCO and benzyl bromide. To study transalkylation in polymers, linear polyacrylates, functionalized with benzyl bromide groups were crosslinked efficiently with DABCO, resulting in insoluble polymer networks. Addition of excess DABCO de-crosslinked the system resulting in a soluble polymer. DABCO transalkylation proved to be efficient in this network, as in rheological testing the material showed full stress relaxation after 45 minutes at 140 °C.

During the characterization of the produced Diels-Alder polymers unexpected additional curing was observed. A detailed study of the origin for this curing with a non-reversible material unequivocally showed that a small oscillatory strain applied above T_g is responsible for the observed additional curing. The effect was observed with both tensile strain, DTMA, and shear strain, rheometry. Both are important characterization techniques used to study (dynamic covalent) polymer systems. It is important to keep in mind that while measuring the properties of a system, this system might change.

6.3 Future perspectives

Use of the Diels-Alder monomer described in Chapter 2 would be of interest to improve the lifetime of products produced via stereolithography. To really improve the material properties, the amount of bond reformation should be increased. The material used is highly crosslinked which strongly restricts the mobility of the exchangeable bonds and possibly hinders reformation of the Diels-Alder moeity.[13,14] A possible solution to this is the incorporation of additional reactive groups in the network. If the concentration of a functional group is increased, the chance of reformation with an opened reaction partner is increased.

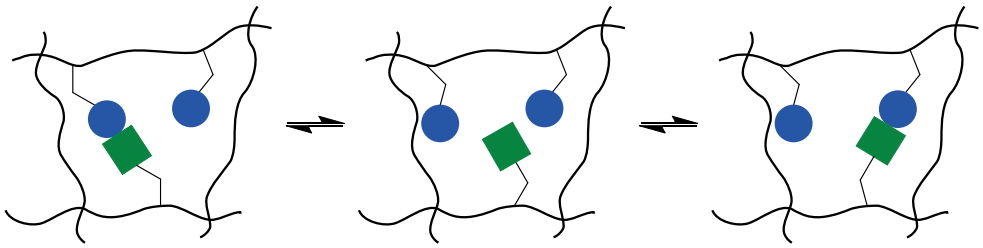

Scheme 6.1. Additional 'acceptor groups' increase the concentration of reversible bonds, which will facilitate bond reformation.

For the Diels-Alder system, the best candidate for an 'acceptor group' is the furan, as maleimide groups can initiate side reactions at elevated temperatures.[15] A furan acceptor could be synthesized via reaction of furfuryl alcohol and acryloyl chloride, Scheme 6.2.[16]

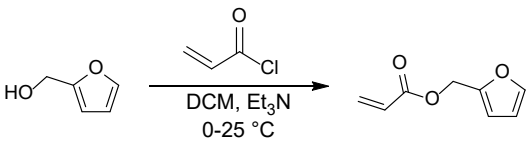

Scheme 6.2. The proposed reaction for the synthesis of a furan acceptor monomer to facilitate Diels-Alder reformation in a network.

For the transalkylation system, a dimethacrylate monomer was obtained by reacting the synthesized BrEMA monomer with DABCO, Scheme 6.3, resulting in a colorless precipitate. Centrifugation yielded the pure product. This monomer contained a bisbenzyl-DABCO moiety as the reversible group which showed efficient exchange reactions in small molecule kinetic studies.

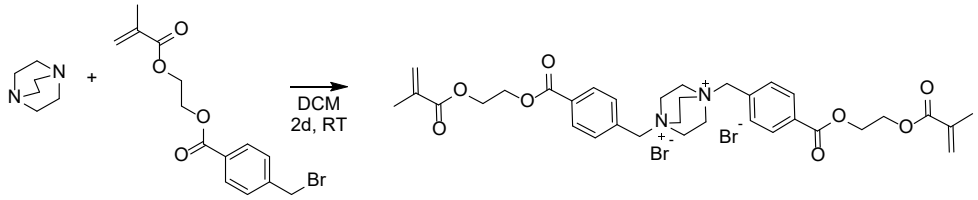

815 mg, 2 eq. 157 mg, 1 eq. yield = 62%

Scheme 6.3. Synthesis of a di-methacrylate monomer containing a bisbenzyl-DABCO moiety for relaxation of stresses through transalkylation in an acrylate resin.

To study if additional groups on the benzyl ring affected the reactivity of the system a kinetic experiment with free DABCO was performed, similar to the reaction reported in section 4.2. The reactants were mixed in a 1:1 ratio in DMSO and heated to 60 °C. The formation of monobenzyl-DABCO [P] was monitored via *in situ* ^{1}H NMR spectroscopy. The results are shown in Figure 6.4 where the same experiment without the polymerizable side chains was shown as a reference. The observed reaction rates are very similar, indicating that addition of polymerizable groups on the aromatic ring does not affect the reactivity of the system.

(a)

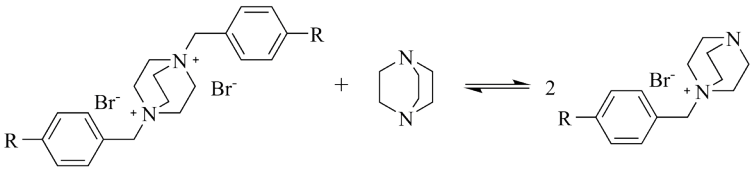

R= H for small molecule
R= acrylate-glycol-carbonyl for polymerizable side chain

(b)

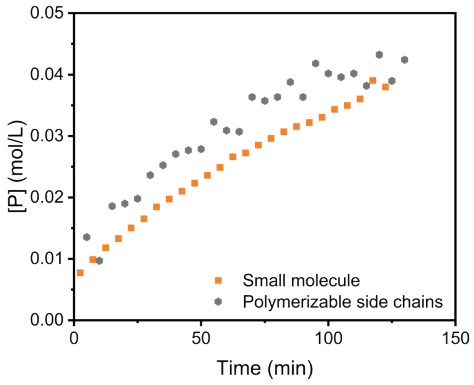

Figure 6.4. (a) Exchange reaction of bisbenzyl-DABCO (S) and free DABCO (D), for the diacrylate (R= acrylate-glycol-carbonyl) and model compound (R=H). **(b)** Formation of monobenzyl-DABCO at 60 °C with a concentration of 0.04 M for all reactants.

The transalkylation monomer was obtained as a solid, so incorporation into a resin will require more effort than with the previously described Diels-Alder containing monomer. If the monomer is not soluble in commonly used monomers, an oligomer or prepolymer could be synthesized, which might result in a liquid monomer that can be mixed in the resin.

For the transesterification system no new monomers were synthesized. A possible synthetic route towards a dimethacrylate monomer is shown in Scheme 6.4. The reaction between pyromellitic dianhydride and an alcohol to form a monoalkyl ester will occur readily at elevated temperatues.[17] A potential problem is that the elevated temperatures required for the reaction will cause spontaneous polymerization, hence the choice for methacrylate groups, as these are more thermally stable than acrylate groups. Addition of an inhibitor and careful tuning of the reaction conditions might help overcome this problem. Another issue is the hydrolysis of the pyromellitic dianhydride, which could be overcome by performing the reaction in dry conditions.

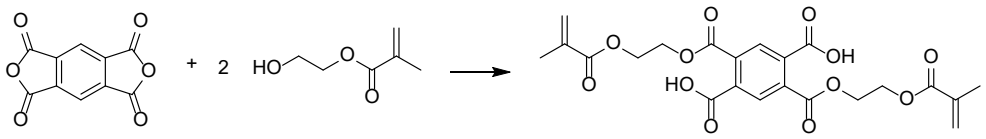

Scheme 6.4. The proposed reaction for the synthesis of monomers containing reversible transesterification groups.

Adaptable networks are not only interesting for reducing stress in photopolymers, but can be used in many applications to enhance material properties. By dynamic covalent chemistry, strong and solvent resistance polymer networks can be formed which are still moldable and recylabe.[18] Crosslinking of pre-formed linear polymers would offer opportunities to tune the dynamic properties of a network by adaptation of a small crosslinker molecule rather than the need for new monomer designs. Guan *et al.* showed that by using different crosslinkers, the reactivity of a reversible network is strongly influenced.[19] By changing the neighboring groups of the boronic ester crosslinks, they were able to tune the rate of exchange for different applications.

For example, the research described in this thesis showed that crosslinking of linear polymer chains with pyromellitic dianhydride yielded polymer networks which could be reshaped by compression molding at elevated temperatures. The carboxylic acid which is formed during the crosslinking reaction acts as an internal catalyst for the exchange reactions. Bates and coworkers investigated the catalytic strength of several Brønsted acids for transesterification reactions.[20] By combining this knowledge, it possible to design materials with tunable temperature dependence depending on the acid anhydride used for the crosslinking.

6.4 Conclusions

In this thesis, it was shown that incorporating dynamic covalent bond in polymers is a promising strategy to obtain materials with enhanced mechanical properties. Although many general concepts already have been known for years, the implementation in existing production methods is not trivial due to the need for specific raw materials demands which differ for each production method. Some potential strategies for the implementation in stereolithography discussed here are very promising. For other applications, a more convenient approach could be the crosslinking of commodity polymers with dynamic crosslinks. Besides enhanced mechanical properties, dynamic covalent bonds are also suitable to incorporate additional material functions such as shape memory, self-healing or recyclability. Given the many possibilities, dynamic covalent polymers have to offer, I expect there is a very promising future ahead for these polymers. And although the numerous examples that have already been shown, a few in this thesis and numerous in literature, additional reversible chemistries will certainly be developed and their areas of application will continue to grow.

6.5 References

(1) Wong, K. V.; Hernandez, A. A Review of Additive Manufacturing. *ISRN Mech. Eng.* **2012**, *2012*, 1–10.

(2) Tumbleston, J. R.; Shirvanyants, D.; Ermoshkin, N.; Janusziewicz, R.; Johnson, A. R.; Kelly, D.; Chen, K.; Pinschmidt, R.; Rolland, J. P.; Ermoshkin, A.; et al. Continuous Liquid Interface Production of 3D Objects. *Science.* **2015**, *347* (6228), 1349–1352.

(3) Karalekas, D.; Aggelopoulos, A. Study of Shrinkage Strains in a Stereolithography Cured Acrylic Photopolymer Resin. *J. Mater. Process. Technol.* **2003**, *136* (1–3), 146–150.

(4) Kotlinski, J. Mechanical Properties of Commercial Rapid Prototyping Materials. *Rapid Prototyp. J.* **2014**, *20* (6), 499–510.

(5) Davis, F. J.; Mitchell, G. R. Polymeric Materials for Rapid Manufacturing. In *Stereolithography: Materials, Processes and Applications*; Bártolo, P. J., Ed.; Springer US: Boston, MA, 2011; pp 113–139.

(6) Melchels, F. P. W.; Feijen, J.; Grijpma, D. W. A Review on Stereolithography and Its Applications in Biomedical Engineering. *Biomaterials* **2010**, *31* (24), 6121–6130.

(7) Decker, C.; Nguyen Thi Viet, T.; Decker, D.; Weber-Koehl, E. UV-Radiation Curing of Acrylate/Epoxide Systems. *Polymer (Guildf).* **2001**, *42* (13), 5531–5541.

(8) Tasdelen, M. A. Diels-Alder "Click" Reactions: Recent Applications in Polymer and Material Science. *Polym. Chem.* **2011**, *2* (10), 2133–2145.

(9) Chen, X.; Dam, M. A.; Ono, K.; Mal, A. A Thermally Re-Mendable Cross-Linked Polymeric Material. *Science.* **2002**, *295* (March), 1698–1703.

(10) Terryn, S.; Brancart, J.; Lefeber, D.; Van Assche, G.; Vanderborght, B. Self-Healing Soft Pneumatic Robots. *Sci. Robot.* **2017**, *2* (9), 1–13.

(11) Capelot, M.; Unterlass, M. M.; Tournilhac, F.; Leibler, L. Catalytic Control of the Vitrimer Glass Transition. *ACS Macro Lett.* **2012**, *1* (7), 789–792.

(12) Hendriks, B.; Waelkens, J.; Winne, J. M.; Du Prez, F. E. Poly(Thioether) Vitrimers via Transalkylation of Trialkylsulfonium Salts. *ACS Macro Lett.* **2017**, *6* (9), 930–934.

(13) Monzón, M.; Ortega, Z.; Hernández, A.; Paz, R.; Ortega, F. Anisotropy of Photopolymer Parts Made by Digital Light Processing. *Materials (Basel).* **2017**, *10* (1), 1–15.
(14) Cook, W. D.; Scott, T. F.; Quay-Thevenon, S.; Forsythe, J. S. Dynamic Mechanical Thermal Analysis of Thermally Stable and Thermally Reactive Network Polymers. *J. Appl. Polym. Sci.* **2004**, *93* (3), 1348–1359.
(15) Turkenburg, D. H.; Fischer, H. R. Diels-Alder Based, Thermo-Reversible Cross-Linked Epoxies for Use in Self-Healing Composites. *Polymer (Guildf).* **2015**, *79*, 187–194.
(16) Chen, Y.; Spiering, A. J. H.; Karthikeyan, S.; Peters, G. W. M.; Meijer, E. W.; Sijbesma, R. P. Mechanically Induced Chemiluminescence from Polymers Incorporating a 1,2-Dioxetane Unit in the Main Chain. *Nat. Chem.* **2012**, *4* (7), 559–562.
(17) Esterification. *Van Nostrand's Scientific Encyclopedia*. April 14, 2006.
(18) Montarnal, D.; Capelot, M.; Tournilhac, F.; Leibler, L. Silica-like Malleable Materials from Permanent Organic Networks. *Science.* **2011**, *334* (6058), 965–968.
(19) Cromwell, O. R.; Chung, J.; Guan, Z. Malleable and Self-Healing Covalent Polymer Networks through Tunable Dynamic Boronic Ester Bonds. *J. Am. Chem. Soc.* **2015**, *137* (20), 6492–6495.
(20) Self, J. L.; Dolinski, N. D.; Zayas, M. S.; Read De Alaniz, J.; Bates, C. M. Brønsted-Acid-Catalyzed Exchange in Polyester Dynamic Covalent Networks. *ACS Macro Lett.* **2018**, *7* (7), 817–821.

Curriculum Vitae

Eveline E. L. Maassen was born on 25th September 1990 in Beek, The Netherlands. After finishing her Higher General Secondary Education at Graaf Huyn College, Geleen, she began her studies in Chemistry at the Hogechool Zuyd, Heerlen. Internships were performed at MSD in Oss and at DSM Innovative Synthesis BV, Geleen. In 2012 she received her bachelor's degree after which she started the master's degree program Molecular Engineering at the TU/e, Eindhoven. In her final year, she completed a research project in the group of Prof. Rint Sijbesma on the synthesis of bisurea-based bolaamphiphiles with charged end groups; towards strain stiffening supramolecular hydrogels. She received her Master of Science degree in 2014. In March 2015, she began her PhD research on reversible chemistries for UV curable materials in the Supramolecular Polymer Chemistry group at the TU/e under supervision of Prof. Rint Sijbesma and Dr. Hans Heuts. The most important results are presented in this thesis.

List of Publications

Peer reviewed journal publications

- Anastasio, R.; Maassen, E.E.L.; Cardinaels, R.; Peters, G.W.M.; Breemen van, L.C.A. Thin film mechanical characterization of UV-curing acrylate systems. *Polymer*, **2018**, 150, 84-94
- Maassen, E.E.L.; Anastasio, R.; Breemen van, L.C.A.; Sijbesma, R.P.; Heuts, J.P.A. Thermal Stress Relaxation in Acrylate Networks via Reversible Diels-Alder Reactions. *Submitted*
- Maassen, E.E.L.; Anastasio, R.; Poto, S.; Cardinaels, R.; Sijbesma, R.P.; Breemen van, L.C.A.; Heuts, J.P.A. Strain-induced post-curing of thermosets: a DMTA study. *Submitted*
- Maassen, E.E.L; Heemskerk, X.R.; Ziegenbalg, N.; R.; Sijbesma, R.P.; Heuts J.P.A. Stress relaxation in dynamic polymer networks via transalkylation using DABCO. *To be Submitted*

Conference contributions, *poster, †oral:

- Dutch Polymer Days (DPD), March 2019, Lunteren, the Netherlands †
- Chemistry as Innovating Science (CHAINS), December 2018, Veldhoven, the Netherlands †
- Dutch Polymer Days (DPD), April 2018, Lunteren, the Netherlands †
- ICMS outreach symposium, February 2018, Eindhoven, the Netherlands (poster pitch award by popular vote)*
- Chemistry as Innovating Science (CHAINS), December 2017, Veldhoven, the Netherlands *
- Advanced Polymers via Macromolecular Engineering (APME), May 2017, Gent, Belgium *
- Dutch Polymer Days (DPD), March 2017, Lunteren, the Netherlands *
- Chemistry as Innovating Science (CHAINS), December 2016, Veldhoven, the Netherlands *
- Dutch Polymer Days (DPD), March 2016, Lunteren, the Netherlands *
- Third Belgian-German Macromolecular meeting - Dynamic and Responsive Polymer Systems, February 2016, Houffalize, Belgium *
- Chemistry as Innovating Science (CHAINS), December 2015, Veldhoven, the Netherlands *

Acknowledgements

Na (ruim) vier jaar is het zover, het proefschrift is af en daarmee is het einde van mijn PhD in zicht! We zijn heel wat experimenten, typewerk, en wetenschappelijke discussies verder. Toch zijn het niet de uren in het lab of achter de PC die ik me zal herinneren over een paar jaar, maar de mensen op de uni of thuis die me altijd geholpen en gesteund hebben. Een aantal mensen in het bijzonder wil ik hier bedanken.

After four years the moment has arrived, my thesis is finished, and the end of my PhD is approaching. It took a lot of experiments, typing and scientific discussions to get to this point. Still, it will be the people around me during these years that are the most memorable, and therefore I would like to thank several people here.

Allereerst natuurlijk Rint en Hans, voor dit uitdagende en leuke project. Rint, na mijn afstuderen was het jouw rotsvaste overtuiging dat ik een PhD moest gaan doen dat uiteindelijk de doorslag heeft gegeven om de stap te wagen. Bedankt voor het vertrouwen, niet alleen tijdens mijn promotie maar ook al daarvoor. Hans, het maakt niet uit wat de resultaten van een experiment zijn, jij bent altijd enthousiast en vol nieuwe ideeën voor verder onderzoek. De uurtjes bij jou op kantoor discussiëren over data of presentaties perfectioneren met het bijbehorende 'teske koffie' waren vaak precies wat ik nodig had om weer de volgende stap te zetten.

Prof. Dr. Francesco Picchioni and Prof. Dr. Rolf van Benthem, thank you for taking the time to critically read my work and for being part of my committee. Prof. dr. Dick Broer, bedankt voor de uitleg over alignment en suggesties voor POM-metingen. Daarnaast wil ik u ook bedanken voor het deelnemen in mijn commissie. Prof. dr. Gerrit Peters en dr. Tessa ten Cate, ik heb jullie input en suggesties tijdens de BMC-AM meetings altijd zeer op prijs gesteld, bedankt dat jullie tijd wilden vrij maken om deel uit te maken van de promotiecommissie. Als laatste wil ik Prof. dr. ir. Emiel Hensen bedanken voor het voorzitten van de verdediging.

Een deel van deze thesis is tot stand gekomen door samenwerkingen met collega's en studenten. Rosaria, I enjoyed our update meetings in the library, the halfway point between chemistry and mechanical engineering. Our collaboration already resulted in one published paper and two more manuscripts are submitted. Mallika, as my first student you put a lot of time in the 'spin-speed-calculator', I think one of my most used excel spreadsheets, thank you for that. Remon and Nicolle, your work greatly contributed to Chapter 4, thank you for all the time and effort you guys put in unraveling the kinetics. Stijn en Jaap, ondanks dat de resultaten uit jullie projecten niet in dit boekje staan, waren ze niet minder belangrijk en hebben beide projecten geleid tot veel nieuwe inzichten.

Zonder alle supportstaf zou deze thesis er niet zijn en een hoop andere wetenschap niet plaats kunnen vinden. De hulp en steun van het fantastische secretaresseteam is voor ons allemaal onmisbaar, net als de koffie bij Henk en de bestellingen van Hans. Dank ook aan alle mensen (zowel staf als PhD studenten) die zich inzetten om alle apparatuur up en

running te houden. Jolanda, jij bedankt voor alle praktische tips en tricks en natuurlijk mijn adoptie op lab 2 toen we naar vloer 4 zijn verhuisd.

Gedurende de jaren hier zijn er zo veel mensen die hier of daar ergens mee helpen, een kritische vraag tijdens een colloquium, een suggestie bij een groupmeeting, nieuwe inzichten door een praatje op kantoor of op het lab. Het is onmogelijk jullie allemaal persoonlijk te bedanken dus bij dezen wil ik iedereen binnen SMO, alle (ex)leden van de Sijbesma group in het bijzonder, bedanken voor de super werksfeer.
Naast het werk binnen SMO heb ik ook behoorlijk wat uurtjes gebruik mogen maken van apparatuur en labruimtes bij SFD en bij mechanical engineering, ook hier wil ik iedereen bedanken voor de gastvrijheid en input.
Bovenop alle werk gerelateerde zaken denk ik ook met heel veel plezier terug aan al die minder serieuze momenten met alle collega's tijdens de lunch, koffiepauze, borrels, conferenties of uitjes.

Daarnaast wil ik nog een aantal mensen extra bedanken die de term collega inmiddels ontgroeid zijn. Allereest natuurlijk mijn paranimfen! Lieve Annelore en Ellen, wat was ik blij dat jullie allebei volmondig 'JA!' zeiden om op 2 oktober naast mij te staan. Niet alleen die dag; tijdens die behoorlijk hectische schrijfperiode gingen we gezellig even ontspannen bij de salsalessen en toen het manuscript af was stonden jullie daar met feestbubbels. Natuurlijk ook mijn (kantoor)maatje Jody, van gesprekken over de wetenschap tot gesprekken over het (PhD) leven, je verrast me altijd weer met jouw kijk op dingen. Wat ben ik blij dat ik je af en toe even kon bellen toen je de TU verlaten had. Gilles, Marc, Stijn, Fabian, Simon, Tom, Jeroen en alle andere ameeeezing mensen die ervoor zorgen dat onze lunchgesprekken in een film gecensureerd zouden worden, ik ga die uurtjes zeker missen.

Uiteraard ook een stukje voor mijn lieve familie en vrienden, bedankt voor al jullie interesse en de betrokkenheid de afgelopen jaren! Ook hier weer een paar mensen in het bijzonder. Jolien, mijn cover is precies wat ik wilde, maar toch mooier dan ik had durven dromen, vooral met het achterliggende persoonlijke tintje. Iris, onze jarenlange vriendschap is voor mij onbetaalbaar. Een trip naar Londen of een verrassingspakketje in de brievenbus, laten we de memory jar die jij mij een tijd geleden gegeven hebt nog maar flink uitbreiden. Mijn toppers van (reserve)zusjes Angeline, Myrthe en hun mannen, of we nu foto's maken in Maastricht of frietjes met zuurvlees eten thuis, met jullie is het altijd feest. Ik kan me geen leuker gezin wensen. Pap en mam, wat er ook gebeurt, jullie zijn er altijd voor me, met advies, hulp of wat dan ook, ik hoef het vaak niet eens te vragen. Het is dankzij jullie dat ik hier nu sta, bedankt voor alles. En pa, natuurlijk bedankt voor de holpijpjes.

Als allerlaatste natuurlijk Davey, bij jou kan ik met alles terecht en helemaal mezelf zijn, bedankt voor al je hulp, steun en liefde. Op naar jouw promotie en nog veel meer mooie momenten samen!

Bedankt voor de onvergetelijke tijd,
Eveline
♥